

International conference

# Functional Inorganic Materials



# FIM 2022

Abstract book



VILNIUS UNIVERSITY PRESS



Vilnius  
University



CENTER  
FOR PHYSICAL SCIENCES  
AND TECHNOLOGY



kaunas  
university of  
technology



Lithuanian  
Chemical  
Society

## **CONTENTS**

Scientific committee	4
Organizing committee	5
Conference programme	6
Invited speakers	12
Invited speaker lecture abstracts	15
Short presentation lecture abstracts	36
Poster presentation abstracts	55
Index	84

Copyright © 2022 [Authors]. Published by Vilnius University Press

This is an Open Access article distributed under the terms of the Creative Commons Attribution Licence, which permits unrestricted use, distribution, and reproduction in any medium, provided the original author and source are credited.

<https://doi.org/10.15388/Proceedings.2022.29>

ISBN 978-609-07-0777-7 (digital PDF)



International Conference  
**Functional Inorganic Materials 2022**

**Sponsors**





## **SCIENTIFIC COMMITTEE**

Prof. dr. Kęstutis Baltakys (*Kaunas University of Technology*)

Prof. (HP) dr. Aldona Beganskienė (*Vilnius University*)

Prof. habil. dr. Aivaras Kareiva (*Vilnius University*)

Prof. habil. dr. Rimantas Ramanauskas (*CPST, Institute of Chemistry*)

Prof. (HP) dr. Almira Ramanavičienė (*Vilnius University*)



## **ORGANIZING COMMITTEE**

Assoc. prof. dr. Živilė Stankevičiūtė (*Vilnius University*), **Chairperson**

Assoc. prof. dr. Justina Gaidukevič (*Vilnius University*)

Dr. Andrius Laurikėnas (*Vilnius University*)

Dr. Jolanta Raudonienė (*Vilnius University*)

Dr. Eva Raudonytė-Svirbutavičienė (*Vilnius University*)

PhD student Greta Inkrataitė (*Vilnius University*), **scientific secretary**

PhD student Justinas Januškevičius (*Vilnius University*)

PhD student Dovydas Karoblis (*Vilnius University*)

PhD student Rūta Aukštakojtė (*Vilnius University*)

PhD student Andrius Pakalniškis (*Vilnius University*)

PhD student Gintarė Rimkutė (*Vilnius University*)



## CONFERENCE PROGRAMME

### 5<sup>th</sup> of October. Arrival day.

17:00–20:00 Participant meeting at Vilnius Airport.

### 6<sup>th</sup> of October

Vilnius University seminar room 239, Universiteto St. 3 (live or online).

Time	Presenter	Institution	Title of the Lecture
8:00–9:00	Participant registration		
9:00–9:10	Welcome speech from the vice rector of Vilnius University Prof. (HP) Dr. Edita <b>Sužiedelienė</b>		
9:10–9:20	Welcome speech from Prof. Habil. Dr. Jūras <b>Banys</b> , the president of the Lithuanian Academy of Sciences		
9:20–9:30	Information from the chairman of the organizational committee Prof. Habil. Dr. Aivaras <b>Kareiva</b>		
<b>Oral session</b> (Chairperson Prof. Dr. Simas <b>Šakirzanovas</b> )			
9:30–10:00	Invited Speaker Prof. Dr. Pierre <b>Rabu</b>	University of Strasbourg, <i>France</i>	Insertion-Grafting to Exfoliation in Layered Functional Systems
10:00–10:30	Invited Speaker Prof. Dr. Aleksej <b>Žarkov</b>	Vilnius University, <i>Lithuania</i>	Phase Transformations in Calcium Phosphates
10:30–11:00	Invited Speaker Dr. Simonas <b>Ramanavičius</b>	Center for Physical Sciences and Technology, <i>Lithuania</i>	Formation and Applications of Nonstoichiometric Titanium Oxides and MXenes (Ti <sub>3</sub> C <sub>2</sub> T <sub>x</sub> ) Nanostructures
11:00–11:30	<b>Coffee break</b>		
11:30–12:00	Invited Speaker Prof. Dr. Koichiro <b>Hayashi</b>	Kyushu University, <i>Japan</i>	Carbonate Apatite Honeycomb Scaffolds for Bone Regeneration
12:00–12:30	Invited Speaker Prof. Dr. Artūras <b>Katelnikovas</b>	Vilnius University, <i>Lithuania</i>	Inorganic CsPbX <sub>3</sub> (X = Cl, Br, I) Perovskite Quantum Dots: Synthesis, Properties, and Applications
12:30–14:00	<b>Lunch break</b>		
<b>Oral session</b> (Chairperson Prof. (HP) Dr. Aldona <b>Beganskienė</b> )			
14:00–14:30	Invited Speaker Prof. Dr. Vytautas <b>Getautis</b>	Kaunas University of Technology, <i>Lithuania</i>	Advanced Organic Molecules for New Generation Solar Cells
14:30–15:00	Invited Speakers Prof. Habil. Dr. Wojciech	Nicolaus Copernicus	The Properties of Polymeric and Ceramic Membranes in Gas and Liquid Separation



	<b>Kujawski</b> , Guoqiang Li, Dr. Katarzyna Knozowska, habil. Dr. Joanna Kujawa	University in Toruń, <i>Poland</i>	
15:00–15:30	Invited Speaker Prof. Dr. Rasa <b>Pauliukaitė</b>	Center for Physical Sciences and Technology, <i>Lithuania</i>	Can Graphene Be Sensitive?
15:30–16:00	Invited Speaker Assoc. Prof. Dr. Lina <b>Mikoliūnaitė</b>	Center for Physical Sciences and Technology, <i>Lithuania</i>	Effect of Silver to Magnetite Properties in Ag/Fe <sub>3</sub> O <sub>4</sub> Nanoparticles Composite
16:00–16:20	<b>Coffee break</b>		
16:20–17:30	<b>Poster session</b>		
19:00	<b>Dinner (Universiteto St. 3)</b>		

### 7<sup>th</sup> of October

Vilnius University seminar room 239, Universiteto St. 3 (live or online).

Time	Presenter	Institution	Title of the Lecture
8:30–9:00	Participant registration		
<b>Oral session</b> (Chairperson Prof. Dr. Artūras <b>Katelnikovas</b> )			
9:00–9:30	Invited Speaker Prof. Dr. Kęstutis <b>Baltakys</b>	Kaunas University of Technology, <i>Lithuania</i>	Characterization of Functional Inorganic Materials by X-Ray Diffraction Methods
9:30–10:00	Invited Speaker Dr. Michele <b>Back</b>	University of Venice, <i>Italy</i>	Cr <sup>3+</sup> -Activated Phosphors: Effective Luminescent Thermometers?
10:00–10:30	Invited Speaker Dr. Anton <b>Popov</b>	Vilnius University, <i>Lithuania</i>	Surface Plasmon Resonance Spectroscopy as a Key to the Development of Sensitive Biosensors
10:30–11:00	Invited Speaker Prof. Dr. Anja Verena <b>Mudring</b>	Aarhus University, <i>Denmark</i>	How to Use Ionic Liquids to Make Inorganic Nanomaterials
11:00–11:30	<b>Coffee break</b>		
11:30–12:00	Invited Speaker (HP) dr. Jurgis <b>Barkauskas</b>	Vilnius University, <i>Lithuania</i>	Graphene-Based Materials: Synthesis, Chemistry and Applications
12:00–12:30	Invited Speaker Prof. dr. Malle <b>Krunks</b>	Tallinn University of Technology, <i>Estonia</i>	Antimony Chalcogenide Thin Film Solar Cells – Challenges and Prospects



*International Conference*  
**Functional Inorganic Materials 2022**

12:30–14:00 <b>Lunch break</b>			
<b>Oral session</b> (Chairperson Prof. Dr. Rasa <b>Pauliukaitė</b> )			
14:00–14:30	Invited Speaker Prof. Dr. Rimantas <b>Ramanauskas</b>	Center for Physical Sciences and Technology, <i>Lithuania</i>	Corrosion Behaviour of Cerium Based Conversion Coatings on Zinc
14:30–15:00	Invited Speakers Habil. Dr. Anna <b>Lukowiak</b>	Polish Academy of Sciences, <i>Poland</i>	Bioactive Glasses with Luminescent Properties
15:00–15:30	Invited Speaker Prof. Dr. Tomas <b>Tamulevičius</b>	Kaunas University of Technology, <i>Lithuania</i>	Nanomaterials and their Structures for Optical Applications
15:30–16:00	Invited Speaker Prof. Habil. Dr. Gerd <b>Meyer</b>	KTH Royal Institute of Technology, <i>Sweden</i>	Small Cause — Great Effect: What the $4f^{n+1}5d^0 \rightarrow 4f^n5d^1$ Configuration Crossover Does to the Chemistry of Divalent Rare-Earth Halides and Coordination Compounds, and How it Makes the Formation of Cluster Complex Compounds and Polar Intermetallics Possible
16:00–17:30 <b>Tour of Vilnius University</b>			

**8<sup>th</sup> of October**

Vilnius University seminar room 239, Universiteto St. 3 (live or online).

Time	Presenter	Institution	Title of the Lecture
8:30–9:00	Participant registration		
<b>Oral session</b> (Chairperson Prof. Dr. Aleksej <b>Žarkov</b> )			
9:00–09:30	Invited Speaker Assoc. Prof. Dr. Linus <b>Vilčiauskas</b>	Center for Physical Sciences and Technology, <i>Lithuania</i>	From Fundamental Understanding to Applications in Energy Storage of Phosphate Framework Materials
9:30–9:40	<b>Agnė Kizalaitė</b>	Vilnius University, <i>Lithuania</i>	Novel Whitlockite Compounds: Structure and Properties
9:40–9:50	<b>Dovydas Karoblis</b>	Vilnius University, <i>Lithuania</i>	Investigation of Various Types Ferrites and Manganites Prepared via Sol-Gel Synthetic Approach
9:50–10:00	<b>Anastasija Afonina</b>	Vilnius University, <i>Lithuania</i>	Investigation of Phase Transformations in the Low





			Temperature Synthesis of Magnesium Whitlockite
10:00–10:10	Dr. Halyna <b>Yankovych</b>	Institute of Geotechnics of the Slovak Academy of Sciences, <i>Slovakia</i>	Photocatalytic Removal of Halogenated Organic Substances and Industrial Dyes by Activated Carbon Composites
10:10–10:20	Dr. Viktoriia <b>Kyshkarova</b>	Institute of Geotechnics of the Slovak Academy of Sciences, <i>Slovakia</i>	Synthesis and Adsorption Potential of Organo-Inorganic Hybrids Based on the Polymers with Carboxyl Groups and Silica
10:20–10:30	Edvardas <b>Brimas</b>	Vilnius University, <i>Lithuania</i>	Analytical Methods Used for the Characterization of Adipose Tissue
10:30–11:00	<b>Coffee break</b>		
<b>Oral session</b> (Chairperson Assoc. Prof. Dr. Živilė <b>Stankevičiūtė</b> )			
11:00–11:10	Rūta <b>Aukštakojtė</b>	Vilnius University, <i>Lithuania</i>	A Dopamine Electrochemical Sensor Based on N-Doped Reduced Graphene Oxide Electrode
11:10–11:20	Monika <b>Baublytė</b>	Vilnius University, <i>Lithuania</i>	GdPO <sub>4</sub> ·H <sub>2</sub> O:Eu <sup>3+</sup> Ceramic Composites – Wood
11:20–11:30	Greta <b>Inkrataitė</b>	Vilnius University, <i>Lithuania</i>	YAG and LuAG Powder, Ceramic and Thin Films. The Effect of Boron Doping on Compounds Luminescence Properties
11:30–11:40	Rasa <b>Karalkevičienė</b>	Vilnius University, <i>Lithuania</i>	Solvothermal Synthesis of Calcium Hydroxyapatite via Hydrolysis of α-Tricalcium Phosphate in Different Aqueous-Organic Media
11:40–11:50	Laura <b>Lukavičiūtė</b>	Vilnius University, <i>Lithuania</i>	Synthesis of Structurized Phosphates and Their Application in Cosmetic Products
11:50–12:00	Andrius <b>Pakalniškis</b>	Vilnius University, <i>Lithuania</i>	Stabilization of Hexagonal Crystal Structure in the Orthorhombic LuFeO <sub>3</sub> Matrix
12:00–12:10	Gintarė <b>Rimkutė</b>	Vilnius University, <i>Lithuania</i>	A Comparative Study of the Effect of Graphite Particle Size on the Formation of Sulfuric Acid Intercalated Graphite and Its Thermal Treatment



12:10–12:20	Rūta <b>Raišeliene</b>	Vilnius University, <i>Lithuania</i>	Synthesis and Investigation of Magnesium Whitlockite Granules
12:20–12:30	Justinas <b>Januškevičius</b>	Vilnius University, <i>Lithuania</i>	Aqueous Sol-Gel Synthesis of Select Orthoferrite Powders, Coatings, Nanotubes
12:30–12:40	Lukas <b>Šerpytis</b>	Vilnius University, <i>Lithuania</i>	Continuous Flow Synthesis of Silicon Dioxide Microparticles
12:40–12:50	Greta <b>Merkininkaitė</b>	Vilnius University, <i>Lithuania</i>	Additive Manufacturing of Inorganic 3D Nanostructures by Combining Laser Lithography and Pyrolysis
12:50–13:00	Davit <b>Tediashvili</b>	Vilnius University, <i>Lithuania</i>	Degradation Study of Vanadium-Based Materials for Aqueous Na-Ion Battery Cathodes
13:00–13:10	Diana <b>Griesiūtė</b>	Vilnius University, <i>Lithuania</i>	Synthesis and Optical Properties of Mn-Doped Calcium Pyrophosphate Polymorphs
13:10–13:40	<b>Conference result review. Scientific discussions. Closing of the conference.</b>		

<b>POSTER SESSION</b> 6 <sup>th</sup> of October, 16:20–17:30		
<b>P1</b>	Dr. Rasa <b>Alaburdaitė</b>	UV Investigation of CdS Layers on Polypropylene Film
<b>P2</b>	Darija <b>Astrauskytė</b>	Deposition of Optical Coatings on Micro-Optics
<b>P3</b>	Darius <b>Budrevičius</b>	The Optimal Eu Concentration for Luminesces Properties of GdPO <sub>4</sub>
<b>P4</b>	Narvydas <b>Dėnas</b>	Enzyme and Prussian Blue Based Detection of Mercury Ions
<b>P5</b>	Marius <b>Dzvinka</b>	Study of Properties of Europium-Doped Sodium Aluminum Germanate
<b>P6</b>	Neringa <b>Gailiūtė</b>	Synthesis and Analysis of Mg <sub>2</sub> /Al <sub>1</sub> -CO <sub>3</sub> and Zn <sub>2</sub> /Al <sub>1</sub> -CO <sub>3</sub> Layered Double Hydroxide Modified Wood
<b>P7</b>	Dr. Yuriy <b>Gerasymchuk</b>	Structure and Morphology of Thin Layers of Bismuth Ferrite Obtained by the Sol-Gel Method Depending on Different Substrates
<b>P8</b>	Erlandas <b>Kabašinskas</b>	Phase Transformations of Amorphous Calcium Phosphate in Molten Salts
<b>P9</b>	Prof. Habil. Dr. Aivaras <b>Kareiva</b>	Novel Co-Substituted Yttrium Gallium Garnets
<b>P10</b>	Gabija <b>Kavaliauskaitė</b>	Prussian Blue in Formation of Bio-Electrochemical Systems



<b>P11</b>	Dr. Valentina <b>Krylova</b>	Functionalization of Polyvinylchloride Textile Surface with Thin Films of Silver Oxide by Chemical Method
<b>P12</b>	Miglė <b>Liudžiūtė</b>	Structural Characterizations of Cadmium Telluride-Cadmium Sulfide Layers on Polyamide 6
<b>P13</b>	Gabija <b>Navašinskaitė</b>	In-situ Synthesis of Calcium Phosphate Bioceramics Derived from Eggshells to Improve Strength and Fire Resistance of Scots Pine Wood
<b>P14</b>	Dr. Neringa <b>Petrasauskienė</b>	UV/Vis Investigation of Cu <sub>x</sub> S Thin Films Deposited on Polypropylene by Chemical Bath Technique
<b>P15</b>	Ignas <b>Pocius</b>	Simulating Microwave Field Distribution in a Novel Superconducting EPR Microresonator
<b>P16</b>	Laura <b>Sakalauskienė</b>	Reagentless Electrochemical Glucose Biosensor Based on Electrochemically Deposited Gold Nanostructures and Prussian Blue
<b>P17</b>	Birutė <b>Serapinienė</b>	Effect of the Acid Sulphate Solution Additives on the Active Real Surface Area of the Electrodeposited Copper Honeycomb-Like Structures
<b>P18</b>	Dr. Monika <b>Skrudienė</b>	Optically Active Yttrium Aluminum Garnet and Silica Glass System
<b>P19</b>	Dr. Robert <b>Tomala</b>	Influence of Grain Size on Properties of Lanthanum Manganite Nanocrystals and Nanoceramics
<b>P20</b>	Justinas <b>Turčak</b>	Overview of Donors in Silicon for Spin-Based Quantum Technologies
<b>P21</b>	Dr. Skirmantė <b>Tutlienė</b>	Substitution Effects on the Stability and Electrochemical Properties of NaTi <sub>2-x</sub> M <sub>x</sub> (PO <sub>4</sub> ) <sub>3</sub> (M = Zr(IV), Hf(IV)) Anodes for Aqueous Sodium Ion Batteries
<b>P22</b>	Gediminas <b>Usevičius</b>	ESEEM Spectroscopy of Methyl Group Quantum Tunneling in Co <sup>2+</sup> -Doped Dimethylammonium Zinc Formate
<b>P23</b>	Dr. Tyrpekl <b>Vaclav</b>	Lanthanide Oxalates: Synthesis, Structure, and Applications
<b>P24</b>	Klaudija <b>Vaičiukynaitė</b>	Formation and Investigation of Cobalt Sulfide Layers on the Surface of Polyamide 6
<b>P25</b>	Kristina <b>Vasiliauskienė</b>	Hydration Properties of Mayenite and Gypsum Mixture
<b>P26</b>	Paulina <b>Verbaitytė</b>	Coupling of Microwaves to a Planar EPR Microresonator via a 3D Cavity
<b>P27</b>	Gerda <b>Žižiūnaitė</b>	Electrochemical Prussian Blue-Based Hypochlorite Sensor
<b>P28</b>	Dr. Edita <b>Zubrytė</b>	The Performance of Waste Nanomaterial in the Remediation of a Real Aluminum Anodizing Wastewater

# INVITED SPEAKERS



Prof. dr. Pierre **Rabu**, University of Strasbourg, *France*.

[From Insertion-Grafting to Exfoliation in Layered Functional Systems](#)



Dr. Aleksej **Žarkov**, Vilnius University, *Lithuania*.

[Phase Transformations in Calcium Phosphates](#)



Dr. Simonas **Ramanavičius**, Center for Physical Sciences and Technology, *Lithuania*.

[Formation and Applications of Nonstoichiometric Titanium Oxides and MXenes \( \$Ti\_3C\_2T\_x\$ \) Nanostructures](#)



Prof. dr. Koichiro **Hayashi**, Kyushu University, *Japan*.

[Carbonate Apatite Honeycomb Scaffolds for Bone Regeneration](#)



Prof. dr. Artūras **Katelnikovas**, Vilnius University, *Lithuania*.

[Inorganic  \$CsPbX\_3\$  \( \$X = Cl, Br, I\$ \) Perovskite Quantum Dots: Synthesis, Properties, and Applications](#)



Prof. dr. Vytautas **Getautis**, Kaunas University of Technology, *Lithuania*.

[Advanced Organic Molecules for New Generation Solar Cells](#)



Prof. habil. dr. Wojciech **Kujawski**, Nicolaus Copernicus University in Toruń, *Poland*

[The Properties of Polymeric and Ceramic Membranes for Gas and Liquid Separation.](#)



Prof. dr. Rasa **Pauliukaitė**, Center for Physical Sciences and Technology, *Lithuania*.

[Can Graphene be Sensitive?](#)



Dr. Lina **Mikoliūnaitė**, Center for Physical Sciences and Technology, *Lithuania*.

[Effect of Silver to Magnetite Properties in Ag/Fe<sub>3</sub>O<sub>4</sub> Nanoparticles Composite](#)



Prof. dr. Kęstutis **Baltakys**, Kaunas University of Technology, *Lithuania*.

[Characterization of Functional Inorganic Materials by X-ray Diffraction Methods](#)



Dr. Michele **Back**, University of Venice, *Italy*.

[Cr<sup>3+</sup>-Activated Phosphors: Effective Luminescent Thermometers?](#)



Dr. Anton **Popov**, Vilnius University, *Lithuania*.

[Surface Plasmon Resonance Spectroscopy as a Key to the Development of Sensitive Biosensors](#)



Prof. dr. Anja Verena **Mudring**, Aarhus University, *Denmark*.

[How to Use Ionic Liquids to Make Inorganic Nanomaterials](#)



Prof. (HP) dr. Jurgis **Barkauskas**, Vilnius University, *Lithuania*.

[\*Graphene-Based Materials: Synthesis, Chemistry and Applications\*](#)



Prof. dr. Malle **Krunk**, Tallinn University of Technology, *Estonia*.

[\*Antimony Chalcogenide Thin Film Solar Cells - Challenges and Prospects\*](#)



Prof. dr. Rimantas **Ramanauskas**, Center for Physical Sciences and Technology, *Lithuania*.

[\*Corrosion Behaviour of Cerium Based Conversion Coatings on Zinc\*](#)



Dr. habil. Anna **Lukowiak**, Polish Academy of Sciences, *Poland*.

[\*Bioactive Glasses with Luminescent Properties\*](#)



Prof. dr. Tomas **Tamulevičius**, Kaunas University of Technology, *Lithuania*.

[\*Nanomaterials and their Structures for Optical Applications\*](#)



Prof. habil. dr. Gerd **Meyer**, KTH Royal Institute of Technology, *Sweden*.

[\*Small Cause — Great Effect: What the  \$4f^{n+1}5d^0 \rightarrow 4f^n5d^1\$  Configuration Crossover Does to the Chemistry of Divalent Rare-Earth Halides and Coordination Compounds, and How it Makes the Formation of Cluster Complex Compounds and Polar Intermetallics Possible\*](#)



## **INVITED SPEAKER LECTURE ABSTRACTS**

# From Insertion-Grafting to Exfoliation in Layered Functional Systems

Pierre Rabu <sup>1,\*</sup>

<sup>1</sup>Institute of Physics and Chemistry of Materials of Strasbourg, CNRS-University of Strasbourg, 23 rue du Loess  
67034 Strasbourg, France

\*Corresponding author, e-mail: pierre.rabu@ipcms.unistra.fr

Chemical and structural versatility of layered metal hydroxides and oxides allows for insertion and grafting of various kinds of functional molecules in between magnetic or ferroelectric sheets. This ability is promising for generating multi-functionality. Numerous properties can be combined as conductivity, luminescence, chirality, magnetism electro-activity, catalysis, etc ... In addition, these functionalities can be rather easily modulated by changing the host structure as well as the inserted species. Such “Lego©” chemistry seems really appropriate and we obtained many magnetic (2D-3D), magneto-luminescent and magneto-electric systems.<sup>1,2</sup> Although successful, this approach is still quite serendipitous and a better control *a priori* of the synthesis and precise knowledge of the structure of these hybrid materials are necessary to help the designing of new layered hybrids.

We present here recent results concerning magnetic and multifunctional layered hydroxides (LSH) and oxides (Aurivillius phases) illustrating the mechanisms involved in insertion-grafting reactions, up to exfoliation. Our results enlarge the library of molecular species that is possible to graft into inter-lamellar space using various activation conditions.<sup>2-5</sup> We will describe efficient structural characterization techniques and analytical tools (TEM, XRD analysis and modeling) that were developed to investigate the structural features of these systems, allowing for establishing structure-properties relationships, together with improvement of the design of layered functional materials.

**Acknowledgements:** CNRS, University of Strasbourg, Région Grand Est, contract No. ANR-14-CE07-0004-01 (HYMN)) and the Labex NIE (ANR-11-LABX-0058\_NIE within the Investissement d’Avenir program ANR-10-IDEX-0002-02).

## References:

1. Rabu, P.; Delahaye, E.; Rogez, G. Hybrid Interfaces in Layered Hydroxides: Magnetic and Multifunctional Superstructures by Design. *Nanotechnol. Rev.* **2015**, *4* (6), 557–580. <https://doi.org/10.1515/ntrev-2015-0017>.
2. Evrard, Q.; Chaker, Z.; Roger, M.; Sevrain, C. M.; Delahaye, E.; Gallart, M.; Gilliot, P.; Leuvrey, C.; Rueff, J.-M.; Rabu, P.; Massobrio, C.; Boero, M.; Pautrat, A.; Jaffrès, P.-A.; Ori, G.; Rogez, G. Layered Simple Hydroxides Functionalized by Fluorene-Phosphonic Acids: Synthesis, Interface Theoretical Insights, and Magnetoelectric Effect. *Adv. Funct. Mater.* **2017**, *27* (41), 1703576. <https://doi.org/10.1002/adfm.201703576>.
3. Evrard, Q.; Leuvrey, C.; Farger, P.; Delahaye, E.; Rabu, P.; Taupier, G.; Dorkenoo, K. D.; Rueff, J.-M.; Barrier, N.; Pérez, O.; Rogez, G. Noncentrosymmetric Cu(II) Layered Hydroxide: Synthesis, Crystal Structure, Nonlinear Optical, and Magnetic Properties of Cu<sub>2</sub>(OH)<sub>3</sub>(C<sub>12</sub>H<sub>25</sub>SO<sub>4</sub>). *Cryst. Growth Des.* **2018**, *18* (3), 1809–1817. <https://doi.org/10.1021/acs.cgd.7b01692>.
4. Wang, Y.; Leuvrey, C.; Delahaye, E.; Leroux, F.; Rabu, P.; Taviot-Guého, C.; Rogez, G. Tuning the Organization of the Interlayer Organic Moiety in a Hybrid Layered Perovskite. *J. Solid State Chem.* **2019**, *269*, 532–539. <https://doi.org/10.1016/j.jssc.2018.10.034>.
5. Payet, F.; Bouillet, C.; Leroux, F.; Leuvrey, C.; Rabu, P.; Schosseler, F.; Taviot-Guého, C.; Rogez, G. Fast and Efficient Shear-Force Assisted Production of Covalently Functionalized Oxide Nanosheets. *J. Colloid Interface Sci.* **2022**, *607*, 621–632. <https://doi.org/10.1016/j.jcis.2021.08.213>.



# Phase Transformations in Calcium Phosphates

A. Zarkov<sup>1,\*</sup>, D. Griestiute<sup>1</sup>, A. Kizalaite<sup>1</sup>, E. Raudonyte-Svirbutaviciene<sup>1</sup>,  
V. Klimavicius<sup>2</sup>, A. Kareiva<sup>1</sup>

<sup>1</sup> Institute of Chemistry, Vilnius University, Naugarduko 24, LT-03225 Vilnius,  
Lithuania

<sup>2</sup> Institute of Chemical Physics, Vilnius University, Sauletekio 3, LT-10257, Vilnius,  
Lithuania

\*Corresponding author, e-mail: aleksej.zarkov@chf.vu.lt

Calcium phosphates (CPs) are a family of materials widely used in biomedical applications and especially bone regeneration due to their structural and compositional similarity to natural bone [1]. The compositional and structural variety of CPs leads to their different physicochemical, mechanical and biological properties, which allows the application of these materials in medicine in various forms from cements to ceramics and coatings [2].

While some CPs can be prepared directly by precipitation from aqueous solution, some phases can only be obtained by employing thermal treatment. Conventionally, for thermally induced synthesis, Ca and P salts are thoroughly mixed and annealed at an appropriate temperature. This approach is commonly applied for the preparation of CP phases such as calcium hydroxyapatite (HA,  $\text{Ca}_{10}(\text{PO}_4)_6(\text{OH})_2$ ), tricalcium phosphate (TCP,  $\text{Ca}_3(\text{PO}_4)_2$ ) or calcium pyrophosphate (CPP,  $\text{Ca}_2\text{P}_2\text{O}_7$ ). It should be underlined that the Ca/P ratio in starting materials and final products is expected to be identical and precursors are used in strictly stoichiometric ratios. It is generally assumed that only the structural components such as  $\text{H}^+$ ,  $\text{OH}^-$ ,  $\text{H}_2\text{O}$ , and  $\text{CO}_3^{2-}$  are removed during annealing in the form of volatile species.

Another way to obtain some CPs considers the thermal conversion of less stable phases. For instance, calcium-deficient hydroxyapatite (Ca/P ratio 1.5:1) is commonly used for the preparation of  $\beta$ -TCP. Thermal treatment at higher temperature allows the  $\alpha$ -TCP polymorph to be synthesized as well. Depending on the annealing temperature, amorphous CP (Ca/P ratio 1.5:1) can be converted to both TCP polymorphs, moreover, it is a suitable precursor for the preparation of low-temperature metastable  $\alpha$ -TCP. Additionally, phase transformations in CPs can occur in aqueous medium, where the presence of other ions and medium pH are the most important factors. Overall, the phase transformations in CPs highly depend on the origin of starting material, the presence of impurities and processing conditions.

## Acknowledgements

This research was funded by a grant WHITCERAM (No. S-LJB-22-1) from the Research Council of Lithuania.

## References

1. W. Habraken, P. Habibovic, M. Epple and M. Böhner, *Mater. Today*, **19** (2016) 69–87.
2. S. V. Dorozhkin and M. Epple, *Angew. Chem., Int. Ed.*, **41** (2002) 3130–3146.

# Formation and Applications of Nonstoichiometric Titanium Oxides and MXenes ( $\text{Ti}_3\text{C}_2\text{T}_x$ ) Nanostructures

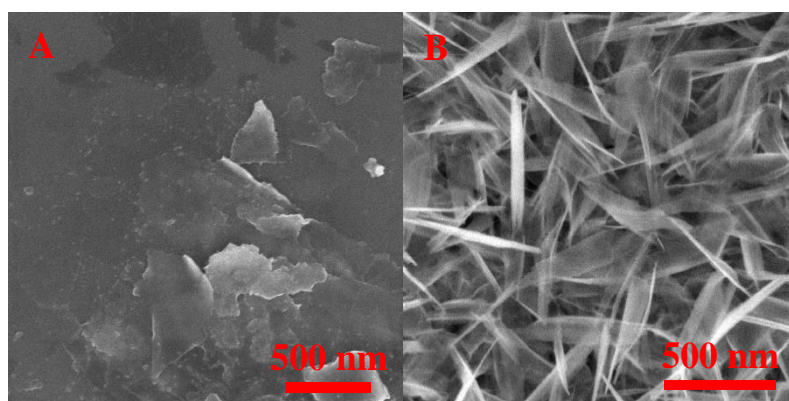
S. Ramanavičius

State research institute Center for Physical Sciences and Technology, Savanorių Ave. 231, LT-02300 Vilnius, Lithuania

\*Simonas Ramanavičius, simonas.ramanavicius@ftmc.lt:

In addition to stoichiometric  $\text{TiO}_2$ , recently, various nanostructured non-stoichiometric titanium oxides, which by different authors are abbreviated as  $\text{TiO}_n$ , or  $\text{TiO}_{2-x}$  and Magnéli phases ( $\text{Ti}_n\text{O}_{2n-1}$ ), have received significant attention in the development of various sensors [1]. Also, recent progress in the formation of optically active titanium carbides ( $\text{Ti}_3\text{C}_2\text{T}_x$ ) so-called MXenes encourages applications of these new 2D materials in the design of sensors, bioelectronics and some breakthrough in these areas are foreseen. The advantageous properties of MXenes are suitable for biosensing applications but are not the limitation. The other important property of MXenes is their high and near metallic conductivity altered by their surface termination groups [2], leading to a possible application as supercapacitors [3], resistive sensors [4] and other applications in electrochemistry [5], electronics [6].

This research is dedicated to investigate new ways for non-stoichiometric titanium oxides and their based nanostructures formation by wet chemical methods and searching for new applications. The main focus is on gas and biologically active molecules sensors and catalysts for hydrogen evolution reaction.



**Fig. 1.** SEM images of A – MXenes ( $\text{Ti}_3\text{C}_2\text{T}_x$ ) sheets, B –  $\text{TiO}_x$  nanostructures.

## References

1. Y. Wang, T. Wu, Y. Zhou, C. Meng, W. Zhu, L. Liu,  $\text{TiO}_2$ -Based Nanoheterostructures for Promoting Gas Sensitivity Performance: Designs, Developments, and Prospects. *Sensors*, **17**, (2017), 1971.
2. J.L. Hart, K. Hantanasirisakul, A.C. Lang, B. Anasori, D. Pinto, Y. Pivak, J.T., van Omme; S.J. May, Y.; Gogotsi, M.L. Taheri, Control of MXenes' Electronic Properties through Termination and Intercalation. *Nat. Commun.*, **10**, (2019), 522.
3. S.A. Melchior, K. Raju, I.S. Ike, R.M. Erasmus, G. Kabongo, I. Sigalas, S.E. Iyuke, K.I. Ozoemena, High-Voltage Symmetric Supercapacitor Based on 2D Titanium Carbide (MXene,  $\text{Ti}_2\text{CT}_x$ )/Carbon Nanosphere Composites in a Neutral Aqueous Electrolyte. *J. Electrochem. Soc.*, **165**, (2018), A501–A511.
4. L. Lorencova, T. Bertok, E. Dosekova, A. Holazova, D. Paprckova, A. Vikartovska, V. Sasinkova, J. FilipP., Kasak, M. Jerigova, Electrochemical Performance of  $\text{Ti}_3\text{C}_2\text{T}_x$  MXene in Aqueous Media: Towards Ultrasensitive  $\text{H}_2\text{O}_2$  Sensing. *Electrochim Acta*, **235**, (2017), 471–479.
5. D. Song, X. Jiang, Y. Li, X. Lu, S. Luan, Y. Wang, Y. Li, F. Gao, Metal–organic Frameworks-Derived  $\text{MnO}_2/\text{Mn}_3\text{O}_4$  Microcuboids with Hierarchically Ordered Nanosheets and  $\text{Ti}_3\text{C}_2$  MXene/Au NPs Composites for Electrochemical Pesticide Detection. *J. Hazard Mater.* **373**, (2019), 367–376.
6. H. Kim, Z. Wang, H.N. Alshareef, MXetronics: Electronic and Photonic Applications of MXenes. *Nano Energy*, **60**, (2019), 179–197.

# Carbonate Apatite Honeycomb Scaffolds for Bone Regeneration

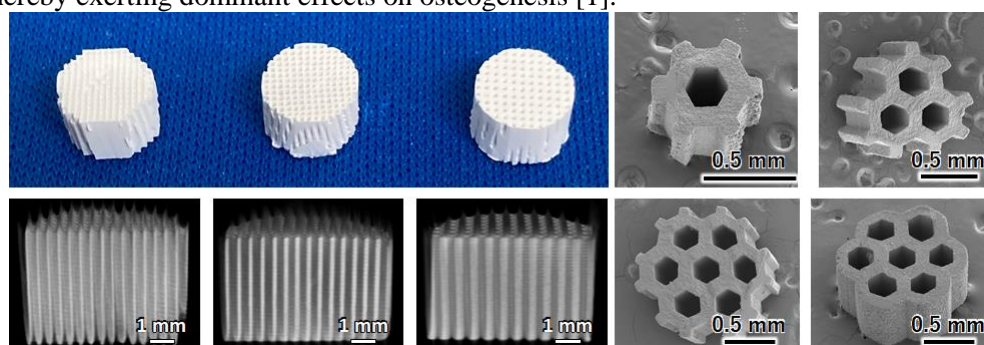
K. Hayashi<sup>1,\*</sup>

<sup>1</sup>Kyushu University, 3-1-1, Maidashi, Higashi-ku, Fukuoka 812-8582 Japan

\*Corresponding author, e-mail: khayashi@dent.kyushu-u.ac.jp

As the global population is aging rapidly, healthy life expectancy should accompany this increase. To extend the healthy life expectancy, the maintenance and recovery of oral and locomotory functions are crucial, for which dental implantation and orthopedic bone regeneration are effective.

Scaffolds with uniaxial channels from the bottom face contacting the host bone to the top face, such as honeycomb (HC) scaffolds, are deemed to be favorable for the ingrowth of bone and blood vessels. To date, we fabricated various types of HC scaffolds composed of carbonate apatite (Figure 1), known as a bone mineral analog, by exploiting extrusion molding [1-18]. We demonstrated the effects of the composition [12,16], structure at macro- [3-5,8-14], micro- [17], and nanoscales [15], and shape [1] on osteogenesis and angiogenesis by in vivo evaluations. Carbonate apatite showed a higher osteoconductivity than those consisting of  $\beta$ -tricalcium phosphate and hydroxyapatite [12,16]. Intrascapular channels of 230–300  $\mu\text{m}$  in apertural size prevented the penetration of fibrous tissues into the scaffold [14], thus providing a dominant position for osteogenesis and angiogenesis [3,4,9]. The micro- and nanopores affected osteoclastogenesis and the subsequent resorption of scaffolds by osteoclasts and new bone formation [15,17]. The scaffolds with both channels and micropores exerted osteoinduction [6] and osteoconduction [7,9], and shortened the bone reconstruction period. Furthermore, even tiny protuberances on the scaffold surface affected the percentage of interscaffold space, thereby exerting dominant effects on osteogenesis [1].



**Fig. 1.** Various carbonate apatite HC scaffolds.

In addition, we developed the method for providing antibacterial activity to carbonate apatite HC scaffolds [2]. The antibacterial HC scaffolds perfectly prevented bacterial infection in vivo in the presence of methicillin-resistant *Staphylococcus aureus*, formed new bone at 2 weeks after surgery, and were gradually replaced with a new bone. Thus, the antibacterial honeycomb scaffolds achieved both infection prevention and bone regeneration.

## References

1. K. Hayashi, T. Yanagisawa, R. Kishida, K. Ishikawa ACS Nano 2022, 16, 11755-11768
2. K. Hayashi, M. Shimabukuro, K. Ishikawa, ACS Appl. Mater. Interfaces. 2022, 14, 3762–3772.
3. K. Hayashi, T. Yanagisawa, M. Shimabukuro, R. Kishida, K. Ishikawa, Mater. Today Bio 2022, 14, 100247.
4. K. Hayashi, M. Shimabukuro, R. Kishida, A. Tsuchiya, K. Ishikawa, J. Adv. Res. 2022, in press, DOI: 10.1016/j.jare.2021.12.010.
5. K. Hayashi, A. Tsuchiya, M. Shimabukuro, K. Ishikawa, Mater. Des. 2022, 215, 110468.
6. K. Hayashi, K. Ishikawa, Nano Select 2022, 3, 60–77.
7. K. Shibahara, K. Hayashi, Y. Nakashima, K. Ishikawa, Front. Bioeng. Biotechnol. 2022, 10, 825831.
8. K. Hayashi, N. Kato, M. Kato, K. Ishikawa, Mater. Des. 2021, 204, 109686.
9. K. Hayashi, K. Ishikawa, ACS Appl. Bio Mater. 2021, 4, 721–730.
10. Y. Sakemi, K. Hayashi, A. Tsuchiya, Y. Nakashima, K. Ishikawa, J. Biomed. Mater. Res. 2021, 109, 1613–1622.
11. K. Shibahara, K. Hayashi, Y. Nakashima, K. Ishikawa, ACS Appl. Bio Mater. 2021, 4, 6821–6831.
12. K. Hayashi, R. Kishida, A. Tsuchiya, K. Ishikawa, ACS Appl. Bio Mater. 2020, 3, 1787–1795.
13. K. Hayashi, M. L. Munar, K. Ishikawa, Mater. Sci. Eng. C-Mater. Biol. Appl. 2020, 111, 110848.
14. K. Hayashi, M. Shimabukuro, R. Kishida, A. Tsuchiya, K. Ishikawa, Mater. Adv. 2021, 2, 7638–7649.
15. K. Hayashi, K. Ishikawa, J. Mater. Chem. B 2020, 8, 8536–8545.
16. K. Hayashi, R. Kishida, A. Tsuchiya, K. Ishikawa, Mater. Today Bio. 2019, 4, 100031.
17. K. Hayashi, R. Kishida, A. Tsuchiya, K. Ishikawa, Adv. Biosyst. 2019, 3, e1900140.
18. K. Hayashi, M. L. Munar, K. Ishikawa, Ceram. Int. 2019, 45, 15429–15434.

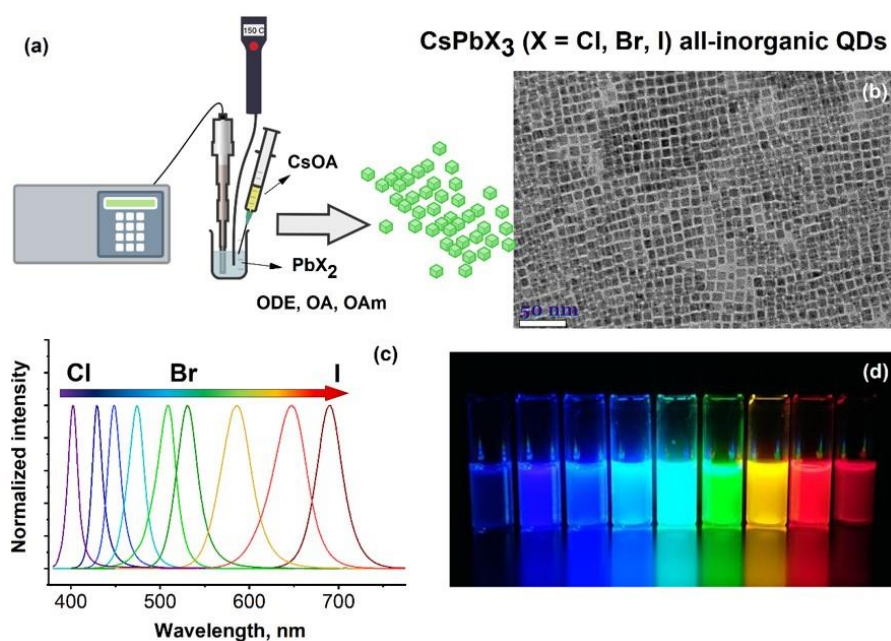
# Inorganic CsPbX<sub>3</sub> (X = Cl, Br, I) Perovskite Quantum Dots: Synthesis, Properties, and Applications

V. Klimkevičius<sup>1</sup>, M. Steponavičiūtė<sup>1</sup>, E. Ežerskytė<sup>1</sup>, A. Katelnikovas<sup>1,\*</sup>

<sup>1</sup>Institute of Chemistry, Vilnius University, Naugarduko 24, LT-03225 Vilnius, Lithuania

\*Corresponding author, e-mail: arturas.katelnikovas@chf.vu.lt

All-inorganic perovskite quantum dots (QDs), due to their outstanding power conversion efficiency, strong absorption, and narrow and tunable emission band, have already found applications in LEDs, solar cells, photodetectors, etc. In the past decade, there have been thousands of publications dedicated to the perovskite QDs structure-property relationship and their application in various optoelectronic fields [1,2]. The first inorganic lead perovskite QDs synthesis employing the hot-injection method was reported by Kovalenko et al. in 2015 [3]. Since then, the demand for novel, easier, and faster perovskite QDs synthesis methods has gradually increased. Thus, simple, easy, and highly reproducible lead perovskite QDs synthesis routes are very desirable. This study presents a novel approach to obtain perovskite QDs. The crucial synthesis parameters, such as temperature, isolation conditions, or optical density, on the changes in optical properties were investigated in detail. The detailed verification of different parameters showed that the proposed ultrasound-induced synthesis method (see Figure 1) is superior to the conventional hot-injection method since it offers not only higher reproducibility but also a significantly shorter synthesis time, i.e., from several hours via the traditional hot-injection method to merely 20-30 minutes by our proposed method.



**Fig. 1.** Graphical illustration of the ultrasound-induced synthesis of all-inorganic lead perovskite QDs (a); TEM image of the obtained CsPbBr<sub>3</sub> QDs (b); PL emission spectra (c) and emission color gamut of CsPbX<sub>3</sub> QDs with various compositions ( $\lambda_{\text{ex}} = 365$  nm) (d).

**Acknowledgement.** The authors acknowledge financial support from the European Regional Development Fund (project No 01.2.2-LMT-K-718-03-0048) under a grant agreement with the Research Council of Lithuania (LMTLT).

## References

1. M.B. Faheem, B. Khan, C. Feng, M.U. Farooq, F. Raziq, Y.Q. Xiao, Y.B. Li, ACS Energy Lett., **5** (2020) 290-320.
2. W.G. Chi, S.K. Banerjee, Angew. Chem.-Int. Edit. **61** (2022) e20211241219.
3. L. Protesescu, S. Yakunin, M.I. Bodnarchuk, F. Krieg, R. Caputo, C.H. Hendon, R.X. Yang, A. Walsh, M.V. Kovalenko, Nano Lett., **15** (2015) 3692-3696.

# Advanced Organic Molecules for New Generation Solar Cells

V. Getautis

*Kaunas University of Technology, Radvilėnų st., LT-50254 Kaunas, Lithuania  
vytautas.getautis@ktu.lt*

The application of solar cells is one of the most promising solutions for satisfying the ever-increasing global energy demand. First generation (1G) solar cells contain silicon wafers, which, although having high efficiency, are expensive to produce. Second-generation thin-film solar cells contain a layer of amorphous silica; however, their performances are poorer than their 1G counterparts. Hence after two decades of research, efforts are now centered on the development of a third generation (3G) of newly emerging solar cells. 3G solar cells include copper/zinc/tin sulfide solar cells, dye-sensitized solar cells (DSSCs), organic solar cells, polymer solar cells, quantum dot (QD) solar cells, and perovskite solar cells (PSCs). Recently, organic-inorganic hybrid lead halide PSCs are gathering attention and have emerged as an extremely promising photovoltaic technology due to their remarkable photovoltaic performance and potentially low production cost. To date, progress has been made on each layer, with major emphasis on perovskite film processing and relevant material design. Consequently, the power conversion efficiency of lead halide perovskite based thin film photovoltaic devices has skyrocketed from 3.8% to 25.8% in just ten years [1].

Despite significant efforts dedicated towards development of new hole transporting materials (HTMs) the field is still dominated by 2,2',7,7'-tetrakis(*N,N*-di-*p*-methoxyphenylamine)-9,9'-spirobifluorene (Spiro-OMeTAD) [2]. This compound combines high solubility, good film-forming ability, and suitable frontier molecular orbitals energy levels, resulting in excellent performance and ease of use [3]. However, the synthesis of Spiro-OMeTAD is expensive and its purification is tedious, which limits its application to the large-scale fabrication of PSCs [4]. Although many HTMs with comparable performance to Spiro-OMeTAD have been reported, multistep synthetic procedures are still required in most cases. More work is therefore needed to develop truly low-cost and efficient HTMs needed for the commercialization of PSCs.

This lecture will cover results of our recent investigations in the field of molecular engineering of small molecule hole transporting materials for perovskite solar cells. Our group has been successful in creating several classes of novel organic charge transporting materials, which are on a par with or even better than Spiro-OMeTAD. The molecularly engineered new hole transporting materials were synthesized in one or two steps from commercially available and relatively inexpensive starting reagents, resulting in up to several fold cost reduction of the final product compared with Spiro-OMeTAD. High solubility in organic solvents and ease of preparation makes these molecules very appealing for commercial prospects of photovoltaic devices.

## References

1. H. Min, D.Y. Lee, J. Kim, G. Kim, K.S. Lee, J. Kim, M. J. Paik, Y.K. Kim, K.S. Kim, M.G. Kim, T.J. Shin, S.I. Seok, *Nature*, **598** (2021) 444-450.
2. A. Farokhi, H. Shahroosvand, G.D. Monache, M. Pilkington, M.K. Nazeeruddin, *Chem. Soc. Rev.*, **51** (2022) 5974-6064.
3. F.M. Rombach, S.A. Haque, T.J. Macdonald, *Energy Environ. Sci.* **14** (2021) 5161-5190.
4. D. Vaitukaityte, Z. Wang, T. Malinauskas, A. Magomedov, G. Bubniene, V. Jankauskas, V. Getautis, H.J. Snaith, *Adv. Mater.*, **30** (2018)1803735.

# The Properties of Polymeric and Ceramic Membranes for Gas and Liquid Separation

**Wojciech Kujawski\*, Guoqiang Li, Katarzyna Knozowska, Joanna Kujawa**

*Membranes and Membrane Processes Research Group, Emerging Field "Polymer Sciences and Multifunctional Nanomaterials"; Faculty of Chemistry, Nicolaus Copernicus University in Toruń, 7 Gagarina Street, 87-100 Toruń, Poland*

*\*Corresponding author, e-mail:wkujawski@umk.pl*

Membrane technology plays an important role in various areas replacing or enriching the classical separation method. Since 1980s, membrane processes have become well-accepted in industry and medicine. The separation with the use of a membrane is based on the presence of a polymeric or inorganic barrier which splits the separated mixture into two effluents: the permeate, containing species transported preferentially through the membrane and the retentate, which contains the particles rejected by the membrane. A membrane phase (solid, liquid, or gaseous) introduces an interface between two other phases involved in the separation and acts as a permselective barrier.

The use of membranes is nowadays a part of the class of operations termed separation technology and in general, membrane processes are used for purification, concentration, fractionation, and distribution. The membrane is a key component of the separation system and its morphology is dependent on the final destination. In general, membranes can be classified according to different criteria such as a material used for the membrane preparation, membrane structure (morphology), methods of the membrane preparation, principle of separation, and the final application.

Paper will discuss various methods for optimizing membranes for given separation purposes, focusing mostly on membranes for gas separation and liquid-liquid separation by pervaporation. The goal of this optimization is to improve the affinity between membrane and separating systems. By merging material and membrane science, materials with adjusted morphology and controlled separation features can be prepared. The modification can be related to the adjustment of the surface nano-architecture and/or bulk membrane structure. Polymeric membranes with commercial and synthesized nanofillers will be described in detail. The surface modification of ceramic materials will be also discussed. Eventually, several practical applications of the pristine and modified membranes in gas separation and pervaporation will be presented.

# Can Graphene be Sensitive?

**J. Gaidukevič<sup>1,2</sup>, R. Aukstakojyte<sup>2</sup>, M. Kozłowski<sup>3</sup>, J. Barkauskas<sup>2</sup>, R. Pauliukaite<sup>1,2\*</sup>**

<sup>1</sup>*Department of Nanoengineering, Center for Physical Sciences and Technology, Savanoriu Ave. 231, LT-02300 Vilnius, Lithuania*

<sup>2</sup>*Faculty of Chemistry and Geosciences, Vilnius University, Naugarduko str. 24, LT-03225, Vilnius, Lithuania*

<sup>3</sup>*Faculty of Chemistry, Adam Mickiewicz University in Poznań, Uniwersytetu Poznańskiego 8, 61-614 Poznań, Poland*

*\*rasa.pauliukaite@ftmc.lt*

Graphene and its oxide (GO) due to its properties are widely applied in electrochemical research as an electrode material. The immobilization of GO and its related nanomaterials into electrochemical sensors has shown great promise due to its high surface area, chemical stability, electron transfer rate, and easy functionalization. However, the field of graphene-based sensors is still in its early development stage, and several key challenges need to be addressed. The current progress has proved that the doping of heteroatoms (such as N, P, and B) in the graphene lattice is a feasible method to modulate the surface chemistry and electronic properties of graphene [1]. Therefore, this work aimed to produce N-doped reduced graphene oxide (rGO) and investigate its suitability in electrochemical sensing.

In this work, GO was prepared from natural graphite using the synthesis protocol reported by Yan et al. [2]. The obtained pre-oxidized graphite was subjected to oxidation by Hummers' method using NaNO<sub>3</sub>, H<sub>2</sub>SO<sub>4</sub>, and KMnO<sub>4</sub> [3]. The rGO was produced from GO using a thermal shock method. The dried GO powder was quickly inserted into a preheated tubular furnace at a temperature of about 800 °C in the Ar atmosphere. To introduce N-functionalities, the rGO surface was modified with gaseous ammonia at temperatures of 850 °C and 950 °C for 4 and 8 h, respectively [4]. To achieve a complete comprehension of the effect on N-doped rGO structure, the nature of N-functionalities introduced during the functionalization and composition, a combination of various analysis methods such as Raman spectroscopy, X-ray photoelectron spectroscopy, SEM investigations, were used. Electrochemical measurements, in particular, cyclic voltammetry and chronoamperometry were used to evaluate the sensitivity of the obtained samples toward H<sub>2</sub>O<sub>2</sub> and glucose detection.

The results demonstrated that the amount and type of N-containing functional groups introduced during the functionalization of rGO surface plays a crucial role in controlling the structure and the application potential of rGO. Moreover, it was observed, that various nitrogen species including pyridinic-N, pyrrolic-N, and quaternary-N were detected in the N-doped rGO. Also, it was demonstrated, that the N-doping at higher temperatures and longer time dramatically interrupts the carbon lattice and causes a high defective degree. Electrochemical studies showed that the attachment of a greater content of quaternary nitrogen species onto the rGO surface significantly improves electrocatalytic activity toward H<sub>2</sub>O<sub>2</sub> reduction and glucose oxidation. The analytical performances of such sensors will be presented and discussed.

## Acknowledgments

This project has received funding from European Social Fund (project No 09.3.3-LMT-K-712-19-0050) under grant agreement with the Research Council of Lithuania (LMTLT).

## References

1. Z. Zhu, Nano-Micro Letters, **9** (2017) 25.
2. X. Yan, J. Chen, J. Yang, Q. Xue, P. Miele, App. Mater., **9** (2010) 2521–2529.
3. W. S. Hummers, R. E. Offeman, J. Am. Chem. Soc., **80** (1958) 1339.
4. J. Gaidukevič, J. Barkauskas, A. Malaika, V. Jasulaitienė, M. Kozłowski, Appl. Surf. Sci. **554** (2021) 149588.

# Effect of Silver to Magnetite Properties in Ag/Fe<sub>3</sub>O<sub>4</sub> Nanoparticles Composite

L. Mikoliunaite<sup>1,2\*</sup>, M. Talaikis<sup>1</sup>, G. Zambzickaite<sup>1</sup>, G. Niaura<sup>1</sup>

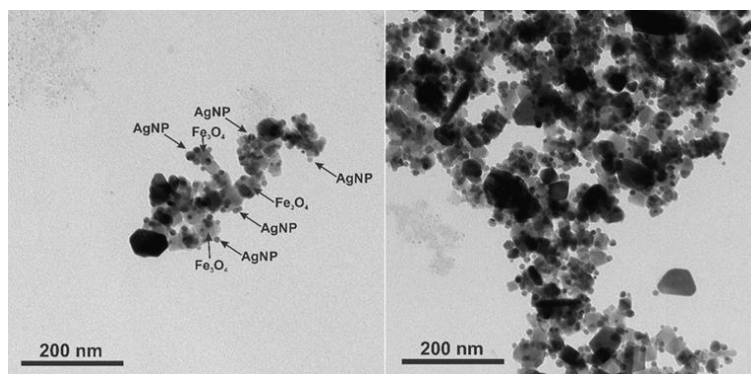
<sup>1</sup>Center for Physical Sciences and Technology, Department of Organic Chemistry, Sauletekio av. 3, LT-10257, Vilnius, Lithuania

<sup>2</sup>Vilnius University, Faculty of Chemistry and Geosciences, Naugarduko st. 24, LT-03225, Vilnius, Lithuania

\*Corresponding author, e-mail: lina.mikoliunaite@ftmc.lt

Bifunctional magneto-plasmonic nanoparticles that exhibit synergistically magnetic and plasmonic properties are advanced substrates for surface-enhanced Raman spectroscopy (SERS) due to their excellent controllability and improved detection potentiality. Surface-enhanced Raman spectroscopy [1] is known for its sensitivity to detect extremely low concentrations of analytes. Rough noble metal structures, such as silver and gold nanoparticles provide plasmon resonance that enhances Raman signal allowing to detect the analyte at concentrations as low as 10<sup>-9</sup> M. However, this method has some difficulties, such as low analyte concentration and large solution volumes hamper the detection of Raman spectrum or require long acquisition time. One solution, suggested by scientists and dedicated for sample concentration, was to supplement plasmonic properties having particles with magnetic properties by preparing noble metal-coated or decorated nanocomposites [2-5]. The magnetic part of the composite allows concentrating material together with adsorbed analyte while plasmonic silver/gold part provides the SERS signal.

In this work 50 nm size magnetite nanoparticles were decorated with 13 nm size silver nanoparticles and their optical properties were investigated. It was noticed, that not only analyte's signal is enhanced in the presence of AgNP, but magnetite nanoparticles are affected as well. Usually, the heating of the sample is present during the illumination of the laser. The heating of magnetite results in the change of its crystallographic structure, which at certain temperatures changes to the hematite form. However, due to attached silver nanoparticles, magnetite was able to endure higher power of laser radiation. In addition to this, we estimated the SERS enhancement factors of hybrid nanoparticles for five laser excitations, with the highest found for 633 nm to be  $3.1 \times 10^7$ .



**Fig. 1.** TEM images of cubic magnetite covered with spherical silver nanoparticles.

## References

1. J. Langer, D.J. De Aberasturi, J. Aizpurua, R.A. Alvarez-Puebla, B. Augu  , J.J. Baumberg, G.C. Bazan, S.E.J. Bell, A. Boisen, A.G. Brolo, A.G.; et al., *ACS Nano*, 14 (2020) 28–117.
2. K.-H. Huynh, E. Hahm, M.S. Noh, J.-H. Lee, X.-H. Pham, S.H. Lee, J. Kim, W.-Y. Rho, H. Chang, D.M. Kim, et al., *Nanomaterials*, 11 (2021) 1215.
3. C. Wang, M.M. Meloni, X. Wu, M. Zhuo, T. He, J. Wang, C. Wang, P. Dong, *AIP Advances*, 9 (2019) 010701.
4. M. G  hlke, S. Selve, J. Kneipp, *J. Raman Spectrosc.*, 43 (2012) 1204–1207.
5. H. Lai, F. Xu, L. Wang, *J. Mater. Sci.*, 53 (2018) 8677–8698.



# Characterization of Functional Inorganic Materials by X-ray Diffraction Methods

**K. Baltakys, T. Dambrauskas**

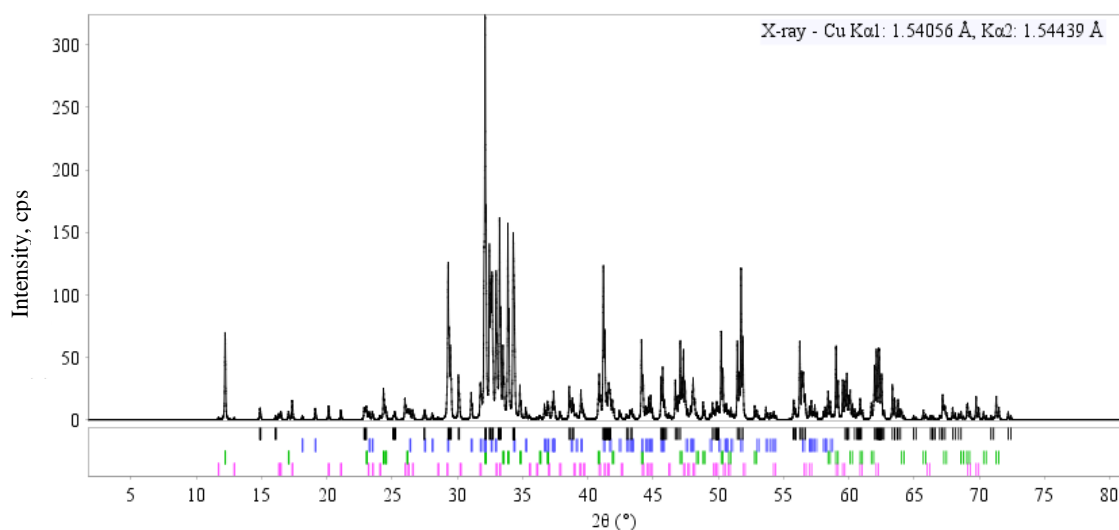
*Kaunas University of Technology, Radvilenu st. 19-236, LT-50524 Kaunas, Lithuania*

*\*Corresponding author, e-mail: kestutis.baltakys@ktu.lt*

Rapid advances in material science have been achieved thanks to a variety of new instrumental techniques for characterising the crystal structure of functional inorganic materials and the application of these techniques to quantitative analysis. Recently, the Rietveld method in quantitative phase analysis has been increasingly applied to the analysis of X-ray diffraction profiles of functional inorganic materials and their main constituents, calcium silicate hydrates and/or calcium silicates, etc. The Rietveld quantitative phase analysis is the only method that evaluates crystallographic changes in the components of the material under investigation [1, 2].

The essence of the Rietveld method is that a theoretical model of the crystal structure of the material is calculated using a theoretical diffraction pattern of the material and appropriate shape and background functions for the profile of the diffraction maxima [1, 2]. The intensity values of the calculated and experimental diffraction profiles of the test material at each point are compared with each other and the difference between them is minimised by the least squares method by varying various structural parameters in the initial model. The difference shall be close to zero and, for a fully refined material structure, the calculated diffraction profile shall be similar to that measured experimentally. It is worth highlighting, that Rietveld method is inherently a structure refinement method but not a structure solution method. Therefore, to perform accurate analysis, it is necessary to have an accurate initial structure model for each crystalline phase in the sample.

The quantitative analysis is a challenging process for all materials. For example, ordinary Portland cement (OPC) consists of four main phases, alite, belite, tricalcium aluminate, and brownmillerite (Fig. 1).



**Fig. 1.** X-ray diffraction analysis pattern of Portland cement clinker sample

During synthesis, foreign ions can intercalate into the structure of mentioned compounds, which complicates the analysis. Therefore, the quantitative Rietveld analysis with 3% error is considered accurate. Even more complex analysis is characterization of OPC hydration products.

## References

1. Scrivener K., Snellings R., Lothenbach B. (2016). A Practical Guide to Microstructural Analysis of Cementitious Materials: edited book. Boca Raton, FL: Taylor & Francis, 540 p.
2. Pecharsky, V.K., Zavalij, P.Y. (2005). Fundamentals of Powder Diffraction and Structural Characterization of Materials. New York: Springer Science+Business Media. 721 p.

# Cr<sup>3+</sup>-Activated Phosphors: Effective Luminescent Thermometers?

M. Back

Department of Molecular Sciences and Nanosystems, Ca' Foscari University of Venice, Via Torino 155, 30170, Venezia-Mestre, Italy  
e-mail: michele.back@unive.it

The development of contactless luminescent thermal sensors able to locally probe temperature is becoming very popular due to the interesting fields of application ranging from biology to catalysis, aerospace and microfluidic, to name a few [1].

Among the strategies proposed to probe the temperature, the use of the ratio between two luminescent signals coming from two thermally coupled excited states of a luminescent ion has been recognized as one of the most reliable techniques [1-3]. Despite the interesting results obtained with lanthanide ions, the ratio between the <sup>4</sup>T<sub>2</sub> and <sup>2</sup>E emissions of Cr<sup>3+</sup> ions can also be used as ratiometric thermometer [4-9]. To design a Cr<sup>3+</sup>-activated thermometer, the emission from both <sup>4</sup>T<sub>2</sub> and <sup>2</sup>E is necessary. This can be achieved by controlling the octahedral site of the host to fall in the so-called intermediate crystal field (CF) range in which the suitable <sup>4</sup>T<sub>2</sub>-<sup>2</sup>E energy gap ( $\Delta E$ ) play a critical role on the thermometric performances.

Here, as a case study, the mullite-type Bi<sub>2</sub>M<sub>4</sub>O<sub>9</sub>:Cr<sup>3+</sup> (M=Ga, Al) crystal system [4-6] is considered to discuss the potentials and the limits of the Cr<sup>3+</sup>-activated thermometers. The role of the CF and its effect on the electronic levels of Cr<sup>3+</sup> are spectroscopically investigated. The CF strength  $10Dq$  and the Racah parameters  $B$  and  $C$  are calculated and exploited in the framework of Tanabe-Sugano diagram. The electron-phonon interaction is discussed in terms of phonon energy and the potential of the systems as luminescent thermal sensors is assessed by analyzing the temperature dependence of the PL spectra. In the Bi<sub>2</sub>M<sub>4</sub>O<sub>9</sub>:Cr<sup>3+</sup> (M=Ga, Al) systems, the <sup>2</sup>E is split into two  $R$ -lines (called  $R_1$  and  $R_2$ ) allowing to simultaneously define two thermometric parameters (based on <sup>4</sup>T<sub>2</sub>-<sup>2</sup>E and  $R_1$ - $R_2$  couples) working into two different temperature ranges in the same compound. The thermometric performances of the systems are compared with the literature discussing parameters such as the relative sensitivity ( $S_r$ ), the temperature uncertainty ( $\delta T$ ) and the reproducibility ( $R$ ). For singly-activated ratiometric thermometers based on the Boltzmann distribution, the absolute sensitivity ( $S_a$ ) is also a good parameter, describing the extent of the change of the thermometric parameter with the temperature, very important from the application point of view. The effect of  $\Delta E$  variation on  $S_r$  and  $S_a$  is discussed. The absolute sensitivity of Boltzmann distribution-based systems is theoretically investigated demonstrating the potential of Cr<sup>3+</sup>-activated phosphors as luminescent thermometers. Finally, the flexibility of this class of thermometers will be discussed and an example of real application will be introduced, showing the possibility of this family of thermometers to locally probe the temperature of a metallic catalyst during the catalytic reaction of C<sub>2</sub>H<sub>4</sub> hydrogenation [8].

## References

1. C. D. S. Brites, S. Balabhadra, L. D. Carlos, *Adv. Optical Mater.*, **7** (2018) 1801239.
2. E. J. McLaurin, L. R. Bradshaw, D. R. Gamelin, *Chem. Mater.*, **25** (2013) 1283.
3. M. Suta, A. Meijerink, *Adv. Theory Simul.*, **3** (2020) 2000176.
4. M. Back, E. Trave, J. Ueda, S. Tanabe, *Chem. Mater.*, **28** (2016) 8347.
5. M. Back, J. Ueda, M. G. Brik, T. Lesniewski, M. Grinberg, S. Tanabe, *ACS Appl. Mater. Interfaces*, **10** (2018) 41512.
6. M. Back, J. Ueda, J. Xu, K. Asami, M. G. Brik, S. Tanabe, *Adv. Optical Mater.*, **8** (2020) 2000124.
7. M. Back, J. Ueda, M. G. Brik, S. Tanabe, *ACS Appl. Mater. Interfaces*, vol. **12** (2020) 38325.
8. M. Back, J. Ueda, H. Nambu, M. Fujita, A. Yamamoto, H. Yoshida, H. Tanaka, M. G. Brik, S. Tanabe, *Adv. Optical Mater.*, **9** (2021) 2100033.
9. J. Ueda, M. Back, M. G. Brik, Y. Zhuang, M. Grinberg, S. Tanabe, *Opt. Mater.*, **85** (2018) 510.

# Surface Plasmon Resonance Spectroscopy as a Key to the Development of Sensitive Biosensors

**A. Popov, V. Lisyte, A. Kausaite-Minkstimiene, A. Ramanaviciene**

*NanoTechnas – Center of Nanotechnology and Materials Science, Institute of Chemistry, Faculty of Chemistry and Geosciences, Vilnius University, Naugarduko str. 24, LT-03225 Vilnius, Lithuania;*

*\*Anton Popov, e-mail: anton.popov@chgf.vu.lt*

An immunosensor is a type of biosensor that is designed to monitor the interaction between an antibody or antigen and an analyte. The formation of immune complex on the surface of transducer generates a measurable signal in response to a change in analyte concentration [1]. The immunosensors can be used to detect various biomarkers whose concentration in body fluids is usually quite low. Therefore, it is important to apply sensitive method of detection. One of the most sensitive methods is surface plasmon resonance (SPR) spectroscopy [2].

The main advantage of SPR technique is the real-time monitoring of analyte without any labels. Moreover, the binding kinetics of molecules can be investigated while measuring a low concentration of the analyte from relatively small volume [3]. Detection is possible under complex matrix conditions in the presence of high level of foreign substances, which eliminates the complex and time-consuming procedure of sample preparation and concentration. SPR biosensing is suitable for multiple use in automatic mode and can be applied for rapid quantifying of multiplex analytes. Moreover, examples of wearable SPR sensors can be found in the literature [4].

According to sensing principle, the detection of low molecular weight biomarkers is complicated using SPR spectroscopy. The application of sandwich immunoassay format could be a solution to this issue. Moreover, the detection of small biomarkers at low concentration could be reached using various nanostructures [3, 5].

## Acknowledgments

This research was funded by a grant (No. S-MIP-22-46) from the Research Council of Lithuania.

## References

1. A. Ramanaviciene, A. Kausaite-Minkstimiene, A. Popov, B. Brasiunas, A. Ramanavicius, Ed. B. Ozkan, Bakirhan, Mollarasouli, Academic Press, 2022, p. 303.
2. J. Zhoua, Q. Qi, C. Wang, Y. Qian, G. Liu, Y. Wang, L. Fu, Biosens. Bioelectron., **142** (2019) 111449.
3. A. Kausaite-Minkstimiene, A. Popov, A. Ramanaviciene, ACS Appl. Mater. Interfaces, **14** (2022) 20720-20728.
4. J. Qu, A. Dillen, W. Saeys, J. Lammertyn, D. Spasic, Anal. Chim. Acta, **1104** (2020) 10-27.
5. F. Fathi, M. R. Rashidi, Y. Omid, Talanta, **192** (2019) 118-127.

# How to Use Ionic Liquids to Make Inorganic Nanomaterials

A.-V. Mudring\*


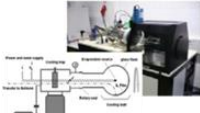
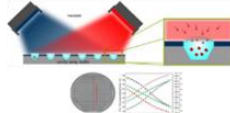
<sup>1</sup>Department of Chemistry and iNANO, Aarhus University, Langelandsgade 140, 8000 Aarhus C, Denmark

\*A.-V. Mudring, e-mail: anja-verena.mudring@chem.au.dk

Nanomaterials have become indispensable for modern life. Many technologies depend critically on nanomaterials with engineered properties and structures, particularly those related to clean energy applications such as photocatalysts, light phosphors, thermoelectrics and others. Technological borders could be pushed further and improved materials would become available if more powerful tools for the tailored synthesis of nanomaterials could become available. In this, ionic liquids (ILs, room temperature molten salts) have the potential to become a true game changer. These unconventional solvents are permitting more efficient, safer and environmentally benign preparation of high quality products.

ILs, which can be built by a wide variety of cation-anion combinations with different functionalities, can act as the reaction medium, particle stabilizing and templating agent all-in-one, sometimes even as the reaction partner. IL based nanomaterial synthesis is faster, safer, and more energy- and atom-efficient than comparable methods. It uses less toxic chemicals, omits the use of auxiliary substances such as stabilizers, and minimizes waste. Through coupling with unconventional synthetic routes (physical vapor deposition, microwaves, ultrasound) that take advantage of their unique properties, ILs become even more powerful in nanomaterials synthesis (Fig. 1).

Because of their high modularity, ILs can be tailored for a specific synthesis through chemical structure variations unlike any conventional solvents. Unique to ILs is their truly multifunctional character, which allows them to serve more than just as the solvent and reaction medium. With ILs properties and property combinations can be achieved that are unattainable from conventional solvents. This also allows to use unconventional synthetic methods and develop new techniques. It is expected that the presented, universal methods for the production of nanomaterials from ILs, will allow for the manufacturing of improved products and devices and open up new horizons for nanosynthesis. The methods are generally, faster, safer, more energy- and atom (material)-efficient, use less and less toxic chemicals, negate the use of auxiliary substances (such as surfactants and stabilisers), reduce the risk of pollution, reduce and prevent waste, thus, reduce the risk to human health and minimise the impact on the environment, yet are economically viable. In addition, these unconventional production methods allow us to develop new and improved nanomaterials, pertinent for a wide number of applications such as catalysis and wastewater treatment, solar cells and solid-state lighting as well as biomedicine.

Conversion Method	Bottom-up Chemical		Top-down Physical	
	Microwave	Ultrasound	PVD	Sputtering
<b>Technology Enabler</b>	 High dielectric susceptibility of ILs	 viscosity and thermal conductivity of ILs	 low vapor pressure of ILs which allows for working under vacuum	
<b>Added Value</b>	efficient heating, fast, high nucleation rates, small particles, kinetic reaction products become available	low overall temperature, high energy efficiency	high mass/atom efficiency, no byproducts, less waste	product formation not restricted by thermodynamic stability
<b>Materials Classes</b>	<b>Metals &amp; alloys</b>		<b>Semiconductors</b>	<b>Ceramics</b>
<b>Applications</b>	Catalysts High density magnetic storage Hydrogen storage Memory materials / Superalloys ...		Phosphors Medical Imaging Labelling and Tracing Thermoelectrics ...	(Photo-)Catalysts Fuel Cells Coatings Phosphors (CFLs, LEDs) ...

**Fig. 1.** Bottom-up vs. top-down methods for the synthesis of nanomaterials from ionic liquids.

## References

- O. Hammond, A.-V. Mudring, Chem. Commun. **58** (2022) 3865-3892 and references therein.

# Graphene-Based Materials: Synthesis, Chemistry and Applications

J. Barkauskas\*, J. Gaidukevič

Vilnius University, Institute of Chemistry, Naugarduko 24, LT-03225, Vilnius, Lithuania

\*Corresponding author, e-mail: jurgis.barkauskas@chf.vu.lt

Graphene-based materials (GBM) comprise an important class of materials including graphene itself, graphene oxide (GO), reduced graphene oxide (rGO), exfoliated graphene flakes, graphene nanoplatelets, as well as chemically functionalized versions of all these. GBM attracts the attention of many researchers due to their exceptional properties (high electric and thermal conductivity, mechanical strength and flexibility, chemical stability, biocompatibility), and thereof emerging fields of application (electronics, energy conversion and storage, light processing, biomedicine, environmental cleaning, composite production, etc.).

In this research, the expertise of the Laboratory of Carbonaceous Materials in synthesis, investigation and application of different GBM is presented. rGO is among the most often used GBM for application. Using thermal shock equipment, rGO fractions were produced from GO, and applied as electrode materials for amperometric glucose biosensors with direct electron transfer capacity [1]. Hybrid single-walled carbon nanotube and GO coatings also demonstrate the same effect of direct electron transfer [2]. The C<sub>3</sub>O<sub>2</sub> additive used during the process of thermal reduction of GO improves the electrical conductivity of the product. The rGO obtained this way was used as effective component in dopamine biosensor [3]. Based on the fact that GO is especially hydrophilic material, GO synthesized by modified Hummer's method was applied for surface acoustic wave humidity sensors [4]. The GO nanocomposites with organic dye molecules are suitable to prepare coatings, which can be further used for laser scribing and biosensor application [5]. Another promising application for GO coatings is their antimicrobial properties. We used direct oxidation of graphene layer coated on the polypropylene surface [6]. Functionalized rGO tailored with appropriate functional groups was used as efficient catalyst in transesterification reaction [7]. Another preparation protocol was based on the reduction of graphite oxide in the melt of boric acid to produce reduced graphene oxide with the structure favorable to fast ion transport in the bulk of carbon network. This sort of rGO was applied as electrodes in supercapacitor [8]. GO nanocomposite with inorganic polymer – parathiocyanogen – was used as prospective electrode (cathode) material in fuel cells. It works as metal-free catalyst, and thus makes it possible to dispense with the use of expensive platinum [9]. We also performed detailed studies of the mechanism and kinetics of thermal decomposition of GO. This study revealed the ways which may be used to produce rGO with controllable properties [10]. Low-defective graphene may be produced by using GIC. In our study we used the GIC with sulfuric acid for this purpose [11]. In each case, the relationship between the structure of GBM and its properties is discussed in detail.

## References

1. I. Šakinytė, J. Barkauskas, J. Gaidukevič, J. Razumienė. *Talanta*, **144** (2015) 1096–1103.
2. A. Ramanavicius, I. Morkvenaite-Vilkonciene, U. Samukaite-Bubnieneabe, J.J. Petroniene, J. Barkauskas, P. Genys, V. Ratautaite, R. Viterg, I. Iatsunskyi, A. Ramanaviciene. *Colloid. and Surf. A*, **624** (2021) 126822.
3. J. Gaidukevic, R. Aukstakojyte, J. Barkauskas, G. Niaura, T. Murauskas, R. Pauliukaite. *Appl. Surf. Sci.*, **592** (2022) 153257.
4. R. Rimeika, J. Barkauskas, D. Čiplys. *Appl. Phys. Lett.*, **99** (2011) 051915.
5. R. Trusovas, K. Ratautas, G. Račiukaitis, J. Barkauskas, I. Stankevičienė, G. Niaura, R. Mažeikienė. *Carbon*, **52** (2013) 574-582.
6. J. Barkauskas. *Eur. Pat. EP 2 832 802 B1*. 11.05.2016. *Bulletin* 2016/19.
7. J. Gaidukevič, J. Barkauskas, A. Malaika, V. Jasulaitienė, M. Kozłowski. *Appl. Surf. Sci.*, **554** (2021) 149588.
8. J. Gaidukevič, R. Pauliukaitė, G. Niaura, I. Matulaitienė, O. Opuchovič, A. Radzevič, G. Astromskas, V. Bukauskas, J. Barkauskas. *Nanomaterials*, **8** (2018) 889.
9. J. Gaidukevič, J. Razumienė, I. Šakinytė, S. L. H. Rebelo, J. Barkauskas. *Carbon*, **118** (2017) 156–167.
10. J. Barkauskas, J. Gaidukevič, G. Niaura. *Carbon Lett.*, **31** (2021) 1097-1110.
11. G. Rimkute, M. Gudaitis, J. Barkauskas, A. Zarkov, G. Niaura, J. Gaidukevic. *Crystals*, **12** (2022) 421.

# Antimony Chalcogenide Thin Film Solar Cells - Challenges and Prospects

**M. Krunks**

*Tallinn University of Technology, Ehitajate tee 5, 19086 Tallinn, Estonia  
e-mail:malle.krunks@taltech.ee*

Photovoltaic (PV) solar energy conversion is one of the leading green technologies towards pollution-free production of electricity. For new PV technologies is not sufficient to be only competitive with the Si and CdTe technologies in efficiency and reliability but one should also rely on environmentally friendly and stable materials and green processing technologies. An emerging class of highly promising PV materials currently under widespread investigation in the PV community are the inorganic antimony chalcogenide compounds. Despite of their recent addition to the PV thin film family, efficiency values of these devices have climbed rapidly and are now approaching 10%.

This talk will discuss the latest achievements in antimony chalcogenide thin film solar cell technology with the main emphasis on  $\text{Sb}_2\text{S}_3$  and  $\text{Sb}_2\text{Se}_3$  compounds produced by cost efficient technologies of ultrasonic spray pyrolysis and closed space sublimation. The presentation will review key processing strategies to optimize absorber material properties as well as the selection of electron transport layers (ETL) and hole transport materials (HTM) in solar cell structure glass/TCO/ETL/ $\text{Sb}_2\text{S}_3$ ; ( $\text{Sb}_2\text{Se}_3$ )/HTM/Au. Based on the state-of-the art progress in performance, a roadmap of applications including semitransparent and tandem PV devices for building integrated PV, product integrated PV and IoT markets will be presented.

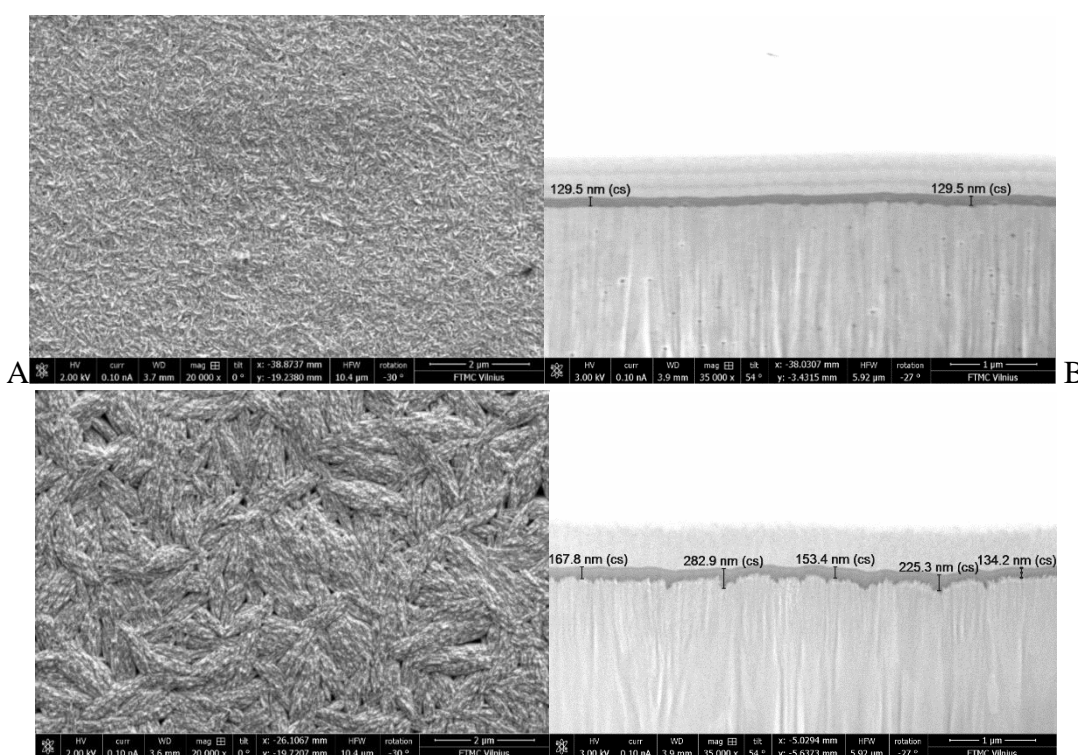
# Corrosion Behaviour of Cerium Based Conversion Coatings on Zinc

A. Kirdeikienė, L. Gudavičiūtė, J. Pilipavičius, R. Juškėnas, A. Selskis, R. Ramanauskas\*

Center for Physical Science and Technology, Saulėtekio al. 3, LT-10257 Vilnius, Lithuania

\*Corresponding author, e-mail: rimantas.ramanauskas@ftmc.lt

Ce based coatings can be considered as environmentally friendly alternative to chromium conversion coatings to protect Zn against corrosion. These coatings can be produced by chemical treatment of metal surface in a  $\text{Ce}(\text{NO}_3)_3$  solution and usually present a mixture of Ce (III) and Ce (IV) oxides and hydroxides. The disadvantage associated with oxide film deposition process is a crack formation through the deposited layer due to gas evolution caused by decomposition of electrolytes. Therefore, Ce based coatings did not show always a sufficient corrosion resistance. The aim of this investigation was to study the influence of the base metal Zn structural parameters on the protective and self-healing abilities of Ce based conversion coatings formed on Zn surface. Different surface analytic techniques, including SEM, XRD, XPS together with electrochemical measurements (EIS) were applied in order to obtain complementary information of this coating system.



**Fig. 1.** SEM images of the initial Zn surface topography (left side) and cross-sections of Ce based coatings on Zn (right side), produced by direct current (A) and pulse (B) electrolysis.

Non-stationary (pulse) electrodeposition was applied for modification of Zn structural parameters, what resulted in formation of the Zn coating with the large crystallite aggregates (SEM data) and, at the same time, in two-fold reduction of the grain size and consequently increase in the number of lattice imperfection (XRD data) in comparison with a direct current (DC) plated sample. The mentioned structural differences affected significantly the process of Ce conversion film formation. It was established that Zn topography peculiarities ( $\mu\text{m}$  level) and the grain size (nm level) variations affect the rate of the film formation, its composition (XPS data), thickness and compactness. Ce conversion coatings deposited on the pulse plated Zn layer exhibited higher corrosion resistance (one order lower  $i_{\text{corr}}$  values) and, at the same time, higher self-healing ability in respect to DC plated sample. Lower Ce based coating porosity (higher compactness) and the higher amount of Ce (IV) oxide (XPS data) in the film, were the main reasons of the higher corrosion resistance of Ce coatings deposited on the pulse plated Zn.

# Bioactive Glasses with Luminescent Properties

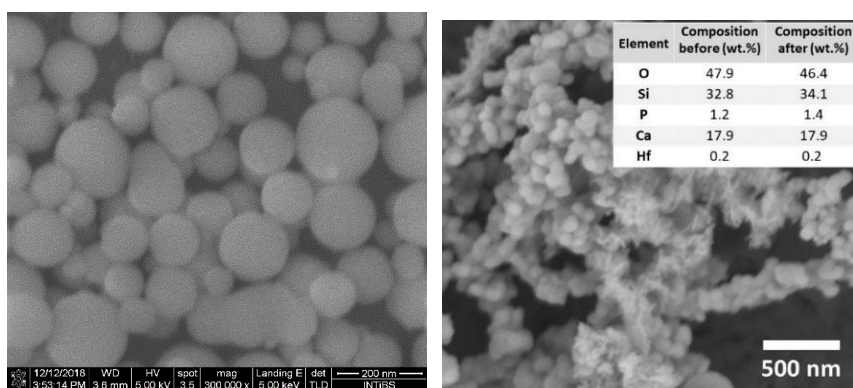
A. Lukowiak<sup>1,\*</sup>, K. Halubek-Gluchowska<sup>1</sup>, B. Borak<sup>2</sup>, D. Szymański<sup>1</sup>, Y. Gerasymchuk<sup>1</sup>

<sup>1</sup> Institute of Low Temperature and Structure Research, Polish Academy of Sciences, Wrocław Poland

<sup>2</sup> Department of Mechanics, Materials and Biomedical Engineering, Wrocław University of Science and Technology, Wrocław, Poland

\*Corresponding author, e-mail: A.Lukowiak@intibs.pl

Various types of nanomaterials play currently important roles in different fields of medicine. For example, silica–calcia system is a well-known basic composition of bioactive glasses used in regenerative medicine. Glass nanostructures might show higher activity and broader range of applications in comparison to their well-known microsized counterparts. We present studies on nanoparticles (average diameter <100 nm) of bioactive glass showing photoluminescence due to a modified composition of silica–calcia system. The sol–gel route was used to fabricate the particles. To ensure photoactivity, the composition of glass was modified by the addition of lanthanide ions or phthalocyanine complexes with metals. The optical properties (absorption and photoluminescence spectra) of the samples as well as their structural and morphological properties were examined. The results showed that glasses were active in different spectral ranges of the electromagnetic spectrum depending on the activators. Photoactivity was observed as luminescence, singlet oxygen generation or photocatalytic dyes degradation. The bioactivity tests indicated that when particles were immersed in the simulated body fluid, ions were released into the medium, and hydroxyapatite formed on the glass surface. Described systems could be used, for example, for monitoring structural changes of the glass immersed in biological fluids, bioimaging, photodynamic therapy, or photocatalysis.



**Fig. 1.** SEM images of SiO<sub>2</sub>–CaO–P<sub>2</sub>O<sub>5</sub> glasses activated with Eu<sup>3+</sup> (left) or PcHfCl<sub>2</sub> (right). Inset shows initial and final (based on EDX analysis) glass composition. Right panel from [3] (published with CC BY license).

## Acknowledgment

The research was supported by the National Science Centre (Poland) grant No. 2016/22/E/ST5/00530.

## References

1. N. A. Spaldin, R. Ramesh, *Nature Mater.*, **18** (2019) 203.
2. S. Shevlin, *Nature Mater.*, **18** (2019) 191.
3. Y. Gerasymchuk, A. Wedzynska, A. Lukowiak, *Nanomaterials*, **12** (2022) 1719, <https://doi.org/10.3390/nano12101719>.



# Nanomaterials and their Structures for Optical Applications

**T. Tamulevičius<sup>1,2,3\*</sup>, J. Mykolaitis<sup>2</sup>, M. A. Baba<sup>1</sup>, N. Khinevich<sup>1</sup>, A. Tamulevičienė<sup>1,2,3</sup>, M. Juodėnas<sup>1</sup>, D. Peckus<sup>1</sup>, R. Mardosaitė<sup>1,2</sup>, S. Račkauskas<sup>1,2</sup>, S. Tamulevičius<sup>1,2</sup>**

<sup>1</sup>*Institute of Materials Science of Kaunas University of Technology, K. Baršausko St. 59, LT-51423, Kaunas, Lithuania*

<sup>2</sup>*Department of Physics of Kaunas University of Technology, Studentų St. 50, LT-51368, Kaunas, Lithuania*

<sup>3</sup>*UAB “Nanoversa”, K. Baršausko St. 59, LT-51423, Kaunas, Lithuania*

*\*Corresponding author, e-mail: tomas.tamulevicius@ktu.lt*

Silver, gold, and copper nanoparticles are an excellent platform for the manifold of applications not limited to sensing, biomedicine, and nanophotonics [1]. These metal nanostructures demonstrate the remarkable size and shape-determined optical properties related to localized surface plasmon resonance (LSPR) which appears as strong light scattering and/or absorption bands. Dense random ensembles of Ag and Au nanoparticles increase the light fields and are beneficial for surface-enhanced Raman spectroscopy (SERS). Light scattered by the subwavelength period regular arrays of nanoparticles on the surfaces can interact resonantly narrowing down the LSPR peaks into high-quality factor surface lattice resonances (SLR). Such structures are called metasurfaces and find numerous applications in optics and nanophotonics [2]. Different nanomaterial synthesis approaches are developed enabling control of the size, shape, structure, and surface quality of the nanomaterials [3,4].

In this work, silver, gold, and copper nanoparticle colloids were synthesized employing chemical or photophysical synthesis methods seeking applications in metasurface-based SERS substrates, lateral flow assays, and of antiviral surfaces.

Nanoparticle colloids were chemically synthesized using the seed growth method or femtosecond laser ablated from pure metal targets employing Yb:KGW femtosecond laser Pharos (Light Conversion). The nanoparticle sizes were inspected with the field emission scanning electron microscope and transmission electron microscopes (FEI). Monodisperse nanoparticles were deposited into polymer replica templates using the capillarity-assisted particle assembly (CAPA) method. The optical density of the colloids and nanoparticle arrays were evaluated with the steady state (Avantes) and transient absorption (Light Conversion) spectrometers. Field enhancement of nanoparticle assemblies was investigated by a Raman spectrometer (Renishaw).

Strongly absorbing silver, gold, and copper colloids of yellow, dark green, and pink color were synthesized.

Multi-wavelength Raman measurements of SERS substrates with 532 nm matched SLR peak indicated strong signal enhancement for detection of the 2NT analyte molecule. In cooperation with UAB “Imunodiagnostika” the antibody functionalized gold nanoparticles were successfully used to detect SARS-CoV-2 nucleoprotein in lateral flow assay tests. Aerograph spray deposited copper nanoparticles on glass substrates demonstrated antiviral efficacy against BHV-1 and IBV.

## Acknowledgments

This work was supported by the Agency for Science, Innovation and Technology, Grant No. Biotech-02-014 and the European Regional Development Fund, Grant No. 13.1.1-LMT-K-718-05-0018.

## References

1. K. M. Mayer et al. *Chem. Rev.* **111** (2011) 3828–3857.
2. D. Peckus et al. *Optics Express* **30** (2022) 27730–27745.
3. M. Juodėnas et al. *ACS Nano* **13** (2019) 9038–9047.
4. V. G. Kravets et al. *Chem. Rev.* **118** (2018) 5912–5951.

# Small Cause — Great Effect: What the $4f^{n+1}5d^0 \rightarrow 4f^n5d^1$ Configuration Crossover Does to the Chemistry of Divalent Rare-Earth Halides and Coordination Compounds, and How it Makes the Formation of Cluster Complex Compounds and Polar Intermetallics Possible

Gerd H. Meyer<sup>1,\*</sup>

<sup>1</sup>Department of Chemistry, University of Cologne, Greinstraße 6, D-50939 Köln, Germany

The rare-earth elements in the divalent state, i.e. with oxidation number +2, may either have the electron configuration  $4f^{n+1}5d^0$  (symbolized as  $R^{2+}$ ) or  $4f^n5d^1$  ( $R^{3+e^-}$ ). As  $R^{2+}$  ( $R = \text{Eu}, \text{Yb}, \text{Sm}, \text{Tm}, \text{Dy}, \text{Nd}$ ) they can either be contained in extended solids as in the insulating diiodides  $RI_2$ , or in coordination complexes such as samarocene, Kagan's reagent, or  $\text{TmI}_2(\text{DME})_3$ , Fig. 1. In the case of  $R^{3+e^-}$ , the "excess" d electron can either be delocalized and cause (semi)metallic behavior in extended solids, e.g. in  $\text{LaI}_2$ , or localized with the  $R^{3+e^-} = 4f^n5d^1$  ion trapped in a coordination complex with (super)bulky ligands such as in  $[\text{K}(2.2.2\text{-crypt})][[\text{LaCp}''_3]]$ . Thus, the seemingly small cause of a one-electron configuration crossover,  $4f^{n+1}5d^0 \leftrightarrow 4f^n5d^1$  has a large effect on the chemical behavior and physical properties of the respective compounds where atomic properties and ligand effects play important roles [1].

Sc										
Y										
La	Ce	Pr	Nd	Pm	Sm	Eu	Gd			
	Tb	Dy	Ho	Er	Tm	Yb	Lu			

Sc										
Y										
La	Ce	Pr	Nd	Pm	Sm	Eu	Gd			
	Tb	Dy	Ho	Er	Tm	Yb	Lu			

**Fig. 1.** Rare-earth elements  $R$  exhibiting the oxidation state +2 under ambient conditions as diiodides,  $RI_2$ , (left) and in coordination compounds (right) with their respective electron configurations: Highlighted in blue:  $4f^{n+1}5d^0$ , and in red:  $4f^n5d^1$ .

In the solid state, dihalides with  $R$  in the  $4f^n5d^1$  configuration (including  $R = \text{Y}, \text{Tb}, \text{Ho}, \text{Er}, \text{Lu}$ ) compete with cluster complex halides,  $\{Z_rR_r\}X_x$ , or polar intermetallics,  $\{Z_rR_r\}$ . In both cases,  $Z$  atoms center an  $R_r$  cluster. The endohedral atom  $Z$ , either non- or semi-metal ( $Z = E$ ) or (transition) metal atom ( $Z = T$ ) is mandatory for heteroatom  $Z-R$  bonding. So far,  $\{Z_rR_r\}X_x$  type compounds are known with  $r$ , i.e. the coordination number (CN) of the endohedral atom, ranging from 3 to 8. Smaller atoms like  $E = \text{B}, \text{C}, \text{N}, \text{O}$  afford smaller CN's (3–6), while larger atoms like  $T = \text{Os}$  (and many other transition metal atoms) demand CNs of 6 to 8 [2, 3].

Bonding in these cluster complex halides  $\{Z_rR_r\}X_x$  is predominantly a symbiosis of polar, heteroatomic  $Z-R$  (intermetallic-like, multi-center covalent) and  $R-X$  (salt-like, ionic) character. Increasing cluster condensation pushes isolated clusters into oligomers, chains, double chains, then layers and, finally, three-dimensional structures. Ultimate cluster condensation, at which end all the halide ligands are eliminated, constitutes polar intermetallics.

When the electronegativity of the halide increases, there is an increasing competition of cluster complex halide *versus* intermetallic and salt. For example, when  $\{\text{PtPr}_3\}\text{Cl}_3$  was targeted, the intermetallic  $\{\text{Pt}_3\text{Pr}_4\}$  as well as remaining  $\text{PrCl}_3$  was obtained, the latter apparently working as a flux for crystal growth. Although the system  $\text{Pt}/\text{Pr}$  seems to have been investigated thoroughly, the new  $\text{Pt}_3\text{Pr}_4$  does not exist in the phase diagram [4]. Other fluxes, such as sodium chloride instead of  $\text{PrCl}_3$  or tin melts, resulted in the formation of what might be considered as a new modification of  $\text{Pt}_2\text{Pr}_3$  and a number of ternary  $\text{Pt}/\text{Sn}/\text{Pr}$  intermetallics [5].

## References

1. G. Meyer, *J. Solid State Chem.* **270** (2019) 324-334.
2. G. Meyer, in *The rare earth elements: fundamentals and applications*; Ed. D. A. Atwood, John Wiley and Sons, Inc., pp 161-173, 2012.
3. G. Meyer, in *Handbook on the Physics and Chemistry of Rare Earths*; Ed. J.-C. Bünzli, V. K. Pecharsky, vol. 45, 111-178, Elsevier 2014.
4. M. L. Rhodehouse, T. Bell, V. Smetana, A.-V. Mudring, G. H. Meyer, *Inorg. Chem.* **57** (2018) 9949-9961.
5. M. L. Rhodehouse, V. Smetana, C. Celandia, A.-V. Mudring, G. H. Meyer, *Inorg. Chem.* **59** (2020) 7352-7359.

# From Fundamental Understanding to Applications in Energy Storage of Phosphate Framework Materials

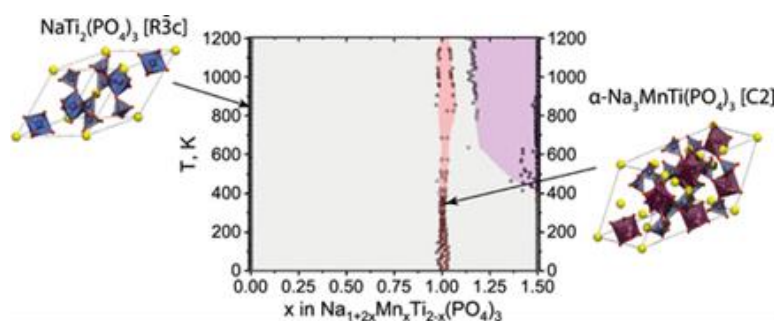
Linās Vilčiauskas\*

<sup>1</sup>Center for Physical Sciences and Technology (FTMC), Saulėtekio al. 3, LT-10257 Vilnius, Lithuania

<sup>2</sup>Institute of Chemistry, Vilnius University, Saulėtekio al. 3, LT-10257 Vilnius, Lithuania

\*Corresponding author, e-mail: linas.vilciauskas@ftmc.lt

Na-ion batteries are deemed to be promising candidates for the future sustainable stationary energy storage systems. However, there is still a number of issues to be solved before their full potential could be utilized. In addition to finding suitable electrode materials there are also issues related to the stability of the aqueous electrolyte/electrode interface. Some of our recent contributions in terms of understanding and enabling of phosphate framework materials for the use in aqueous Na-ion batteries will be reviewed. The thermodynamic limitations in terms of phase formation, electrochemical stability issues and the origin of these effects in NASICON-structured  $\text{Na}_{1+2x}\text{MnTi}_{2-x}(\text{PO}_4)_3$  ( $0.0 < x < 1.5$ ) and  $\text{Na}_{3-x}\text{V}_{2-x}\text{Ti}_x(\text{PO}_4)_3$  ( $0.0 < x < 1.0$ ) and several other phosphates systems as potential cathode materials for aqueous Na-ion batteries will be covered and discussed in detail [1-4].



**Fig. 1.** Temperature-composition phase diagram of  $\text{Na}_{1+2x}\text{MnTi}_{2-x}(\text{PO}_4)_3$  ( $0.0 < x < 1.5$ ) calculated by the first principles calculations [2].

## References

1. G. Plečkaitytė, M. Petrulevičienė, L. Staišiūnas, D. Tediashvili, J. Pilipavičius, J. Juodkazytė, L. Vilčiauskas, *J. Mater. Chem. A*, **9**, (2021) 12670-12683.
2. G. Snarskis, J. Pilipavičius, D. Gryaznov, L. Mikoliūnaitė, L. Vilčiauskas, *Chem. Mater.*, **33**, (2021) 8394-8403.
3. D. Tediashvili, G. Gečė, J. Pilipavičius, S. Daugėla, T. Šalkus, J. Juodkazytė, L. Vilčiauskas, *Electrochim. Acta*, **417**, (2022) 140294.
4. M. Petrulevičienė, J. Pilipavičius, J. Juodkazytė, D. Gryaznov, L. Vilčiauskas, *Electrochim. Acta*, **424**, (2022) 140580.



**SHORT PRESENTATION LECTURE ABSTRACTS**

# Novel Whitlockite Compounds: Structure and Properties

**A. Kizalaite, D. Griesiute, A. Zarkov**

*Institute of Chemistry, Vilnius University, Naugarduko g. 24, LT-03225, Vilnius, Lithuania  
agne.kizalaite@chgf.vu.lt*

One of the major minerals in human body is magnesium whitlockite ( $\text{Ca}_{18}\text{Mg}_2\text{H}_2(\text{PO}_4)_{14}$ ). This compound constitutes to approximately 20-35 wt% of human bone tissue and plays an important role in various bone formation processes [1]. Magnesium whitlockite is known for its excellent osteogenic capability as well as having an active role in natural bone healing processes, therefore it is a promising candidate for application in bone regenerative medicine and tissue engineering [2]. In recent years this compound has attracted a lot of attention and the scientific community is looking for methods to improve its' biological properties. One of the potential ways to achieve this goal is to introduce other bioactive ions instead of magnesium into the structure of the material.

In the present work, we present a simple way to reliably synthesize pure-phase whitlockite compounds substituted with different metal ions. Pure-phase whitlockite compounds containing Zn, Cu and Mn ions were successfully synthesized by dissolution-precipitation process. The effect of various synthesis conditions on particle size and morphology was investigated.

Synthesized compounds were analyzed by X-ray diffraction (XRD), Fourier-transform infrared spectroscopy (FTIR), scanning electron microscopy (SEM) and Raman spectroscopy. Rietveld analysis was employed to calculate the structural parameters of the materials.

## **Acknowledgments**

This research was funded by a grant WHITCERAM (No. S-LJB-22-1) from the Research Council of Lithuania.

## **References**

1. H. Cheng et al. *Acta Biomater.* 69 (2018), 342-351.
2. H. L. Jang et al. *Adv. Healthc. Mater.* 5 (2015), 128-136.

# Investigation of Various Types of Ferrites and Manganites Prepared via Sol-Gel Synthetic Approach

D. Karoblis<sup>1,\*</sup>, A. Žarkov<sup>1</sup>, R. Diliautas<sup>1</sup>, K. Mažeika<sup>2</sup>, D. Baltrūnas<sup>2</sup>, G. Niaura<sup>3</sup>, M. Talaikis<sup>4</sup>, E. Garškaitė<sup>5</sup>, A. Beganskienė<sup>1</sup>, A. Kareiva<sup>1</sup>

<sup>1</sup>*Institute of Chemistry, Vilnius University, Naugarduko 24, 03225, Vilnius, Lithuania*

<sup>2</sup>*Center of Physical Sciences and Technology, Sauletekio Ave. 3, 10257, Vilnius, Lithuania*

<sup>3</sup>*Institute of Chemical Physics, Faculty of Physics, Vilnius University, Sauletekio Ave. 3, 10257, Vilnius, Lithuania*

<sup>4</sup>*Department of Bioelectrochemistry and Biospectroscopy, Sauletekio Ave. 7, 10257, Vilnius, Lithuania*

<sup>5</sup>*Wood Science and Engineering, Department of Engineering Sciences and Mathematics, Luleå University of Technology, Forskargatan 1, 931 87, Skellefteå, Sweden*

\*Corresponding author, e-mail: Dovydas.karoblis@chgf.vu.lt

Multiferroics are described as materials with the presence of two or more ferroic orders (such as magnetic, electric or elastic). While both piezoelectrics (where ferroelectricity occurs with ferroelasticity) and piezomagnetism (where ferromagnetism and ferroelasticity coexists) are investigated, the main research focus is on magnetoelectric multiferroics [1]. Out of all multiferroics, the bismuth ferrite ( $\text{BiFeO}_3$ ) is considered to be the most prominent one [2]. It displays antiferromagnetic and ferroelectric properties with a strong remnant polarization of  $\sim 100 \mu\text{C}/\text{cm}^2$  at room temperature [3]. Moreover, bismuth manganite ( $\text{BiMnO}_3$ ), yttrium ferrite ( $\text{YFeO}_3$ ), yttrium manganite ( $\text{YMnO}_3$ ), gadolinium ferrite ( $\text{GdFeO}_3$ ) and gadolinium manganite ( $\text{GdMnO}_3$ ) have also demonstrated multiferroic properties.

One of the ways to tune the physical properties of the materials is by preparing solid solutions. For this reason few different composition  $\text{Y}_{1-x}\text{Gd}_x\text{FeO}_3$  [4],  $\text{Y}_x\text{Gd}_{1-x}\text{Mn}_{0.97}\text{Fe}_{0.03}\text{O}_3$  [5] and  $\text{Bi}_{1-x}\text{Gd}_x\text{Fe}_{0.85}\text{Mn}_{0.15}\text{O}_3$  solid solutions series were prepared by sol-gel synthesis technique using ethylene glycol and citric acid as complexing agents. For the obtained samples structural, morphological and magnetic properties were investigated with different characterization techniques. It was observed that by varying  $\text{Gd}^{3+}$  content for  $\text{Y}_{1-x}\text{Gd}_x\text{FeO}_3$  samples, the magnetization changed from hysteresis characteristic of  $\text{YFeO}_3$ , to almost linear dependence of magnetization of  $\text{GdFeO}_3$ . With the increasing amount of the  $\text{Gd}^{3+}$  the crystal structure of  $\text{Y}_{1-x}\text{Gd}_x\text{Mn}_{0.97}\text{Fe}_{0.03}\text{O}_3$  gradually transformed from hexagonal to orthorhombic one. While most samples were monophasic, the sample containing 60 mol% of yttrium was mixture between hexagonal and orthorhombic structures. After annealing  $\text{Bi}_{1-x}\text{Gd}_x\text{Fe}_{0.85}\text{Mn}_{0.15}\text{O}_3$  compounds at 500 °C temperature, it was seen that only 10 mol% of  $\text{Gd}^{3+}$  ions can be introduced into the  $\text{BiFe}_{0.85}\text{Mn}_{0.15}\text{O}_3$  structure. Heat treatment at higher temperatures (650 and 800 °C) led to formation of solid solutions in the whole compositional range.

## References

1. C. Lu, M. Wu, L. Lin, J. M. Liu, *Natl. Sci. Rev.* **6** (2019), 653-668.
2. N. Wang, X. Luo, L. Han, Z. Zhang, R. Zhang, H. Olin, Y. Yang, *Nanomicro Lett.* **12**(1) (2020), 1-23.
3. B. Jana, K. Ghosh, K. Rudrapal, P. Gaur, P. K. Shihabudeen, A. Roy Chaudhuri, *Front. Phys.* (2022), 810.
4. D. Karoblis, A. Zarkov, E. Garskaite, K. Mazeika, D. Baltrunas, G. Niaura, A. Beganskiene, A. Kareiva, *Sci. Rep.*, **11**(1) (2021), 1-14.
5. D. Karoblis, A. Zarkov, K. Mazeika, D. Baltrunas, G. Niaura, A. Beganskiene, A. Kareiva, *Solid State Sci.* **118** (2021), 106632.

# Investigation of Phase Transformations in the Low Temperature Synthesis of Magnesium Whitlockite

A. Afonina\*, I. Grigoraviciute, A. Kareiva

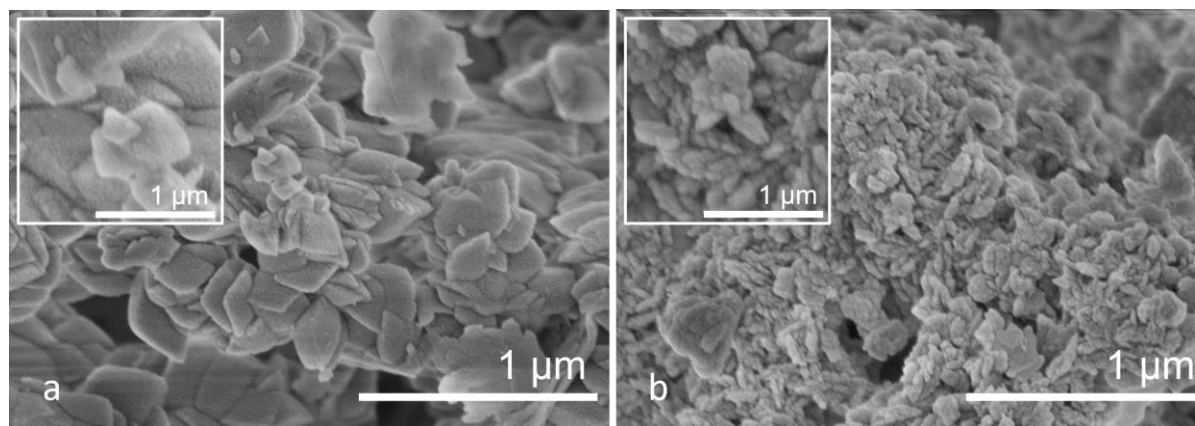
Faculty of Chemistry and Geosciences, Institute of Chemistry, Vilnius University,  
Naugarduko 24, LT-03225 Vilnius, Lithuania.

\*E-mail: anastasija.afonina@stud.chgf.vu.lt

Bone tissue maintains its healthy condition by constantly regenerating the affected areas, but in case of more serious lesions or traumas, the human body needs help – implantology or transplantology. The inorganic part of the bone tissue consists mainly of calcium based phosphates: carbonated B type hydroxyapatite ( $\text{CO}_3\text{-Ap}$ ,  $\text{Ca}_{10-x}(\text{PO}_4)_{6-x}(\text{CO}_3)_x(\text{OH})_{2-x}$  ( $0 \leq x \leq 2$ )) and magnesium whitlockite (WH,  $\text{Ca}_{18}\text{Mg}_2(\text{HPO}_4)_2(\text{PO}_4)_{12}$ ) [1-3]. Thus, calcium phosphates are substances that are excellent for use as alloplasts. HAp ( $\text{Ca}_{10}(\text{PO}_4)_6(\text{OH})_2$ ) is the most commonly used ceramic in this area, but some recent studies showed, that WH can deal with this task even better [4].

In this work we prepared nanopowders of WH from gypsum. A dissolution-precipitation synthesis of WH samples was performed at  $80^\circ\text{C}$  in the presence of  $\text{Mg}^{2+}$  ions. We studied the stages of formation of WH in time under different synthesis conditions: the processing was made in an oven (static condition) and in a shaker (rotating condition).

WH samples were successfully synthesized, regardless of the type of synthesis conditions used. We found some differences in the obtained products' phase composition while evaluating phase transformations in the synthesis of WH. It was also observed that the synthesis under rotating condition gave rise to a decrease in particle size as illustrated in the scanning electron microscopy image presented in Fig. 1b. As a result, the phase composition and particle size of our biomaterial could be properly tuned in order to fulfil someone's requirements and needs.



**Fig. 1.** SEM images of WH powders synthesized under static (a) and rotating (b) synthesis conditions.

## References

1. L. Bauer, M. Antunovic, A. Rogina, M. Ivankovic, H. Ivankovic, J. Mater. Sci., **56** (2021) 3947-3969.
2. D. Zhou, C. Qi, Y. Chen, Y. Zhu, T. Sun, F. Chen, C. Zhang, Int. J. Nanomedicine, **12** (2017) 2673-2687.
3. H.D. Kim, H.L. Jang, H. Ahn, H.K. Lee, J. Park, E. Lee, E.A. Lee, Y. Jeong, D. Kim, K. T. Nam, N. S. Hwang, Biomaterials, **112** (2017) 31-43.
4. S. Batool, U. Liaqat, Z. Hussain, M. Sohail, J. Nanomater, **10** (2020) 1856.
5. L. Pazourková, P. Peikertová, M. Hundáková, G.S. Martynková, Mater. Today: Proceedings, **5** (2018) S38-S44.

# Photocatalytic Removal of Halogenated Organic Substances and Industrial Dyes by Activated Carbon Composites

H. Yankovych\*, I. Melnyk, M. Vaclavikova

<sup>1</sup>*Institute of Geotechnics Slovak Academy of Sciences, Watsonova 45, 040 01 Kosice, Slovakia*

*\*Corresponding author, e-mail: yankovych@saske.sk*

Halogenated organic substances as well as the industrial dyes are organic pollutants commonly indicated in water. These substances are capable to cause serious environmental and health problems. The very first compounds that launch the formation of complex organohalogenes are the group of 4-halogenphenols: 4-chlorophenol, 4-bromophenol and 4-iodophenol. These organics have specific taste and odour, high lipophilicity that increases the influence on nervous, digestive, and excretory human systems [1] and are formed during water disinfection processes and released with industrial emissions [2,3]. More than 10,000 dyes are commercially available and are using increasingly in textile, plastic, rubber, cosmetics, pharmaceutical, and food industries [4]. During the dyeing processes, these industries lost about 10–15 % of dyes directly to wastewater [5], therefore, the water contamination by dyes is a serious life-threatening problem. The combination of adsorption and photocatalysis is the promising technique in wastewater treatment due to its economic benefits and self-cleaning properties of the composites.

The research deals with the facile *in situ* sol-gel synthesis of composite materials based on titania and titania doped with zirconium(IV), cerium(IV) and copper(II) immobilized granular activated carbon. The deposited semiconductors demonstrate the nanocrystalline nature with particles size near 5nm. The composites possess a developed surface area and keep the porous structure of granular activated carbon carrier. The XRD diffractograms showed the presence of anatase, rutile and brookite in composites that enhances its photocatalytic activity. The benefits of the synthesized materials provide the possibility of their application for photocatalytic removal of 4-halogenophenols as the representatives of halogenated organics and 3 industrial dyes of different nature: Acid Red 88 (AR88) from anionic dyes group, Basic Red 13 (BR13) as cationic dye, and Basic Red 5 (BR5) as neutral dye. The high degradation performance of 4-HPH was achieved for all synthesized composites – up to 99.9% with different half reaction times. Titania loaded granular activated carbon was the best in the removal of 4-chlorophenol, the highest photocatalytic performance in 4-bromophenol's removal was achieved by titania doped with cerium (IV) and copper(II) immobilized activated carbon and 4-iodophenol elimination was equal for all synthesized composites. The photodecomposition of the selected dyes was realised under the same conditions with different efficiency. In case of AR88 removal, zirconium-doped titania loaded activated carbon reached the highest efficiency – 80% during 6h; the elimination of BR13 was equal and the highest for titania and titania doped with cerium and zirconium immobilized activated carbon – 65% for 6h; the photodecontamination of BR5 was near 60% for 5h for zirconium-doped titania activated carbon composite. The synthesized composites showed the different efficiency in the photocatalytic removal of halogenated organics and industrial dyes and can be applied in water cleaning processes.

## References

- 1.E.A. Cooper, D.L. Woodhouse, On the relations of the phenols and their derivatives to proteins. A contribution to our knowledge of the mechanism of disinfection: Part IV. The halogen phenols, *Biochem. J.* 17 (1923) 600.
- 2.N.S. Deshmukh, K.L. Lapsiya, D.V. Savant, S.A. Chiplonkar, T.Y. Yeole, P.K. Dhakephalkar, D.R. Ranade, Upflow anaerobic filter for the degradation of adsorbable organic halides (AOX) from bleach composite wastewater of pulp and paper industry, *Chemosphere*, 75 (2009) 1179-1185.
- 3.Y.W. Xie, L.C. Chen, R. Liu, AOX contamination status and genotoxicity of AOX-bearing pharmaceutical wastewater, *J Environ Sci-China*, 52 (2017) 170-177.
- 4.O. Sharma, M.K. Sharma Copper hexacyanoferrate(II) as photocatalyst: decolorisation of neutral red dye *Int. J. Chemtech Res.*, 5 (2013), pp. 2706-2716.
- 5.J.V. Tolia, M. Chakraborty, Z.V.P. Murthy Photocatalytic degradation of malachite green dye using doped and undoped ZnS nanoparticles *Pol. J. Chem. Technol.*, 14 (2012), pp. 16-21.

**Acknowledgement:** The research has been supported by the project VEGA 2/0156/19 of the Scientific Grant Agency of the MŠVVaŠ SR, the Marie Curie Programme H2020-MSCA-RISE-2016-NANOMED project No 734641 as well as by APVV-19-0302 COMWAT.



# Synthesis and Adsorption Potential of Organo-Inorganic Hybrids Based on the Polymers with Carboxyl Groups and Silica

V. Kyshkarova<sup>1,2</sup>, I. Melnyk<sup>1</sup>

<sup>1</sup>Institute of Geotechnics, Slovak Academy of Sciences, 04001 Košice, Slovakia

<sup>2</sup>Technical University of Košice, Faculty of Materials, Metallurgy and Recycling, 04001 Košice, Slovakia  
kyshkarova@saske.sk

The strong growth of the world population and accelerated industrialization have caused several serious environmental problems in more recent years. Conserving water being the most important one of those topics. Water in aquatic systems is polluted by household waste, mining activities, municipal waste, modern agricultural practices, sea dumping of radioactive waste, oil spills, and leaks from underground storage and industries [1]. Also, the main culprits in the pollution of water resources are industrial units (textiles, steel, tanneries, canneries, refineries, mines, sugar factories, fertilizer production, detergent production, and electroplating units) [2]. Among the pollutants discharged by industrial units, heavy metals and dyes pose a serious threat to human health.

The first goal of the research was to obtain materials with carboxylic groups on the surface. The materials were prepared based on SiO<sub>2</sub> with different polymers by a one-step sol-gel method. By this sol-gel technique, three new materials are synthesized (the samples were labeled based on their composition):

- silica/poly(lactic-co-glycolic acid) (PLGA) - silica/PLGA;
- silica/polystyrene acrylic polymer (Tubifast 4010) - silica/Tubifast 4010;
- silica/carboxyethylsilanetriol disodium salt (CEST) - silica/CEST.

Composition and structure of organo-inorganic composites were investigated with physicochemical methods. IR spectroscopy data and stability in water solutions showed that there is an interaction between organic and inorganic components in the synthesized composites. Based on the elemental analysis of the samples, it was confirmed that the organic moiety of polymer is part of the hybrids with carbon content: silica/PLGA -5.1%, silica/Tubifast 4010 - 9.5% and silica/SAC -6.8% (mass.%). The SEM-EDX spectroscopy confirmed the presence of an inorganic part with silicium content: silica/PLGA -49.7%, silica/Tubifast 4010 - 41.6 % and silica/CEST - 46.5% (wt.%). Furthermore, acid-base titration data ( $C_{(-COOH)}=1.3-6.0$  mmol/g) and isoelectric point values (pH=2.3-3.5) verify the existence of acid groups. The data of low-temperature nitrogen adsorption and S<sub>BET</sub> calculations indicated that porosity depends on the type of polymer: silica/PLGA – 467 m<sup>2</sup>/g, silica/Tubifast 4010 - 484 m<sup>2</sup>/g and silica/CEST- 27 m<sup>2</sup>/g.

The second purpose of this work was to address the problem of polluted water treatment, focusing on the removal of heavy metals and cationic dyes. It was demonstrated that the silica/PLGA material was aimed at effective adsorption of Fe(III) with maximum capacity of 34.1 mg/g, at the optimum pH value of 4.0, and during the adsorption equilibrium time of 240 minutes. Moreover, it was revealed chemisorption takes place during the adsorption and hybrid composite selectively adsorbs Fe (III) ions from aqueous solutions containing the equal amount of Cu (II), Mn (II), Ni (II), and Fe (III) ions (~20 mg/l) [3]. Silica/Tubifast 4010 material, which includes styrene-acrylic copolymer, is widely used as a component in acrylic paints because of its ability to bind easily [4]. Thus, the material has been used to uptake cationic dyes such as Methylene blue and Rhodamine 6G. The maximum adsorption capacity of Methylene blue on this material equals 35.6 mg/g, Rhodamine 6G - 52.4 mg/g. The equilibrium data followed the Langmuir model which indicates chemisorption, but 100% desorption cannot be achieved. Silica/CEST spherical particles demonstrated high efficiency during Ni(II) removal from water. Saturation is reached in 24 hours and the sorption capacity of the sample is 112.6 mg/g, which is a relatively high value.

Summing up, it can be noted that the methods of one-step preparation of silica composites with carboxyl groups, which are effective in the adsorption of cations of various natures, have been developed.

**Acknowledgments:** This work was supported by the APVV-19-0302 project.

## References

1. R. Hlihor, M. Gavrilescu, *Environmental engineering and management J* **8**(2) (2009) 353-372.
2. A.I. Abd-Elhamid et al., *Appl Water Sci* **10** (2020) 10:45.
3. V. Kyshkarova et al., *Appl Nanoscience*, **12** (2022) 1201-1212.
4. H. Suman et al, *J Environmental Chem Engineering*, **5** (2017) 103-113.

# Analytical Methods Used for the Characterization of Adipose Tissue

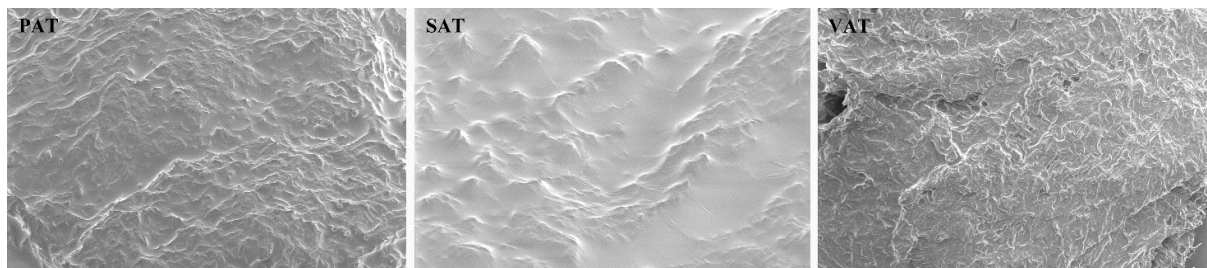
E. Brimas\*, R. Raudonis, A. Kareiva

*Institute of Chemistry, Faculty of Chemistry and Geosciences, Vilnius University, Naugarduko 24, LT-03225  
Vilnius, Lithuania*

*\*Corresponding author, e-mail: edbrimas@gmail.com*

Obesity has become a global pandemic, leading to the development of many common disorders, such as type 2 diabetes, metabolic syndrome, cardiovascular diseases, and even increases the risk of several cancers. In this study several analytical techniques, such as gas and liquid chromatography, Fourier transform infrared (FTIR) and Raman spectroscopies, nuclear magnetic resonance (NMR) spectroscopy, scanning electron microscopy (SEM) and elemental analysis were discussed as the main tools used for the characterization of adipose tissue samples. The emphasis was focused on the relation between the obtained results which provide information about adipose tissue layers chemical and structural composition in human body, as well as main microstructural features and obesity.

The gas and liquid chromatography are conventional methods for determining the composition of fats in the adipose tissue. Liquid chromatography techniques are also very important in lipidomics research. According to FTIR analysis results it was concluded that the main functional groupings in the adipose tissue taken from subcutaneous, preperitoneal and visceral layers of different patients with obesity were different. Therefore, FTIR spectroscopy was successfully used for the analysis and direct qualitative characterization of adipose tissue composition. Raman spectroscopy showed even more possibilities for the analysis of specific features of adipose tissue. It was demonstrated, that  $^1\text{H}$  NMR spectra of adipose tissue samples could be used to predict the different pathologies of patients with obesity. The results of elemental analysis showed various distribution of different metals in adipose tissue of patients with different obesity. It could be concluded, that the results of distribution of some metals in adipose tissue layers of people with overweight are promising for further medical observation. Also, careful morphological observations using SEM and TEM measurements revealed individual surface morphology of adipose tissue samples taken from different patients (Fig. 1).



**Fig. 1.** Typical SEM micrographs of lyophilized adipose tissue obtained from preperitoneal (PAT), subcutaneous (SAT) and visceral (VAT) layers of patients with obesity having different metabolic diseases [1].

From the obtained results were concluded that such characterization of adipose tissue is an essential step for the possible prediction of appearance of symptoms of different diseases, since recent studies have emphasized on a close relationship between adipose tissue properties and development of fat distribution and metabolism, and different diseases. This may facilitate the future development of new prognostic tools useful for personalized treatment strategies that address problems in obesity and its complications. In summary, this review shows interesting findings, which may provide new insights into the treatment of metabolic diseases.

## References

1. G. Brimas, R. Skaudzius, V. Brimiene, R. Vaitkus, A. Kareiva, Microstructural features of lyophilized adipose – A new concept to estimate the metabolic symptoms for obese patients. *Medic. Hypotheses*. 136, 109526 (2020).

# A Dopamine Electrochemical Sensor Based on N-doped Reduced Graphene Oxide Electrode

R. Aukštakojytė<sup>1,\*</sup>, J. Gaidukevič<sup>1,2</sup>, R. Pauliukaitė<sup>2</sup>, J. Barkauskas<sup>1</sup>

<sup>1</sup>*Institute of Chemistry, Faculty of Chemistry and Geosciences, Vilnius University, Naugarduko str. 24, LT-03225 Vilnius, Lithuania*

<sup>2</sup>*Department of Nanoengineering, Center for Physical Sciences and Technology, Savanorių Ave. 231, LT-02300 Vilnius, Lithuania*

\*Corresponding author, e-mail: ruta.aukstakojyte@chgf.vu.lt

Dopamine (DA) is one of the most significant neurotransmitters in our nervous system. It is responsible for our emotions and control of the movements a person makes. Abnormal levels of DA can potentially lead to neurodegenerative disorders such as senile dementia, depression, Parkinson's, and Alzheimer's diseases [1]. Therefore, the sensitive and precise determination of DA has become a vital issue in clinical diagnosis, especially at very low concentrations. The use of graphene-based materials such as graphene oxide (GO) and reduced graphene oxide (rGO) have attracted considerable attention in DA sensing due to their high surface area, chemical stability, and their ability to immobilize a variety of different molecules [2]. Following this, the GO and rGO modification with nitrogen atoms, may modulate and improve the physicochemical characteristics of these carbon materials and create new electrocatalytically active sites for accurate and sensitive DA determination [2,3].

The aim of this study was to synthesize N-doped reduced graphene oxide (N-rGO) samples and investigate their electrochemical performance in the DA detection. GO has been prepared using a modified Hummers' method, including the pre-oxidation of natural graphite powder by the mixture of  $K_2S_2O_8/P_2O_5/H_2SO_4$  [4]. N-rGO samples have been synthesized by a facile and one-pot hydrothermal treatment of GO in the presence of the organic dye "Bismarck Brown Y" (BB) which has been used as a N source for the rGO modification for the first time. Obtained samples (rGO, rGO\_BB20, and rGO\_BB50) have been characterized by Brunauer-Emmett-Teller (BET) analysis, scanning electron microscopy (SEM), X-ray photoelectron (XPS), and Raman scattering spectroscopies. Electrical behavior of prepared materials has also been determined by estimating the dependence between electrical conductivity and bulk density. The electrochemical measurements, including cyclic voltammetry (CV) and chronoamperometry (CA), have been performed to analyse the sensitivity of N-rGO samples toward DA detection.

Results of XPS analysis show that rGO\_BB20 and rGO\_BB50 consist of 5.3 and 14.2 at% of nitrogen, respectively, indicating a successful rGO modification with N atoms.  $I_D/I_G$  values determined from Raman spectra confirm the increase of structural disorders after the use of BB additive. BET analysis shows that specific surface area decreases with the higher amount of BB used in the hydrothermal synthesis. Electrical conductivity measurements demonstrate that rGO and rGO\_BB20 exhibit similar electrical conductivity values, while rGO\_BB50 possesses much lower. From SEM images, it is found that modification with N atoms leads to the corrugation of rGO layers. The CV studies reveal that rGO\_BB20 and rGO\_BB50 samples exhibit prospective electrocatalytic activity towards the DA redox peak. The CA studies show that the proposed sensor based on rGO\_BB50 demonstrates a relatively high sensitivity of  $0.17 \mu A \mu M^{-1} cm^{-2}$  and a low limit of detection (57 nM), suggesting that it is a promising electrode material for the sensitive DA determination.

## References

1. R. Franco, I. Reyes-Resina, G. Navarro, *Biomedicines*, **9** (2021) 109.
2. J. Gaidukevic, R. Aukstakojyte, J. Barkauskas, G. Niaura, T. Murauskas, R. Pauliukaite, *Appl. Surf. Sci.*, **592** (2022) 153257.
3. H. Zhang, S. Liu, *J. Alloys Compd.*, **842** (2020) 155873.
4. X. Yan, J. Chen, J. Yang, Q. Xue, P. Miele, *ACS Appl. Mater. Interfaces*, **2** (2010) 2521–2529.

# GdPO<sub>4</sub>·H<sub>2</sub>O:Eu<sup>3+</sup> Ceramic Composites – Wood Modification

M. Baublytė<sup>1\*</sup>, D. Sokol<sup>1</sup>, R. Skaudžius<sup>1</sup>

<sup>1</sup>Department of Inorganic Chemistry, Faculty of Chemistry, Vilnius University, Naugarduko st. 24, Vilnius

\*Corresponding author, e-mail: monika.baublyte@mb.vu.lt

Thermal and chemical stability, low toxicity, and luminescence of lanthanide orthophosphates offer extensive particle applications in creating multifunctional materials. Thus, the growing demand for multifunctional materials with novel properties has impacted the research of wood structures doped with gadolinium phosphate – wood ceramic composites (WCC) [1,2].

Wood has some adverse properties regarding structural stability, combustibility, and biodeterioration. Many techniques have been used to modify and overcome wood disadvantages (thermal treatment, acetylation, furfurylation, treatments involving organic silicon compounds, etc.) [3]. However, many treatments have several limitations – low effectiveness, expensive production and optimization, and negative environmental and human health impacts [4]. To overcome the issues inorganic dopants are introduced to reinforce polymeric wood matrix to an extent of new properties and increased strength and retardancy.

After in situ GdPO<sub>4</sub>·H<sub>2</sub>O:Eu<sup>3+</sup> synthesis in wood's matrix, the characteristics of the samples were observed by scanning electron microscopy (SEM) and computed tomography (μCT) (Fig.1); optical properties were determined by luminescence analysis. Thermogravimetric (TG) analysis was performed to attest the thermal degradation of composites.

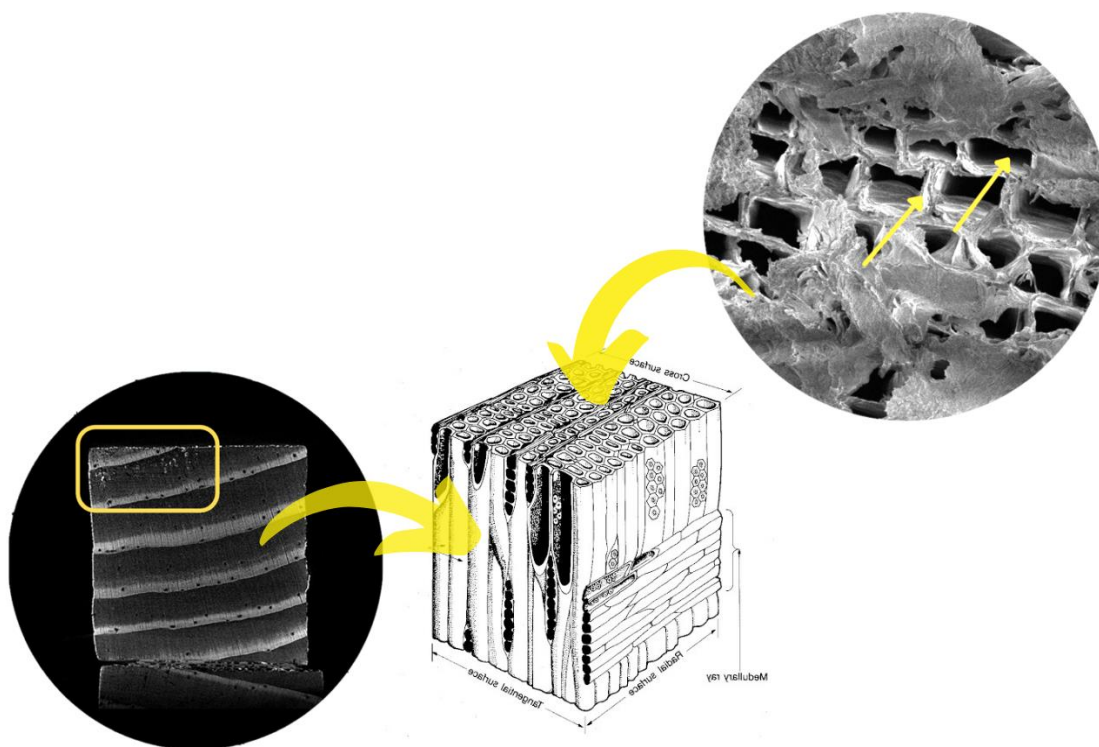


Fig. 1. GdPO<sub>4</sub>·H<sub>2</sub>O:Eu<sup>3+</sup> deposits in woods matrix.

## References

1. H. Khajuria, J. Ladol, S. Khajuria, M. S. Shah, and H. N. Sheikh, Surfactant mediated hydrothermal synthesis, characterization and luminescent properties of GdPO<sub>4</sub>: Ce<sup>3+</sup>/Tb<sup>3+</sup> @ GdPO<sub>4</sub> core shell nanorods, Mater. Res. Bull., 80 (2016) 150–158.
2. K. M. Heffernan, N. L. Ross, E. C. Spencer, and L. A. Boatner, The structural response of gadolinium phosphate to pressure, J. Solid State Chem., 241 (2016) 180–186.
3. Lu, Y., Feng, M. & Zhan, H. Preparation of SiO<sub>2</sub>–wood composites by an ultrasonic-assisted sol–gel technique. Cellulose, 21 (2014) 4393–4403.
4. Miyafuji, H., Saka, S. Fire-resisting properties in several TiO<sub>2</sub> wood-inorganic composites and their topochemistry. Wood Sci. Technol., 31 (1997) 449–455.

# YAG and LuAG Powder, Ceramic and Thin Films. The Effect of Boron Doping on Compounds Luminescence Properties

Greta Inkrataitė<sup>1\*</sup>, Meldra Kemere<sup>2</sup>, Anatolijs Sarakovskis<sup>2</sup>, Ramūnas Skaudžius<sup>1</sup>

<sup>1</sup> Institute of Chemistry, Faculty of Chemistry and Geosciences, Vilnius University, Vilnius, Lithuania

<sup>2</sup> Institute of Solid State Physics, University of Latvia, 8 Kengaraga street, LV-1063, Riga, Latvia  
greta.inkrataite@chgf.vu.lt

To convert high-energy radiation, such as gamma or X-rays, into visible light, a certain type of material is needed. Such compounds are usually referred to as scintillators. Over the years many different candidates to fit the required criteria were examined. Compounds with garnet structure have attracted a particularly large amount of attention as potential scintillators [1]. Cerium doped yttrium and lutetium aluminum garnets (YAG:Ce, LuAG:Ce), have high density, high thermal stability, a rather intensive emission/excitation and high quantum efficiency which are needed for a good scintillator. However, further optimization and improvement are still required, especially towards obtaining high luminescence intensity and even more so on the shortening of the decay time. One way to approach this problem is to alloy the aforementioned compounds with different elements, such as boron and magnesium [2,3]. By replacing one element with another in the crystal lattice it is possible to influence the properties of the materials. As such, by doping we could potentially be able to improve key aforementioned parameters: emission intensity, quantum efficiency and decay times [2]. The form of the samples is also known to be an important factor for scintillators. Although the most common and easiest to work with form of the samples is powder, however coatings and ceramics are more applicable in practice. Therefore, when it comes to scintillators, it is important to consider this as well [4].

In the present work it is investigated the effect of boron doping on the various characteristic of the aforementioned garnets in a different form. This is especially important for ceramics and thin films as most of the scientific data is present only for compounds in powder form. In this research this doping was described as YAG and LuAG garnets in all three forms: powder, thin films and ceramics were synthesized and investigated. Garnets doped with different amounts of boron and/or magnesium were synthesized by the sol-gel method. The coatings were synthesized using the sol-gel spin and dip-coatings methods on different quartz and sapphire substrates and ceramics were obtained using hydrostatic pressure. Crystal structure of the samples was analyzed by means of X-ray diffraction (XRD). Morphology of the compounds was evaluated using scanning electron microscopy (SEM) and atomic force microscopy (AFM). Luminescence properties such as emission, excitation, decay time, quantum efficiency and temperature dependency of emission intensity have been investigated. Radioluminescence was also measured in order to determine the scintillation properties of the samples. The positive impact of boron addition into the garnet structure on the luminescence properties will be discussed in detail.

## Acknowledgements:

This research is funded by the European Social Fund under the No 09.3.3- LMT K-712 “ Development of Competences of Scientists, other Researchers and Students through Practical Research Activities” measure.

## References

1. I.P. Machado, V.C. Teixeira, C.C.S. Pedrosa, et. al., *J. Alloys Compd.*, **777**, 638 – 645 (2019).
2. C. Foster, Y. Wu, M. Koschan, et. al., *J. Cryst. Growth*, **486**, 126 – 129 (2018).
3. M. Lucchini, O. Baganov, E. Auffray, et. al., *J. Lumin.*, **194**, 1 – 7 (2018).
4. D. S. McGregor, *Annu. Rev. Mater. Res.*, **48**, 254-277 (2018).

# Solvothermal Synthesis of Calcium Hydroxyapatite via Hydrolysis of $\alpha$ -Tricalcium Phosphate in Different Aqueous-Organic Media

R. Karalkeviciene<sup>1</sup>, E. Raudonyte-Svirbutaviciene<sup>1,2</sup>, J. Gaidukevic<sup>1</sup>, A. Zarkov<sup>1</sup>,  
A. Kareiva<sup>1,\*</sup>

<sup>1</sup>Institute of Chemistry, Faculty of Chemistry and Geosciences Vilnius University, Naugarduko St. 24, LT-03225 Vilnius, Lithuania

<sup>2</sup>Institute of Geology and Geography, Nature Research Centre, Akademijos Str. 2, LT-08412, Vilnius, Lithuania

\*Correspondence: aivaras.kareiva@chgf.vu.lt

Hydroxyapatite [ $\text{Ca}_{10}(\text{PO}_4)_6(\text{OH})_2$ , HAp] is a major inorganic component in hard tissue [1-3]. HAp is biocompatible and biodegradable substance with a great promise for bone regeneration [4]. It was observed that bone has a great affinity for implants containing high percentages of HAp [5].

In the present work, the effects of various organic solvents and solvothermal conditions on the formation of HAp via hydrolysis of  $\alpha$ -tricalcium phosphate ( $\alpha$ -TCP) were investigated. The hydrolysis reaction was performed in solutions with different water to organic solvent (W:O) ratios under solvothermal conditions at 120 °C for 3 h and at 200 °C for 5 h. Ethyl alcohol (EtOH), isopropyl alcohol (PrOH), and butyl alcohol (BuOH) did not inhibit the hydrolysis of  $\alpha$ -TCP while methyl alcohol (MeOH) and ethylene glycol (EG) had a more prominent inhibitory effect on the formation of single-phased HAp. The samples treated with organic solvent only showed no evidence of HAp formation. This was true for all the organic solvents used under different solvothermal treatments. The morphology of the obtained samples varied from plate-shaped to rod-shaped. From all the solvents analysed, EG had the highest impact on the sample morphology.

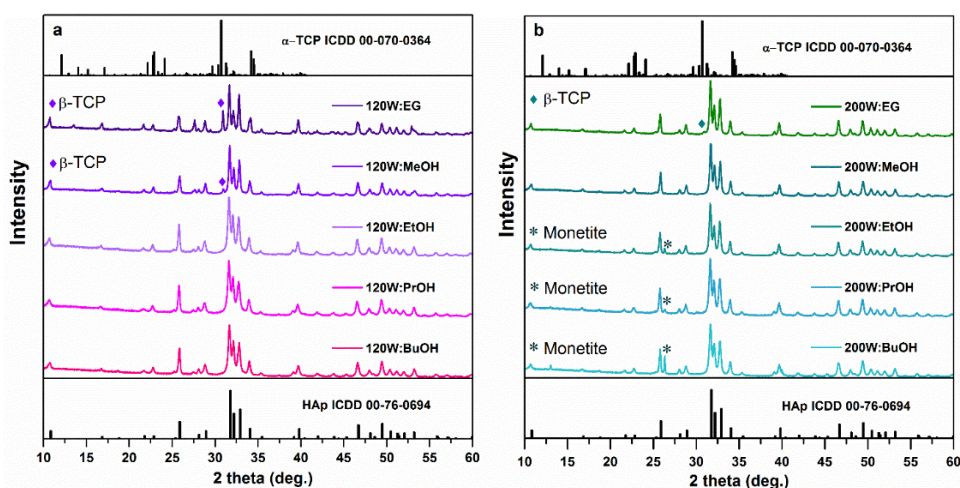


Figure 1. XRD patterns of the samples prepared using water to organic solvent ratio of 40:60 after solvothermal treatment at 120 °C for 3 h (a) and at 200 °C for 5 h (b).

**Acknowledgements:** This work has received funding from the European Social Fund (project No 09.3.3-LMT-K-712-23-0070) under grant agreement with the Research Council of Lithuania (LMTLT).

## References

1. M. J. Olszta; X. Cheng; S. S. Jee; R. Kumar; Y.-Y. Kim; M. J. Kaufman; E. P. Douglas; L. B. Gower. Bone structure and formation: A new perspective. *Mater. Sci. Eng., R* 2007, 58, 77–116.
2. M. Goldberg; A. B. Kulkarni; M. Young; A. Boskey. Dentin: structure, composition and mineralization. *Front. Biosci., Elite Ed.* 2011, E3, 711–735.
3. Y. In; U. Amornkitbamrung; M.H. Hong; H. Shin. On the Crystallization of Hydroxyapatite under Hydrothermal Conditions: Role of Sebacic Acid as an Additive. *ACS omega* 2020, 5, 27204-27210, doi:10.1021/acsomega.0c03297.
4. E. Fiume; G. Magnaterra; A. Rahdar; E. Verné; F. Baino. Hydroxyapatite for Biomedical Applications: A Short Overview. *Ceramics*, 2021, 2571-6131, doi:10.3390/ceramics4040039.
5. J.R. Woodard, A.J. Hilldore, S.K. Lan, C.J. Park, A.W. Morgan, J.C. Ewell, S.G. Clark, M.B. Wheeler, R.D. Jamison and A.J. Wagoner Johnson, "The mechanical properties and osteoconductivity of hydroxyapatite bone scaffolds with multi-scale porosity", *Biomaterials* 28 (2007) 45, doi.org/10.1016/j.biomaterials.2006.08.021.

# The Influence of Fe<sup>2+</sup> on the Transformation of $\alpha$ -TCP

L. Lukaviciute\*, G. Klydziute, E. Raudonyte-Svirbutaviciene, A. Zarkov, A. Beganskiene, A. Kareiva

*Institute of Chemistry, Faculty of Chemistry and Geosciences, Vilnius University, Naugarduko 24, LT-03225  
Vilnius, Lithuania*

*\*Corresponding author, e-mail: lukaviciute.laura@gmail.com*

Synthetic calcium hydroxyapatite (CHA) is widely used to treat bone defects due to their chemical similarity to bone minerals and excellent biocompatibility. Recently it was demonstrated that calcium hydroxyapatite (CHA) could be used as bone implant materials for bones in order to improve and accelerate the process of osseointegration and also play an important role in dentistry (e.g., in the treatment of dental pulp and dentine hypersensitivity). It is very important to avoid inflammation after implantation, because it can lead to rejection of the implant. Partial substitution of Ca by other biologically active ions has been proposed as a promising tool to the superior biological performance of synthetic CHA-based materials. Enhanced antibacterial effect of ternary system (calcium hydroxyapatite, tricalcium phosphate or/and amorphous calcium phosphate) could be achieved by substitution of calcium with specific cations.

Although calcium hydroxyapatite (CHA) is traditionally regarded as a biomaterial for bone repair, it has also been utilised in the field of cosmetics as a more environment friendly alternative for sunscreens, skin cleansers, make-up, hair care and deodorants. Fe doped CHA has been particularly used in sunscreens as it broadens the absorption spectrum from UV to visible light. In order to prepare adsorbents with the possibility to control morphology, it is essential to develop cost-effective and efficient synthesis methods. Huge efforts have been made recently in this field [4-6]. However, the effects of divalent cations on the hydrothermal synthesis of CHA were not investigated so far. The influence of Fe<sup>2+</sup> on the hydrolysis products of  $\alpha$ -TCP has been investigated in this study. For this purpose,  $\alpha$ -TCP was synthesized by wet precipitation method, and the hydrolysis reaction was performed in aqueous solutions of Fe<sup>2+</sup> under various hydrothermal conditions. For the characterization of hydrolysis products the XRD, SEM, and FTIR spectroscopy methods were used.

It was determined, that low concentrations of Fe<sup>2+</sup> did not affect phase purity of the final product. The obtained XRD patterns revealed that single-phase CHA was obtained after the hydrothermal treatment at 120 - 200 °C. With increasing concentration of Fe<sup>2+</sup> to 5-10 mol % the formation of some  $\beta$ -TCP in addition to CHA was observed. The presence of Fe<sup>2+</sup> ion in the reaction solution had no significant effect on the sample morphology: plate-like crystals were obtained when no foreign ion was used, as well as by introducing different concentrations of Fe<sup>2+</sup>.

**Acknowledgements:** This work has received funding from the European Social Fund (project No 09.3.3-LMT-K-712-23-0070) under grant agreement with the Research Council of Lithuania (LMTLT).

# Stabilization of Hexagonal Crystal Structure in the Orthorhombic LuFeO<sub>3</sub> Matrix

A. Pakalniškis<sup>1\*</sup>, R. Skaudžius<sup>1</sup>, G. Niaura<sup>2</sup>, D. Karpinsky<sup>3</sup>, A. Kareiva<sup>1</sup>

<sup>1</sup> Institute of Chemistry, Vilnius University, Naugarduko 24, LT-03225 Vilnius, Lithuania

<sup>2</sup> Department of Organic Chemistry, Center for Physical Sciences and Technology (FTMC), Sauletekio Ave. 3, LT-10257, Vilnius, Lithuania

<sup>3</sup> Namangan Engineering-Construction Institute, Dustlik Avenue 4, 160100 Namangan, Uzbekistan.

\*Corresponding author, e-mail: andrius.pakalniskis@chgf.vu.lt

The crystal structure and properties of compounds with perovskite structure (nominal chemical formula ABO<sub>3</sub>) can be drastically modified by a chemical substitution in A- and/or B- perovskite sublattices. Introduction of elements with different ionic radii leads to a stabilization of structural distortions. The possibility to control physical properties via chemical doping is particularly important when concerning the formation of both electrical and magnetic orderings in the same compounds, which are commonly referred as multiferroics. However, for the most part, due to the conflicting nature of these properties, the coupling between the electrical and magnetic properties is relatively weak. Since magnetic properties usually require the 3d layer to be partially filled by electrons, while electrical properties arise from empty 3d shells. To solve this conundrum, materials with new mechanism for the origin of their ferroelectric properties were discovered, such as lone pair and spin driven mechanisms, that do not require empty electron shells [1]. The second issue that multiferroic compounds suffer from is the fact that most orderings only occur below room temperature. Only few room temperature multiferroics are known, with the main research being focused on BiFeO<sub>3</sub>.

Recently a new class of hexagonal rare earth ferrite perovskite compounds has been found to exhibit multiferroic ordering, with a mechanism and structure similar to that of hexagonal manganites, making them a new avenue for potential research. This new family of room temperature multiferroic compounds are based on LuFeO<sub>3</sub> with hexagonal structure (space group *P6<sub>3</sub>cm*). It has been discovered that LuFeO<sub>3</sub> in the hexagonal state has both ferroelectric and weak ferromagnetic ordering. Furthermore, it has been reported that the compound in orthorhombic phase (space group *Pnma*) is antiferromagnetic below 620 K, while being in hexagonal structure the magnetic transition shifts down to 440 K while also showing weak ferromagnetism, due to a canting of the magnetic moments towards the c-axis, with the polarization being retained up to 1050 K, at least in the case of thin films [2,3].

It should be noted, that the preparation of hexagonal compounds is quite difficult and the crystal structure can be modified either using the chemical substitution or via preparing the compounds in a form of thin films as the crystal lattice is unstable and tends to form an orthorhombic structure. Due to the unstable nature of the lattice and difficulty of preparation and characterization of the hexagonal variant of LuFeO<sub>3</sub>, the main available results have been performed on thin films. However, when analyzing thin films, it is important to take into account the effect of strain and interface interactions as it can significantly affect chemical and physical properties [4].

We provide insights in stabilizing the hexagonal structure in doped LuFeO<sub>3</sub> polycrystalline compounds prepared using aqueous sol-gel synthesis procedure. While also providing further clarification on the concentration ranges of the different structural phases present in the system and analyzed by means of SEM, EDX/EDS, X-ray diffraction technique, and Raman spectroscopy.

**Acknowledgments:** This project has received funding from the European Union's Horizon 2020 research and innovation programme under the Marie Skłodowska-Curie grant agreement No 778070 – TransFerr – H2020-MSCA-RISE-2017.

## References

1. Manish Kumar, Arvind Kumar, et al., Mater. Lett. **277**, (2020), 128369.
2. Wenbin Wang, Jun Zhao, et al., Phys. Rev. Lett. **110**, (2013) 237601.
3. Shi Cao, Xiaozhe Zhang, et al., J. Phys. Condens. Matter **28**, (2016) 156001.
4. Jana Luxová, Petra Šulcová, J. Therm. Anal. Calorim. **138**, (2019) 4303.



# A Comparative Study of the Effect of Graphite Particle Size on the Formation of Sulfuric Acid Intercalated Graphite and its Thermal Treatment

G. Rimkutė<sup>1\*</sup>, J. Gaidukevič<sup>1,2</sup>, G. Niaura<sup>3</sup>, J. Barkauskas<sup>1</sup>

<sup>1</sup>Faculty of Chemistry and Geosciences, Vilnius University, Naugarduko str. 24, LT-03225 Vilnius, Lithuania

<sup>2</sup>Department of Nanoengineering, Center for Physical Sciences and Technology (FTMC), Savanoriu Ave. 231, LT-02300 Vilnius, Lithuania

<sup>3</sup>Department of Organic Chemistry, Center for Physical Sciences and Technology (FTMC), Saulėtekio Ave. 3, LT-10257 Vilnius, Lithuania

\*gintare.rimkute@chgf.vu.lt

Graphite and graphite-related materials are widely used in industry and in the fields of science and technology. Due to the relatively high degree of structural order, scientists focused their attention on graphite intercalation compounds (GICs), which are formed when various atomic, molecular, or ionic species interpose between layers in a graphite material [1]. Depending on the number of graphene layers between the two layers of the intercalant, GICs can be classified by stage. Stage I GICs have one graphene layer in the middle of two layers of intercalant, stage II GICs have two graphene layers between the two layers of intercalant and so on [2,3].

GICs have unique properties that are not characteristic to their precursor materials, and therefore, these compounds have a wide variety of applications. GICs can be used as superconductors, catalysts in organic synthesis, anode materials, in the batteries, and electrode materials [1,4]. Currently, GICs are also used for the preparation of graphite nanoplatelets, exfoliated graphite, and, most importantly, in the production of promising materials such as graphene and graphene oxide. The object of this study is graphite bisulfate (GBS), which forms as an intermediate compound in the preparation of graphene oxide, which is widely used for the further production and processing of graphene. GBS is a GIC with  $\text{HSO}_4^-$  ions and  $\text{H}_2\text{SO}_4$  molecules inserted between graphite layers [2]. However, the synthesis of graphene, starting with the formation of GBS, can usually lead to a defective final product and a ruptured carbon lattice. To improve the quality of chemically synthesized graphene, a more detailed understanding of the synthesis mechanism is needed. As the properties of GBS depend on the graphite precursor, the oxidizing agent, the synthesis conditions, and other factors, it is important to analyze as many different synthesis options as possible [5].

The purpose of this work was to perform a comparative study of the effect of graphite particle size on the formation of GBS and its thermal treatment. The obtained samples were characterized using optical microscopy, Raman spectroscopy, X-ray powder diffraction (XRD), X-ray photoelectron spectroscopy (XPS), and scanning electron microscopy (SEM).

The GBS compounds were synthesized using  $\text{KIO}_4$  oxidizer and three different graphite precursors with grain sizes of  $<50 \mu\text{m}$ ,  $\geq 150$ ,  $\leq 830 \mu\text{m}$  and  $\leq 2000 \mu\text{m}$ . Raman analysis showed that stage I intercalation compound was only obtained using graphite with the smallest grains ( $<50 \mu\text{m}$ ). XRD analysis revealed that intercalation and thermal treatment of the smallest particle size graphite resulted in the largest interplanar distances (0.338 nm) and the smallest crystallite sizes (20.54 nm). XPS analysis demonstrated that thermal treatment of samples obtained from the smallest and medium grains caused a slight increase in the relative concentration of carbon, while the relative concentration of oxygen decreased. SEM images of the annealed samples showed the presence of a lamellar structure with irregular edges. The analysis carried out confirmed the importance of the grain size of the precursor graphite and suggested that graphite, which particle size does not exceed  $50 \mu\text{m}$ , could be the most suitable for the production of a highly intercalated GBS product.

## References

1. K. Tasaki, Density functional theory study on structural and energetic characteristics of graphite intercalation compounds, *Journal of Physical Chemistry C*. **118** (2014) 1443–1450.
2. D.D.L. Chung, A review of exfoliated graphite, *Journal of Materials Science*. **51** (2015) 554–568.
3. F. Bonaccorso, A. Lombardo, T. Hasan, Z. Sun, L. Colombo, A.C. Ferrari, Production and processing of graphene and 2d crystals, *Materials Today*. **15** (2012) 564–589.
4. W. Zhou, P.H.L. Sit, First-Principles Understanding of the Staging Properties of the Graphite Intercalation Compounds towards Dual-Ion Battery Applications, *ACS Omega*. **5** (2020) 18289–18300.
5. M. Salvatore, G. Carotenuto, S. de Nicola, C. Camerlingo, V. Ambrogio, C. Carfagna, Synthesis and Characterization of Highly Intercalated Graphite Bisulfate, *Nanoscale Research Letters*. **12** (2017) 167.

# Synthesis and Investigation of Magnesium Whitlockite Granules

**R. Raiseliene\***, G. Linkaite, I. Grigoraviciute, A. Kareiva

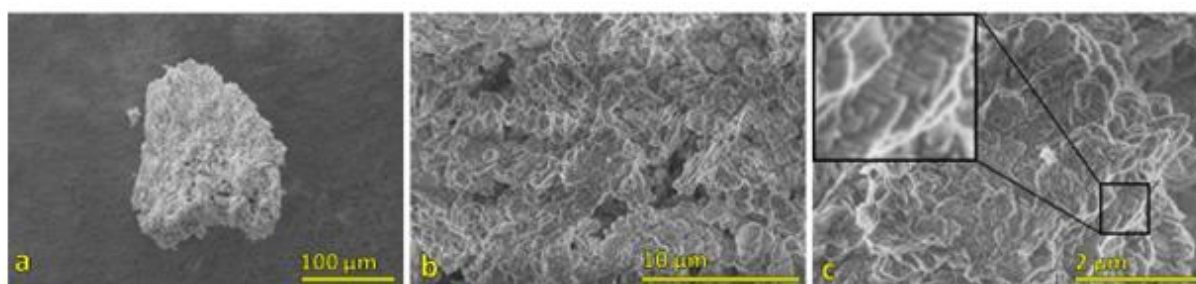
*Faculty of Chemistry and Geosciences, Vilnius University, Naugarduko 24, LT-03225 Vilnius, Lithuania*

*\*Corresponding author, e-mail: ruta.raiseliene@chgf.vu.lt*

Calcium phosphates (CaPs) are the most promising synthetic substitutive biomaterials [1, 2]. However, these biocompounds have some limitations for clinical application as they show low mechanical strength, uncontrolled biodegradation and bioinertness [3].

Magnesium whitlockite (WH,  $\text{Ca}_{18}\text{Mg}_2(\text{HPO}_4)_2(\text{PO}_4)_{12}$ ) is known as the second most abundant mineral in living bone, filling 25-35 wt% of the hard tissue of human bone [4]. As the highlight of WH properties is its better mechanical properties, faster resorbability, and promotional behavior on osteogenesis [4, 5].

In our study, we used a dissolution – precipitation synthesis to fabricate WH granules. Fig. 1 represents scanning electron microscopy (SEM) images of the product.



**Fig. 1.** SEM images of the synthesis product at the different enlargements.

The synthesized samples were also characterized to determine the phase purity and functional groups.

## References

1. J. Lu, H. Yu, C. Chen, *RSC Adv.*, **8** (2018) 2015-2033.
2. P. Wang, L. Zhao, J. Liu, M. D Weir, X. Zhou, H. H K Xu, *Bone Res.*, **2** (2014) 14017.
3. S. Batool, U. Liaqat, B. Babar, Z. Hussain, *J. Kor. Cer. Soc.*, **58** (2021) 530-547.
4. C. Wang, K. J. Jeong, H. J. Park, M. Lee, S. C. Ryu, D. Y. Hwang, K. H. Nam, I. H. Han, J. Lee, *J. Coll. and Int. Sc.*, **569** (2020) 1-11.
5. W. B. Lee, C. Wang, J. H. Lee, K. J. Jeong, Y. S. Jang, J. Y. Park, M. H. Ryu, U. K. Kim, J. Lee, D. S. Hwang, *ACS Appl. Bio Mater.*, **3** (2020) 7762-7768.

# Aqueous Sol-Gel Synthesis of Select Orthoferrite Powders, Coatings, Nanotubes

**J. Januškevičius<sup>1</sup>, Ž. Stankevičiūtė<sup>1</sup>, Thomas C. K. Yang<sup>2</sup>, A. Kareiva<sup>1</sup>**

<sup>1</sup>*Vilnius University, Faculty of Chemistry and Geosciences, Naugarduko st. 24, Vilnius, Lithuania*

<sup>2</sup>*National Taipei University of Technology, Department of Chemical Engineering, No. 1 號 Section 3, Zhongxiao E. Rd., Da'an District, Taipei City, 106, Taipei City, Taiwan (R.O.C.)*

*\*Justinas Januškevičius, justinas.januskevicius@chgf.vu.lt*

Orthoferrites are a promising class of compounds with the general formula of  $RFeO_3$ , where R is a rare earth element. They possess a very malleable perovskite structure (general formula  $ABX_3$ , where A and B are cations and X is the anion), allowing to potentially fine-tune their properties [1]. They have shown promise due to their interesting electromagnetic properties and potential applications in the fields of electronics, catalysis and sensors [2-4]. This malleability of structure and fine-tuning of properties, which is already very high, can be taken even further by applying sol-gel chemistry in order to allow for malleability of large-scale structure and morphology as well, resulting in an incredible number of possible combinations. Better yet – the aqueous sol-gel process is also very simple, scalable and doesn't require and complicated equipment or chemicals [5].

The greatest advantage of the structure – the incredible width of available compound compositions and their combinations with different morphologies – is also the greatest complication [1]. The sheer number of possible structures makes it virtually impossible to test them all. For this reason, a more methodical approach is needed. And, to some degree, there is already some groundwork in this field – for example the Goldschmidt ratio [6], which is a quantity predicting stability of perovskites based on ionic radius of the constituents of the perovskite or DFT calculations which can predict properties of specific structures. However, much work still needs to be done.

That is precisely why in this work, a subset of the perovskite structures – the rare earth orthoferrites – was chosen. Synthesis of select compounds (after some optimization) as well as their coatings and nanotubes was carried out, in the hopes that comparing them may reveal some insights and trends that may help to both find patterns in their properties, which would allow for a more methodical approach for this class of compounds in the future. In addition, the used sol-gel method was developed and shown to be a universal, simple, inexpensive and adaptable method for synthesis of this class of compounds.

## References

1. R. E. Schaak and T. E. Mallouk, *Chem. Mater.*, **14** (2002) 1455-1471.
2. E. A. R. Assirey, *Saudi Pharm. J.*, **27** (2019) 817-829.
3. O. Rosales-González et al, *Ceram. Int.*, **44** (2018) 15298-15303.
4. E. Haye et al, *J. Alloys Compd.*, **657** (2016) 631-638.
5. A. E. Danks, S. R. Hall and Z. Schnepf, *Mater. Horiz.*, **3** (2016) 91-112.
6. K. Y. Tsui, N. Onishi and R. F. Berger, *J. Phys. Chem. C*, **120** (2016) 23293–23298.

# Silica Sol Synthesis and Silica Particles Size Dependence to Environmental Factors

Lukas Šerpytis<sup>1</sup>, Matas Damolskis<sup>2</sup>, Lukas Taujenis<sup>1,2</sup>, Simas Šakirzanovas<sup>1</sup>

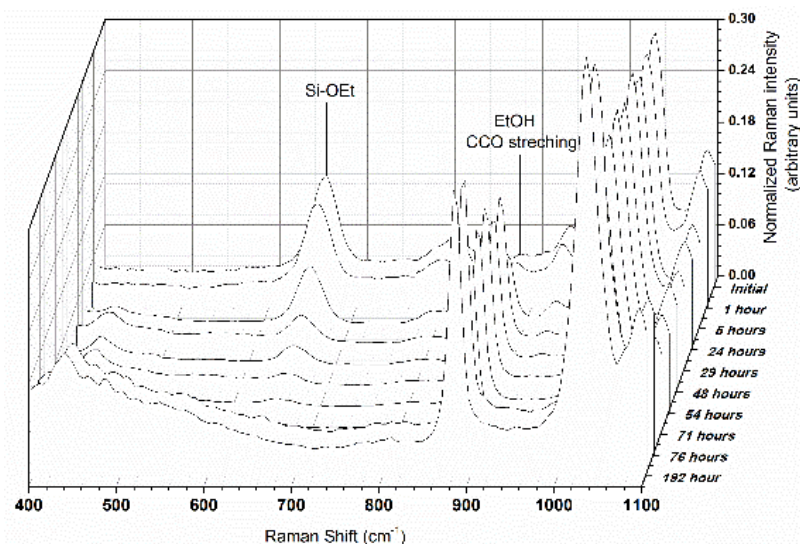
<sup>1</sup> Institute of Chemistry, Faculty of Chemistry and Geosciences, Vilnius University, Lithuania

<sup>2</sup> Thermo Fisher Scientific Baltics, UAB Vilnius, Lithuania

lukas.serpytis@chgf.stud.vu.lt

Acid and base catalyzed polymerized silica sol-gel can be used to form variety of end products such as film, particles coating, wet gel or polymeric colloidal silica particles[1-2]. For instance, mesoporous silica microparticles for liquid chromatography are produced commercially, nevertheless more extensive knowledge on reaction conditions and possible outcome predictions are still relevant.

Investigation is focused on base catalyzed silica sol formation process and characterization of final silica sol colloidal particles formation in different synthesis conditions. To achieve the goal silica sol were prepared using base catalyzed tetraethyl orthosilicate (TEOS) hydrolysis and condensation in methanol and water mixture. Raman spectroscopy and refractive index characterization methods were used to monitor sol formation. The prepared silica sols were tested against different experimental variables: aging, pH, dilution, salts and temperature. Particle size distribution were analyzed using dynamic light scattering method.



**Fig. 1.** Raman spectra of base catalyzed TEOS hydrolysis in methanol and water mixture against hydrolysis time.

**Keywords:** silica sol, pH, sol-gel process.

## References:

- [1] T. W. Zerda, I. Artaki, and J. Jonas, "Study of polymerization processes in acid and base catalyzed silica sol-gels," *J. Non. Cryst. Solids*, vol. 81, no. 3, pp. 365–379, 1986,
- [2] P. P. Ghimire and M. Jaroniec, "Renaissance of Stöber method for synthesis of colloidal particles: New developments and opportunities," *J. Colloid Interface Sci.*, vol. 584, pp. 838–865, 2021.

# Additive Manufacturing of Inorganic 3D Nanostructures by Combining Laser Lithography and Pyrolysis

G. Merkininkaitė<sup>\*1,2</sup>, E. Aleksandravičius<sup>3</sup>, D. Gailevičius<sup>2,3</sup>, M. Malinauskas<sup>3</sup> and S. Šakirzanovas<sup>1,4</sup>

<sup>1</sup>Faculty of Chemistry and Geosciences, Vilnius University, Naugarduko Str. 24, Vilnius LT-03225, Lithuania

<sup>2</sup>Femtika, Saulėtekio Ave. 15, Vilnius LT-10224, Lithuania

<sup>3</sup>Laser Research Center, Physics Faculty, Vilnius University, Saulėtekio Ave. 10, Vilnius LT-10223, Lithuania

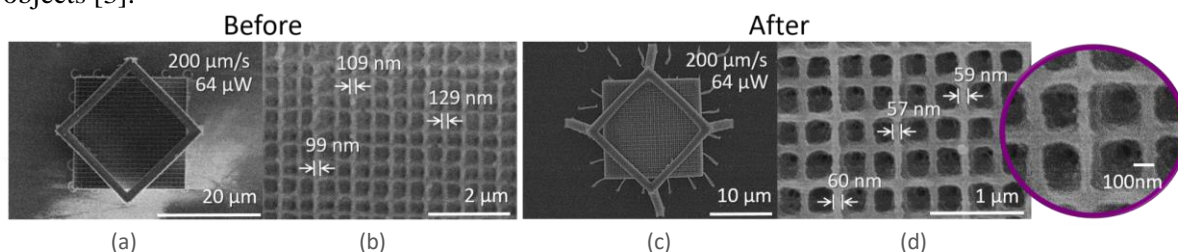
<sup>4</sup>Department of Chemical Engineering and Technology, Center for Physical Sciences and Technology, Saulėtekio Ave. 3, Vilnius LT-10257, Lithuania

\*Corresponding author, e-mail: greta.merkininkaite@chgf.vu.lt

In recent years, the interest in ceramic materials has been growing rapidly due to their unique properties, including high hardness, high strength, chemical stability, biocompatibility and high-temperature performance. Multiphoton polymerization combined with calcination/pyrolysis has been proved to be a powerful tool for the fabrication of fully 3D glass-ceramic micro/nano-objects for a wide range of applications [1].

Nevertheless, to propagate this technology and make it widespread additional optimization of the composition of the starting materials and as well as conditions of calcination have to be fully understood and enhanced. Precursors possessing proper chemical and physical properties are an essential prerequisite for the formation of 3D micro- and nano-dimension ceramic structures by laser lithography.

Therefore, in this work, the focus was on the study of an advanced method for transforming silicon and zirconium metalorganic 3D nano/micro-structures into pure crystalline 3D objects, by combining laser multi-photon lithography and calcination. We synthesized a series of organic- inorganic polymer precursors via sol-gel method varying the molar ratio of silicon (Si) and zirconium (Zr) [2] and investigated the prospects of 3D formation and calcination of these materials. The study shows that structures retain their shape without any distortion. Furthermore, calcination provides a route for the continuous size control and formation of a variety of phase transformations for free-form nano-/micro-objects [3].



**Fig. 1.** Si<sub>9</sub>:Zr<sub>1</sub> woodpiles before heat treatment (a, b) and after heating at 1000 °C under air atmosphere (c, d). The highest resolution of woodpiles was obtained by applying 200 μm/s and 64 μW parameters [3].

Achieved sub-100 nm individual feature dimensions and demonstrated tunability of material makes it a milestone advance in the laser applications field of nano/micro-ceramic manufacturing. The industry of electronics, mechanics and optics will benefit from this investigation as it reveals the potential for manufacturing of 3D ultra-high spatial resolution and highly resilient inorganic structures. Such technology is in a perfect match with the direction for downscaling and increasing functionalities of novel extremely precise devices.

## References

1. D. Gailevičius, V. Padolskytė, L. Mikoliūnaitė, S. Šakirzanovas, S. Juodkakis and M. Malinauskas, Additive-manufacturing of 3D glass-ceramics down to nanoscale resolution, *Nanoscale Horiz.*, 647-651 (2019).
2. A. Ovsianikov, J. Viertl, B. Chichkov, M. Oubaha, B. MacCraith, I. Sakellari, A. Giakoumaki, D. Gray, M. Vamvakaki, M. Farsari, and C. Fotakis, Ultra-Low Shrinkage Hybrid Photosensitive Material for Two-Photon Polymerization Microfabrication, *ACS Nano*, 2(11), 2257–2262 (2008).
3. G. Merkininkaitė, E. Aleksandravičius, M. Malinauskas, D. Gailevičius, S. Šakirzanovas, Laser additive manufacturing of Si/ZrO<sub>2</sub> tunable crystalline phase 3D nanostructures. *Opto-Electron Adv.* 5, 210077 (2022).

# Synthesis and Optical Properties of Mn-Doped Calcium Pyrophosphate Polymorphs

D. Griesiute<sup>1,\*</sup>, V. Klimavicius<sup>2</sup>, A. Antuzevics<sup>3</sup>, A. Katelnikovas<sup>1</sup>, A. Zarkov<sup>1</sup>,  
A. Kareiva<sup>1</sup>

<sup>1</sup> Institute of Chemistry, Vilnius University, Naugarduko 24, LT-03225 Vilnius,  
Lithuania

<sup>2</sup> Institute of Chemical Physics, Vilnius University, Sauletekio 3, LT-10257, Vilnius,  
Lithuania

<sup>3</sup> Institute of Solid State Physics, University of Latvia, Kengaraga 8, LV-1063 Riga, Latvia

\*Corresponding author, e-mail: diana.griesiute@chgf.vu.lt

Calcium phosphates (CPs) are the family of materials, widely used in different areas such as medicine and bone regeneration [1], sensors [2], removal of heavy metals from water [3], etc. Whereas in medicine, mainly calcium orthophosphates such as hydroxyapatite (HA,  $\text{Ca}_{10}(\text{PO}_4)_6(\text{OH})_2$ ), tricalcium phosphate (TCP,  $\text{Ca}_3(\text{PO}_4)_2$ ), or amorphous calcium phosphate (ACP) are used, some recent studies on biomaterials showed the potential of the use of calcium pyrophosphate (CPP,  $\text{Ca}_2\text{P}_2\text{O}_7$ ) for biomedical applications.

One of the strategies for modifying CPs considers partial substitution of  $\text{Ca}^{2+}$  by other biocompatible ions with specific properties [4]. Modification of CPs with magnetic or optically active ions can be used for bio-imaging purposes [5] or monitoring phase transitions in CPs *in situ* [6]. This approach was also employed to tune the properties of CPP.

Manganese is an essential element in the human body that plays a vital role in many biological processes, including bone development. Previously biological properties of different Mn-substituted CPs were investigated, and it was shown that the presence of  $\text{Mn}^{2+}$  ions in the CP matrix provides superior biological performance [7]. However, high concentrations of  $\text{Mn}^{2+}$  result in toxicity of the materials; therefore, Mn content should be limited to a relatively low level [8].

Although CPP has three different polymorphs, most of the works focus exclusively on  $\beta$ -CPP, whereas two others are quite poorly investigated. Studies on  $\alpha$ -CPP are most often related to the preparation of optical materials by substitution of  $\text{Ca}^{2+}$  ions by lanthanides [9]; nevertheless,  $\beta$ -CPP besides of the use in medicine also finds an application in the preparation of phosphors [10]. The least studied polymorph is  $\gamma$ -CPP. This work demonstrates a simple and time-efficient way of preparing  $\text{Mn}^{2+}$ -substituted brushite with subsequent conversion to  $\gamma$ -,  $\beta$ -, and  $\alpha$ -CPP. Structural, optical, and morphological properties of synthesized materials were investigated in detail.

## Acknowledgements

Vilnius University is highly acknowledged for financial support from the Science Promotion Foundation (MSF-JM-5/2021).

## References

1. W. Habraken, P. Habibovic, M. Epple, M. Bohner, *Mater. Today* 2016, 19, 69-87.
2. S. Sun, Q. Chen, S. Sheth, G. Ran, Q. Song, *ACS Sensors* 2020, 5, 541-548.
3. D. Griesiute, J. Gaidukevic, A. Zarkov, A. Kareiva, *Sustainability* 2021, 13.
4. M. Šupová, *Ceram. Int.* 2015, 41, 9203-9231.
5. W. He, Y. Xie, Q. Xing, P. Ni, Y. Han, H. Dai, *J. Lumin.* 2017, 192, 902-909.
6. H. Terraschke, M. Rothe, A. M. Tsigoni, P. Lindenberg, L. Ruiz Arana, N. Heidenreich, F. Bertram, M. Etter, *Inorg. Chem. Front.* 2017, 4, 1157-1165.
7. Y. Huang, H. Qiao, X. Nian, X. Zhang, X. Zhang, G. Song, Z. Xu, H. Zhang, S. Han, *Surf. Coat. Technol.* 2016, 291, 205-215.
8. J. V. Rau, I. V. Fadeeva, A. S. Fomin, K. Barbaro, E. Galvano, A. P. Ryzhov, F. Murzakhanov, M. Gafurov, S. Orlinskii, I. Antoniac, V. Uskoković, *ACS Biomater. Sci. Eng.* 2019, 5, 6632-6644.
9. R. Pang, C. Li, S. Zhang, Q. Su, *Mater. Chem. Phys.* 2009, 113, 215-218.
10. X. Yu, Z. Wang, Q. wang, X. Mi, *J. Alloys Compd.* 2022, 897, 162745.



## **POSTER PRESENTATION ABSTRACTS**

# UV Investigation of CdS Layers on Polypropylene Film

M. Matijūnas, R. Alaburdaite\*

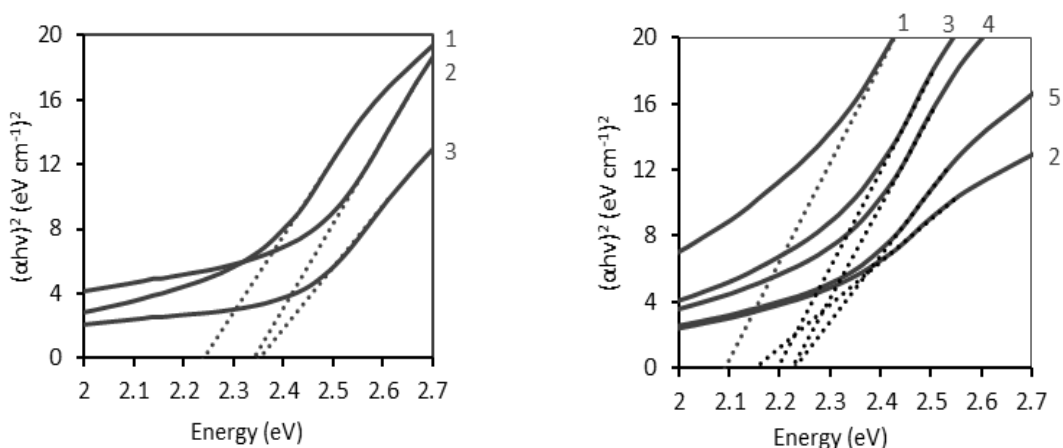
Kaunas University of Technology, Radvilėnų st.19, LT-50254 Kaunas, Lithuania

\*Corresponding author, e-mail: rasa.alaburdaite@ktu.lt

Cadmium sulfide (CdS) as semiconductor often used in solar cells, flat screens, optical device, logical gates [1, 2]. Polypropylene (PP) is a cheap hydrophobic thermoplastic, non-toxic, rigid and widely used [3]. The aim of the experiment is to deposit CdS onto PP thin film (Cd/PP) in order to get the benefits of both materials.

PP is resistant to many chemicals, so modification with thin CdS layers requires additional pre-treatment [4]. Firstly, it was washed in ultrasonic bath with acetone and ethanol, and then was treated at 90 °C for 25 min in oxidation solution of H<sub>2</sub>SO<sub>4</sub>, H<sub>3</sub>PO<sub>4</sub>, and CrO<sub>3</sub>. CdS thin layers were deposited onto PP film via chemical bath deposition using 3 different 0.5 mol/L cadmium salts solutions (Cd(CH<sub>3</sub>COO)<sub>2</sub>, CdCl<sub>2</sub>, CdSO<sub>4</sub>) using thiourea as sulfuring agent. Samples were analyzed using UV-Vis Spectroscopy (spectrometer Spectronic® Genesys™ 8, Perkin Elmer) and band gap was determined by using Tauc plot.

Band gap values of Cd/PP were found 2.24 eV, 2.34 eV, 2.35 eV using Cd(CH<sub>3</sub>COO)<sub>2</sub>, CdCl<sub>2</sub>, CdSO<sub>4</sub> solutions, respectively (Fig.1, a). Band gap of Cd/PP formed using Cd(CH<sub>3</sub>COO)<sub>2</sub> solution increased with increasing treating time: 1 h – 2.09 eV, 2 h – 2.15 eV, 3 h – 2.19 eV, 4 h – 2.22 eV, 5 h – 2.23 eV (Fig.1, b).



**Fig. 1.** Band gap of Cd/PP composite: **a** – formed with different salts: 1 – Cd(CH<sub>3</sub>COO)<sub>2</sub>, 2 – CdCl<sub>2</sub>, 3 – CdSO<sub>4</sub>; **b** – based on reaction time using Cd(CH<sub>3</sub>COO)<sub>2</sub>: 1 – 1 h, 2 – 2 h, 3 – 3 h, 4 – 4 h, 5 – 5 h

## References

1. B. G. An, H. R. Kim, Y. W. Chang, J.G. Park, J. C. Pyun, J. Korean Ceram. Soc. **58** (2021) 631–644.
2. S. S. Shaikh, M. Shkir, E. U. Masumdar, Phy B: Condens Matt, **571** (2019) 64-70.
3. H. A. Maddah, Am. J. Polym. Sci, **6**(1) (2016) 1-11.
4. P. Yang, W. Yang, ACS Appl. Mater. Interfaces, **6** (2014) 3759–3770.



# Deposition of Optical Coatings on Micro-Optics Using Atomic Layer Deposition

D. Astrauskyte<sup>1,\*</sup>, K. Galvanauskas<sup>2</sup>, D. Gailevicius<sup>2</sup>, M. Drazdys<sup>1</sup>, R. Drazdys<sup>1</sup>,  
M. Malinauskas<sup>2</sup>, L. Grineviciute<sup>1</sup>

<sup>1</sup>Center for Physical Sciences and Technology, Savanoriu av. 231, LT-02300, Vilnius, Lithuania

<sup>2</sup>Laser Research Center, Vilnius University, Sauletekio av.10, LT-10223, Vilnius, Lithuania

\*Corresponding author, e-mail: darija.astrauskyte@fmnc.lt

Recent development in 3D printed micro-optical components increases the requirements for optical coatings [1]. The reflection losses of the complex structure optical element can be decreased using the atomic layer deposition (ALD) technique [2]. Compared to physical vapor deposition methods, ALD is advantageous because of the opportunity to synthesize highly conformal coatings over all surfaces of the substrate and strict control of the growth rate [3].

In this work, optical coatings were deposited on microstructures made by femtosecond laser direct-write 3D nanolithography, and fused silica (FS) substrates. The material used for 3D printing was the hybrid organic-inorganic polymer SZ2080<sup>TM</sup> which is widely used for two-photon polymerization [4]. Titanium oxide, aluminum oxide and anti-reflective (AR) coating were synthesized using a plasma-enhanced ALD process. The depositions were performed at 60 °C temperature to prevent micro-optics from thermal damage. Atomic force microscopy was used to evaluate the roughness of the microstructures before and after the deposition. Optical profilometry was used to measure the profile of the micro-lenses. The stress in the thin films was calculated using Stoney formula [5]. Interferometry was used to characterize the curvature of the FS samples.

**Table 1.** Measured characteristics of thin single layers and anti-reflective coating.

Coating	Thickness, nm	Stress, MPa	$\Delta f$ , %
TiO <sub>2</sub>	301	86	7
Al <sub>2</sub> O <sub>3</sub>	302	135	-8
AR coating	153,8	127	2,5

The geometry of micro-lenses is a crucial parameter in applications. This research explores the effect of coatings on micro-lenses focal length. The thin film thickness, stress of the films and the changes in the focal length ( $\Delta f$ ) after the deposition are represented in Table 1. The micro-lens focal length increased after the deposition of titanium oxide and AR coating. Conversely, after the deposition of the alumina focal length decreased. This knowledge is essential in the final element applications – during the fabrication of micro-optics, the coating-induced change of the focal length can be evaluated. In all cases, after the deposition, the surface roughness of the microstructures is reduced.

## References

1. D. L. G. Hernandez, S. Varapnickas, G. Merkininkaitė, A. Ciburyš, D. Gailevicius, S. Sakirzanovas, S. Juodkaziš, M. Malinauskas, Laser 3D printing of inorganic free-form micro-optics, *Photonics*, 8(12), 577 (2021).
2. S. Ristok, P. Flad, H. Giessen, Atomic layer deposition of conformal antireflective coatings on complex 3D printed micro-optical systems, *Opt. Mater. Express* 12(5), 2063 (2022).
3. M. Ritala, J. Niinistö, Chemical Vapor Deposition, *Royal Society of Chemistry*, 9–11, (2009).
4. A. Ovsianikov, et al. Ultra-low shrinkage hybrid photosensitive material for two-photon polymerization microfabrication. *ACS nano* 2.11 (2008).
5. Janssen, Guido CAM, et al. Celebrating the 100th anniversary of the Stoney equation for film stress: Developments from polycrystalline steel strips to single crystal silicon wafers. *Thin Solid Films* 517.6: 1858-1867, (2009).

# The Optimal Eu Concentration for Luminescence Properties of GdPO<sub>4</sub>

D. Budrevičius\*, A. Pakalniškis, A. Kareiva, R. Skaudžius

*Institute of Chemistry, Faculty of Chemistry and Geosciences, Vilnius University, Naugarduko 24, LT-03225  
Vilnius, Lithuania*

*\*Corresponding author, e-mail: darius.budrevicius@chgf.vu.lt*

Due to the strong paramagnetic nature of gadolinium, Gd-based materials are commonly used in medicine as a magnetic resonance contrast agents and in other areas [1,2]. While MRI is a powerful technique used for medical diagnosis, still new ways of improving the imaging are needed. To improve the quality of the MRI, materials are being developed and are already being used to obtain T1 and T2 MRI together, as single mode MRI does not always provide sufficient image quality. Multimodal materials suitable for bioimaging and MRI are also being developed. One such way is to combine the MRI with luminescence measurements. Europium is quite commonly used as a dopant in the preparation of various compounds as it exhibits excellent luminescence properties, even when it is introduced even at small concentrations. Additionally, europium is suitable for the doping of GdPO<sub>4</sub> nanoparticles because it results in emission at ~577 nm, ~590 nm, ~615 nm, ~650 and ~700 nm wavelengths and when considering the interest of the compounds for bioimaging it is quite desirable, since part of the emission, in this case exist in a so-called first biological window, and is absorbed by the tissue to a much lesser extent [3]. Thus, Eu-doped GdPO<sub>4</sub> nanoparticles attract a lot of attention as an efficient single-phase multimodal nanoprobe with both luminescent and magnetic properties [4]. However, the Europium concentration further optimization and investigation is required. This is due to the fact that if the concentration of light emitting dopant introduced into the crystal structure is too large concentration quenching is often observed. In the case of europium, this boundary can change drastically depending on the initial host matrix. Furthermore, irrespective of the crystalline environment, the Eu<sup>3+</sup> ion usually emits red light under UV excitation, however, there have been reports that in certain situations weak emission bands can also be obtained in the green and sometimes blue range [5-8].

Hexagonal gadolinium phosphate hydrate doped with different europium amounts (Gd<sub>1-x</sub>PO<sub>4</sub>:Eu<sub>x</sub>·H<sub>2</sub>O; x = 0.01, 0.05, 0.10, 0.15 and 0.20) was synthesized by the hydrothermal synthesis method and the obtained samples were analyzed giving the optimal dopant concentration. All of the synthesized compounds were analyzed by X-ray diffraction in order to investigate their crystal structure. SEM analysis was used to characterize the morphology of synthesized particles. The luminescence properties were also characterized and discussed in detail.

## References

1. Y. Huang, P.O. Boamah, J. Gong, Q. Zhang, M. Hua, Y. Ye, Gd(III) complex conjugate of low-molecular-weight chitosan as a contrast agent for magnetic resonance/fluorescence dual-modal imaging, *Carbohydr. Polym.* 143 (2016) 288–295.
2. T. Jahanbin, H. Sauriat-Dorizon, P. Spearman, S. Benderbous, H. Korri-Youssoufi, Development of Gd(III) porphyrin-conjugated chitosan nanoparticles as contrast agents for magnetic resonance imaging, *Mater. Sci. Eng. C* 52 (2015) 325–332A.A. Autor, B. Autor, *The Chemical Synthesis*. Wiley & Sons, New York, 1999.
3. S. Golovynskyi, I. Golovynska, L.I. Stepanova, O.I. Datsenko, L. Liu, J. Qu, T.Y. Ohulchanskyy, Optical windows for head tissues in near-infrared and short-wave infrared regions: Approaching transcranial light applications, *J. Biophotonics* 11 (2018).
4. W. Ren, G. Tian, L. Zhou, W. Yin, L. Yan, S. Jin, Y. Zu, S. Li, Z. Gu, Y. Zhao, Lanthanide ion-doped GdPO<sub>4</sub> nanorods with dual-modal bio-optical and magnetic resonance imaging properties, *Nanoscale* 4 (2012) 3754–3760.
5. X.Q. Guo, Y. Yan, H.C. Zhang, Y. Han, J.J. Song, GdPO<sub>4</sub>:Er<sup>3+</sup>/Yb<sup>3+</sup> nanorods: Hydrothermal synthesis and sensitivity of green emission to Yb<sup>3+</sup> concentration, *Ceram. Int.* 42 (2016) 8738–8743.
6. D. Chen, Y. Yu, P. Huang, H. Lin, Z. Shan, Y. Wang, Color-tunable luminescence of Eu<sup>3+</sup> in LaF<sub>3</sub> embedded nanocomposite for light emitting diode, *Acta Mater.* 58 (2010) 3035–3041.
7. H. Lin, S. Tanabe, L. Lin, D.L. Yang, K. Liu, W.H. Wong, J.Y. Yu, E.Y.B. Pun, Infrequent blue and green emission transitions from Eu<sup>3+</sup> in heavy metal tellurite glasses with low phonon energy, *Phys. Lett. Sect. A Gen. At. Solid State Phys.* 358 (2006) 474–477.
8. M. Dejneka, E. Snitzer, R.E. Riman, Blue, green and red fluorescence and energy transfer of Eu<sup>3+</sup> in fluoride glasses, *J. Lumin.* 65 (1995) 227–245.

# Enzyme and Prussian Blue Based Detection of Mercury Ions

N. Dėnas<sup>1,\*</sup>, A. Valiūnienė<sup>1</sup>, P. Virbickas<sup>1</sup>

<sup>1</sup>Vilnius university, Institute of Chemistry, Naugarduko str. 24, LT-03225, Vilnius, Lithuania

\*narvydas.denas@chgf.stud.vu.lt

The toxicity of mercury to humans depends on the form of mercury (elemental, inorganic or organic), the dose and other factors. Inorganic mercury salts are much more dangerous when ingested than elemental mercury because they are more soluble in water. Most of the ingested inorganic mercury salt dose accumulates either in the liver, where it is excreted in the bile, or in the kidneys, where it is excreted in the urine. Symptoms and signs of inorganic mercury poisoning occur in two stages. Burning chest pain, rapid mucosal discoloration (due to protein deposition in the mucosa) and gastrointestinal pain due to direct local damage (due to salt corrosion) occur very soon after ingestion. If the patient survives the initial effects of the venom, systemic effects persist, manifesting as tooth loss and kidney damage [1,2].

Mercury can be determined using various analytical methods as well as biological sensors. Analytical examples of mercury measurement methods include cold vapor atomic absorption spectroscopy (CVAAS), cold vapor atomic fluorescence spectroscopy (CVAFS), and direct analysis by thermal decomposition. In many parts of the world, reduction of aqueous samples and determination of mercury using CVAAS is still the most used method for determining mercury concentrations in samples. The main characteristics of this method are the detection limit is in the row of ng/L and the linear dynamic range is from 1000 to 10000 times. Other atomic spectroscopy techniques such as inductively coupled plasma mass spectrometry (ICP-MS) and inductively coupled plasma optical emission spectrometry (ICP-OES) can be used for mercury analysis. However, these methods, compared to the previously mentioned analytical methods for mercury determination, are problematic for various reasons and are rarely used [3, 4].

Mercury can also be determined using biosensors. Because biosensors are characterized by their inherent simplicity, rapid analysis and easy handling, the use of biosensors to determine the concentration of Hg<sup>2+</sup> in samples has its own advantages over other analytical methods [5]. For example, a biosensor of catalase deposited on a carbon glass electrode. The linear concentration range of this produced biosensor is from 5×10<sup>-11</sup> to 5×10<sup>-10</sup> mol/L. A number of possible interferences in the measurement of mercury concentrations were tested, such as terbutryn, atrazine, cyanazine and Cl<sup>-</sup>, PO<sub>4</sub><sup>3-</sup>, SO<sub>4</sub><sup>2-</sup>, Na<sup>+</sup>, K<sup>+</sup>, Ni<sup>2+</sup>, Co<sup>2+</sup>, Zn<sup>2+</sup>, Cu<sup>2+</sup>, Pd<sup>2+</sup>, Pb<sup>2+</sup> ions and these interferences were found to have little or no effect on biosensor measurements [6].

We used Prussian Blue (PB) with inhibition enzyme to develop Hg<sup>2+</sup> ions sensible biosensor. This biosensor can quickly and using lower potential determine Hg<sup>2+</sup> ions concentration in the sample. Another biosensor advantage is that it is also very stable and can used more than once without losing sensitivity.

## References

1. R.A. Bernhoft, Mercury Toxicity and Treatment: A Review of the Literature, *Journal of Environmental and Public Health*. 2012 (2012).
2. N.J. Langford, R.E. Ferner, Toxicity of mercury, *Journal of Human Hypertension* 1999 13:10. 13 (1999) 651–656.
3. International standart ISO 5666. Water quality - Determination of mercury.
4. Selecting the Best Technique for Mercury Measurement A Practical Guide, (2017). [www.teledyneleemanlabs.com](http://www.teledyneleemanlabs.com)
5. B.D. Malhotra, Md. Azahar Ali, *Nanomaterials in Biosensors: Fundamentals and Application*, *Nanomaterials for Biosensors*. (2018).
6. B. Elsebai, M.E. Ghica, M.N. Abbas, C.M.A. Brett, Catalase based hydrogen peroxide biosensor for mercury determination by inhibition measurements, *Journal of Hazardous Materials*. 340 (2017) 344–350.

# Study of Properties of Europium-Doped Sodium Aluminum Germanate

**Marius Dzvinka**

*Institute of Chemistry, Vilnius University, Naugarduko st. 24 LT-03225 Vilnius, Lithuania  
marius.dzvinka@chgf.stud.vu.lt*

Luminescent materials nowadays are used among a variety of different applications, which attracts a lot of attention for studying such compounds. Many such materials can be obtained by doping a certain matrix with lanthanide ions. This work concentrates on NaAlGeO<sub>4</sub> doped with europium (III) ions, as properties of such compound are relatively unknown.

Samples (Na<sub>1-x</sub>AlGe<sub>1-0,5x</sub>O<sub>4</sub>Eu<sub>x</sub>) were obtained using solid-state synthesis. Stoichiometric amounts of sodium carbonate, aluminum oxide, germanium (IV) oxide and europium (III) oxide were weighed, mixed in agate mortar and sintered in 1000 °C for 6 hours.

The samples were firstly analyzed by X-ray diffractometer. Using the obtained X-ray diffraction results, it was deduced that all of the samples are single-phased. The aforementioned data was also used to refine the existing NaAlGeO<sub>4</sub> unit cell using the Rietveld method. It was determined that the occupancy of europium sites in the crystal cell directly correlates to the bulk concentration of europium during the solid-state synthesis.

The luminescent properties of the specimens were investigated by photoluminescence spectroscopy. Samples with x=0,04 and x=0,08 showed strongest emission when excited by light wavelength of 392,5 nm. The highest emission peaks observed were at 610 nm and 702,5 nm.

# Synthesis and Analysis of $Mg_2/Al_1-CO_3$ and $Zn_2/Al_1-CO_3$ Layered Double Hydroxide Modified Wood

Neringa Gailiūtė, Denis Sokol

Institute of Chemistry, Faculty of Chemistry and Geosciences, Vilnius University, Naugarduko st. 24, LT-03225 Vilnius

\*neringa.gailiute@chgf.stud.vu.lt

Wood has been used extensively for thousands of years and still is crucial to the fuel, construction, furniture and paper industries. Wood products are in high demand, simple to work with and mechanically durable. However, it ignites easily and is susceptible to moisture and various microorganisms [1].

Industrially used wood is usually treated with compounds that enhance its properties. Studies have demonstrated that impregnating wood with  $TiO_2$ ,  $ZnO$ ,  $Al(OH)_3$  and  $CuSO_4$  offers UV protection, hydrophobicity, antibacterial characteristics, reduces flammability and minimizes smoke emission during burning [2,3]. Due to the chemical properties of many commercially available and widely used antipyretics and antifungicides, wood is frequently impregnated only on the surface, which is neither practical, nor effective.

In this work, we used inorganic  $Mg_2/Al_1-CO_3$  and  $Zn_2/Al_1-CO_3$  based layered double hydroxides - LDH - to modify pine wood. Those LDH compounds retain a lot of water in their interlayer, are stable, non-toxic, insoluble in water and absorb heat when they break down into oxides and salts [4]. Zn-LDH has antibacterial properties [5,6]. Our used impregnation method allows wood to be impregnated not only on the surface but also inside, as seen in Figure 1.



**Fig. 1.** Photos of impregnated pine wood cubes, under same impregnation condition, with (left)  $Zn_2/Al_1-CO_3$  layered double hydroxide and (right) Indigo Carmine.

Due to successful and effective impregnation, obtained results of fire retardancy, mechanical and antibacterial tests of  $Mg_2/Al_1-CO_3$  and  $Zn_2/Al_1-CO_3$  LDH modified pine wood are expected to show improved properties.

## References

1. Andersone, Ingeborga & Andersons, Bruno et al., Handbook of wood chemistry and wood composites, second edition. (2012).
2. Guo, B., Liu, Y et al., Efficient Flame-Retardant and Smoke-Suppression Properties of Mg–Al-Layered Double-Hydroxide Nanostructures on Wood Substrate. ACS Applied Materials & Interfaces, 9(27), 23039–23047. (2017).
3. Humar, Miha & Petrič, Marko et al., Leaching of copper from wood treated with copper-based wood preservatives. 111-116. (2001).
4. Lv, S., Kong, X. et al., Flame-retardant and smoke-suppressing wood obtained by In situ growth of hydrotalcite-like compound on the inner surface of vessels. New Journal of Chemistry. (2019)
5. Velázquez-Herrera, F. D., Fetter et al., Effect of structure, morphology and chemical composition of Zn-Al, Mg/Zn-Al and Cu/Zn-Al hydrotalcites on their antifungal activity against *A. niger*. Journal of Environmental Chemical Engineering, 6(2), 3376–3383. 2018.
6. Cheng, H., Gao, X. et al., A novel antimicrobial composite: ZnAl-hydrotalcite with p-hydroxybenzoic acid intercalation and its possible application as food packaging material. New Journal of Chemistry. (2019).

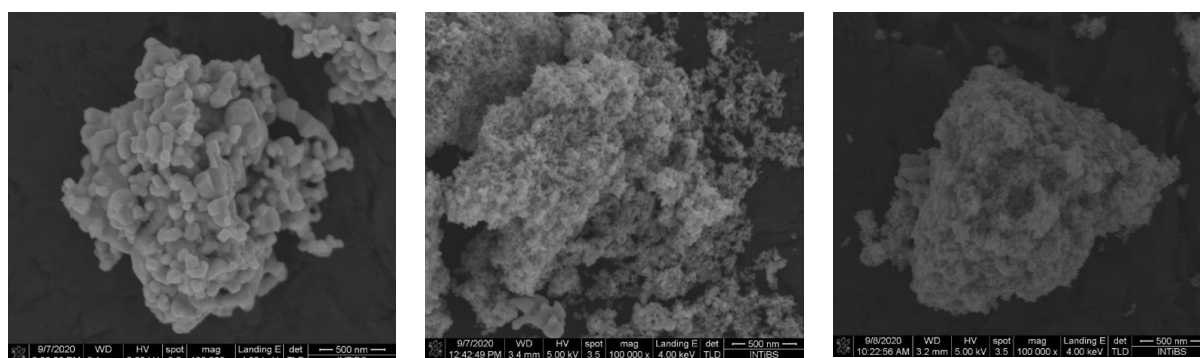
# Structure and Morphology of Bismuth Ferrite Layers Obtained by Sol-Gel Method on Different Substrates

Y. Gerasymchuk\*, A. Wędyńska, R. Tomala, D. Szymański, M. Ptak, W. Stręk,  
A. Łukowiak

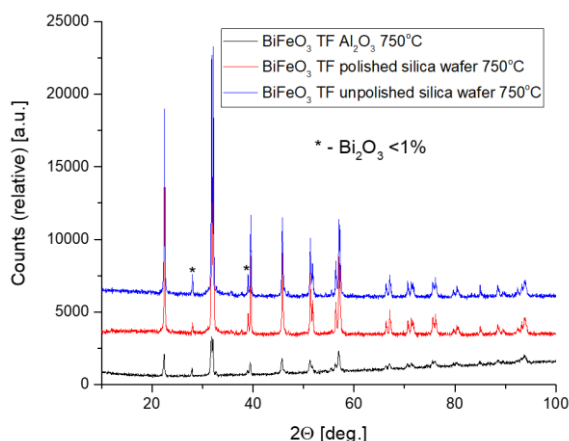
*Institute of Low Temperature and Structure Research, Polish Academy of Sciences, 50-422 Wrocław, Poland*

*\*Corresponding author, e-mail: y.gerasymchuk@intibs.pl*

Bismuth ferrite is one of the unique compounds that have both ferroelectric and antiferromagnetic properties. Its properties can be even more interesting when it is nanostructured and/or deposited as a thin film. In the presented studies, the procedure of obtaining layered structures of  $\text{BiFeO}_3$  was developed on the basis of the previously proposed method of obtaining nanometric ferrite powders [1-3]. After obtaining a gel based on glycine and ethylene glycol containing the starting iron and bismuth nitrates, the gel was applied to polished or unpolished silicon substrates as well as alumina disks using vacuum spraying. After calcination, depending on the type of the substrate, the bismuth ferrite formed on its surface nanocrystallites of various sizes and structures as presented in Figures 1 and 2.



**Fig. 1** SEM images for  $\text{BiFeO}_3$  deposited on corundum (left), unpolished (middle) and polished (right) silicon substrate, annealed at  $750^\circ\text{C}$ , and scratched from the substrates for measurement.



**Fig. 2.** X-ray diffraction patterns for  $\text{BiFeO}_3$  samples deposited on corundum and unpolished and polished silicon after annealing at  $750^\circ\text{C}$ .

## Acknowledgment

The research has received funding from the European Union's Horizon 2020 research and innovation programme under the Marie Skłodowska-Curie grant agreement No. 778070—TransFerr—H2020-MSCA-RISE-2017. Authors would like to thank V. Gaishun, D. Kovalenko, A. Semchanka, D. Karpinsky, and O. Ignatenko for their collaboration.

## References

1. T. Xian et al., *J. Alloys Cmpd.*, **480** (2009) 889–892.
2. J. Wang et al., *Mater. Lett.*, **124** (2014) 242–244.
3. M. Rahimkhania, D. Sanavi Khoshnood, *Procedia Mater. Sci.*, **11** (2015) 238 – 241.

# Phase Transformations of Amorphous Calcium Phosphate in Molten Salts

**E. Kabasinskas\*, D. Griesiute, D. Karoblis, E. Raudonyte-Svirbutaviciene, A. Zarkov**

*Institute of Chemistry, Vilnius University, Naugarduko 24, LT-03225 Vilnius,  
Lithuania*

*\*Corresponding author, e-mail: erlandas.kabasinskas@chgf.stud.vu.lt*

Synthetic calcium phosphates (CPs) are widely used in medicine as bone substitutes due to their excellent biocompatibility, osteoconductivity, and chemical composition similar to those of natural bone [1]. Most frequently, crystalline solids such as calcium hydroxyapatite (HAp,  $\text{Ca}_{10}(\text{PO}_4)_6(\text{OH})_2$ ), tricalcium phosphate (TCP,  $\text{Ca}_3(\text{PO}_4)_2$ ), or octacalcium phosphate (OCP,  $\text{Ca}_8\text{H}_2(\text{PO}_4)_6 \cdot 5\text{H}_2\text{O}$ ) are used for biomedical applications [2]. On the other hand, amorphous calcium phosphates (ACPs) also attract considerable attention in the field of biomaterials science and bone regenerative medicine due to their metastability, which can result in superior biochemical reactivity. Additionally, synthetic ACPs can be used as a precursor for the synthesis of other phosphate crystalline materials. While some CPs can be prepared directly by precipitation from aqueous solution, some phases can only be obtained by employing thermal treatment or conversion of less stable phases.

CPs can be characterized by different Ca-to-P ratios, which is usually fixed for crystalline materials with an exception for calcium-deficient hydroxyapatite (CDHA,  $\text{Ca}_{10-x}(\text{PO}_4)_{6-x}(\text{HPO}_4)_x(\text{OH})_{2-x}$ ), where this ratio can vary. Unlike crystalline solids, synthetic ACPs can be prepared as a substance with different Ca-to-P ratios ranging from 1.2 to 2.2. This ratio strongly depends on the formation conditions such as synthesis media, pH, and presence of foreign ions. In this study, we investigate the crystallization behavior of substituted ACP with a total metal ion-to-P ratio of 1.5:1. Such an elemental ratio is most commonly found in amorphous precipitates obtained in alkaline media. The crystalline analogue of an ACP with that chemical composition is TCP.

The main goal of the present study was to investigate the phase transformations of ACP in different molten salts. The influence of the flux nature, annealing temperature and time, precursors-to-flux ratio were investigated in detail. The crystallinity, crystal structure and structural changes were evaluated by powder X-ray diffraction (XRD), Fourier-transform infrared (FTIR) spectroscopy. Scanning electron microscopy (SEM) was used for the characterization of morphological features of products.

## References

1. W. Habraken, P. Habibovic, M. Epple and M. Böhner, *Mater. Today*, **19** (2016) 69–87.
2. S. V. Dorozhkin and M. Epple, *Angew. Chem., Int. Ed.*, **41** (2002) 3130–3146.

# Novel Co-Substituted Yttrium Gallium Garnets

S. Pazylybek<sup>1</sup>, A. Laurikenas<sup>2</sup>, T. Nurakhmetov<sup>3</sup>, D. Karoblis<sup>2</sup>, D. Vistorskaja<sup>2</sup>, G. Uazyrkhanova<sup>4</sup>, R. Raudonis<sup>2</sup>, A. Beganskiene<sup>2</sup>, A. Zarkov<sup>2</sup>, A. Kareiva<sup>2,\*</sup>

<sup>1</sup>Department of Physics, South Kazakhstan State Pedagogical University, 13 A Baitursynov St, Shymkent 160005, Kazakhstan

<sup>2</sup>Institute of Chemistry, Faculty of Chemistry and Geosciences, Vilnius University, Naugarduko 24, LT-03225 Vilnius, Lithuania

<sup>3</sup>Department of Technical Physics, L.N. Gumilyov Eurasian National University, 2 Satpaeva St, Nur-Sultan ZO1A3D7, Kazakhstan

<sup>4</sup>Department of Physics, D. Serikbayev East Kazakhstan Technical University, 69 Protozanov St, Ust - Kamenogorsk 070004, Kazakhstan

\*Corresponding author, e-mail: aivaras.kareiva@chgf.vu.lt

Mixed-metal garnets with novel chemical compositions ( $Y_{3-x-y-z}C_{ax}Ce_yLi_z1Ga_5O_{12}$ ) have been synthesized by a simple aqueous sol-gel method. The calcium-, cerium- and lithium-substitution effects in these mixed-metal garnets have been investigated. The sol-gel derived garnet samples were characterized by powder thermal analysis, X-ray diffraction analysis, FT-IR spectroscopy and scanning electron microscopy (SEM). The XRD patterns of these samples clearly showed that phase purity of differently co-substituted yttrium gallium garnets depends on chemical composition and the amount of substituent. Thermogravimetric analysis was employed to evaluate thermal decomposition behaviour and determine optimum annealing temperature, which is required for the formation of solid solutions. TG/DTG/DSC curves of the representative precursor gel for  $Y_{2.7}Ca_{0.3}Ga_5O_{12}$  composition compound are presented in Fig. 1.

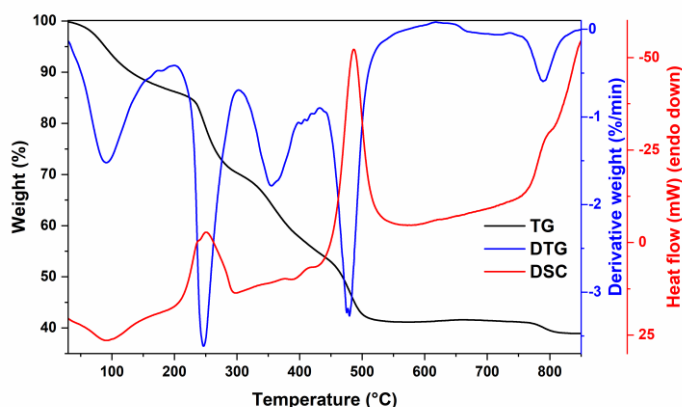


Fig. 1. TG/DTG/DSC curves of precursor gel for  $Y_{2.7}Ca_{0.3}Ga_5O_{12}$  garnet.

The luminescent properties of lanthanide-doped  $Y_{3-x-y-z}C_{ax}Ce_yLi_z1Ga_5O_{12}$  garnets are under investigation.

## Acknowledgements

S. P. is thankful for the Scholarship of the President of the Republic of Kazakhstan "Bolashak" (the Ministry of Education and Science of the Republic of Kazakhstan).



# Prussian Blue in Formation of Bio-Electrochemical Systems

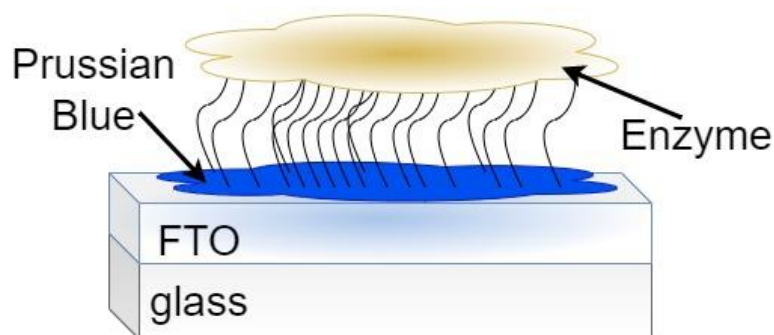
G. Kavaliauskaitė<sup>1\*</sup>, P. Virbickas<sup>1</sup>, A. Valiūnienė<sup>1</sup>

<sup>1</sup>Vilnius university, Institute of Chemistry, Naugarduko str. 24, LT-03225, Vilnius, Lithuania

\*Gabija Kavaliauskaitė, e-mail: gabija.kavaliauskaite@chgf.stud.vu.lt

Iron hexacyanoferrate (Prussian blue (PB)) is an inorganic, electrochromic compound, which is selective for several monovalent ions ( $\text{Cs}^+$ ,  $\text{Rb}^+$ ,  $\text{K}^+$  and  $\text{NH}_4^+$ ). These ions ( $\text{Cs}^+$ ,  $\text{Rb}^+$ ,  $\text{K}^+$  and  $\text{NH}_4^+$ ) are incorporated in the crystal lattice of PB when PB is electrochemically reduced in  $\text{Cs}^+$ ,  $\text{Rb}^+$ ,  $\text{K}^+$  or  $\text{NH}_4^+$  ions containing solution [1]. Moreover, the concentration of PB reduction promoting ions ( $\text{Cs}^+$ ,  $\text{Rb}^+$ ,  $\text{K}^+$  and  $\text{NH}_4^+$ ) affects the reduction potential of PB. For this reason, PB can be used as a signal transducer in optical and electrochemical analytical systems, such as electrochemical ion sensors [2]. Thus, Prussian Blue is often used as a redox mediator and signal transducer in biosensors, for example urea and glucose biosensors [3,4].

In this research work, Prussian Blue was used in formation of glass/FTO/PB/enzyme type electrodes, for the analysis of glucose and urea (Fig.1). Furthermore, these studies introduces the glass/FTO/PB/GOx electrode for optical glucose sensing and the glass/FTO/PB/urease electrode for electrochemical sensing of urea by using electrochemical impedance spectroscopy.



**Fig. 1.** Scheme of glass/FTO/PB/enzyme type electrode construction.

## References

1. A.A. Karyakin, E. E. Karyakina, L. Gorton, On the mechanism of  $\text{H}_2\text{O}_2$  reduction at Prussian Blue modified electrodes, *Electrochemistry Communications* **1**, p. 78 – 82 (1999)
2. A. A. Karyakin, Prussian Blue and Its Analogues: Electrochemistry and Analytical Applications, *Electroanalysis*, No. **10**, 13 (2001).
3. P. Virbickas, A. Valiuniene, G. Kavaliauskaite, A. Ramanavicius, Prussian White-Based Optical Glucose Biosensor, *Journal of The Electrochemical Society*, **166** (12), B927- B932 (2019)
4. A. Valiuniene, G. Kavaliauskaite, P. Virbickas, A. Ramanavicius, Prussian Blue based impedimetric biosensor, *Journal of Electroanalytical Chemistry*, **895**, (2021)

# Functionalization of Polyvinylchloride Textile Surface with Thin Films of Silver Oxide by Chemical Method

V. Krylova<sup>1,\*</sup>, M. Jucienė<sup>1</sup>, V. Dobilaitė<sup>1</sup>

<sup>1</sup>*Kaunas University of Technology, Donelaičio st. 73, LT-44249 Kaunas, Lithuania*

*\*Corresponding author, e-mail: valentina.krylova@ktu.lt*

A detailed analysis of smart textiles for architectural facades has shown that multifunctional textiles with functional coatings and energy recovery additions can provide suitable design solutions for lightweight, durable, low-cost, sustainable, and multifunctional architectural facades. This is a viable and sustainable construction solution [1]. Textile-based solar thermal energy collectors (TSTEC) are one form of novel flexible solar thermal harvesting product, and one that can widely be applied within the fields of building roofs and facades. The study found that the properties of TSTEC in terms of two-layer textile composition were much more efficient when compared to those, which had other numbers of layers. It was also found that a lower airflow velocity contributed to a higher outlet temperature, and that airflow velocity served to increase useful heat levels. It was further proven that an extension to the wind tunnel was very important when it came to being able to increase the efficiency levels of solar thermal energy conversion [2]. Thin film metal oxides are superior solar light absorbers. Many of the metal oxides are n-type semiconductors. Known p-type oxides include silver (I) oxide. They can be combined into a functional material when deposited on polymeric substrates. The optical band gap for Ag<sub>2</sub>O ranges from 1.2 eV [3] to 3.4 eV [4] depending on the stoichiometry, structure and physical properties that result from the deposition method.

In this study, silver oxide films were synthesised on a polyvinylchloride textile (PVC), and an investigation was carried out into the structural, optical, and mechanical properties of the treated fabric. The chemical deposition method was used to modify the PVC textile surface by means of thin silver oxide films. Prior to the process of depositing the materials, the mechanically roughened surface was pre-treated with two different solutions: thermo-alkaline and thermo-oxidative-acidic [5]. An X-ray diffraction (XRD) analysis was carried out in order to provide a level of understanding in regards to the formation of the silver oxide phase and its crystalline structure following the completion of the reactive thermo-chemical treatment of the prepared samples. The XRD analysis revealed that deposited films exist as polycrystalline mixed-phase material, which is composed of Ag<sub>2</sub>O, AgO, and metallic Ag. Ultraviolet-visible (UV-Vis) diffuse reflectance spectra were recorded to study the optical properties of deposited films. It was found that Ag-O/PVC composites are direct band gap semiconductors; the optical band gap is 0.89±0.02eV.

A determination was made of percentage changes for the fabric thickness, total mass per unit area after modification and tensile, and tear tests were carried out. The results showed that the treatment did not serve to negatively affect the structural properties of the PVC textile, while any relative difference of thickness is negligible. When evaluating the material for tear strength, it was found that after both alkaline and oxidative-acid treatments, no noticeable change in tear strength was observed in the longitudinal and transverse directions of the samples. When analysing the tensile characteristics, it was found that due to thermochemical treatment, the tensile strength of architectural textiles decreased in both directions.

## References

1. W.D. Abdul Jalil, IOP Conf. Ser.: Mater. Sci. Eng. **737** (2020) 012078.
2. H. Jia, X. Cheng, J. Zhu, Z. Li, J. Guo. Renew. Energy, **129** (2018) 553-560.
3. E. Fortiu, F.L. Weichman. Phys. Stat. Sol. B, **5** (1964) 515-524.
4. E. Lund, A. Galeckas, A. Azarov, E.V. Monakhov, B.G. Svensson. Thin Solid Films, **536** (2013) 156-159.
5. V. Krylova, N. Dukštienė, M. Lelis, S. Tučkutė. Surf. Interfaces, **25** (2021) 101184.

# Structural Characterizations of Cadmium Telluride-Cadmium Sulfide Layers on Polyamide 6

Miglė Liudžiūtė<sup>1\*</sup>, Skirma Žalėnienė<sup>1</sup>

<sup>1</sup> Department of Physical and Inorganic chemistry of Kaunas University of Technology,  
Radvilėnu St. 19, 50254 Kaunas, Lithuania  
miglė.liudziute@ktu.edu

Polyamide 6 is a polymer molecule which has the following characteristics: great mechanical properties, abrasion, long term heat resistance and others [1]. These days one of the choices for substrate to make photovoltaic cells is polyamides due to their mechanical flexibility, low-cost, etc. [2]. These polymers can be coated with a variety of semiconductor materials. One of those substances are cadmium chalcogenides (CdX, X=Te,Se S). This family of compounds can be included in manufacture of light emitting diodes, solar cells, transistors [3]. Cadmium telluride (CdTe) is one the most important semiconductor material due to its optimum band gap, high absorption coefficient, n-type, p-type conductivity [4]. Most often CdTe is mixed with cadmium sulphide (CdS) owing to the same reasons: optimum band gap, p-n junction, great sunlight absorption [5]. However, great properties of binary semiconductor are highly dependent on the structural, optical, compositional and other properties [4]. This experiment reviews the structural properties of CdTe-CdS mixture.

Polyamide 6 films used in this study were 500 μm thick, with the density of 1.13 g/cm<sup>3</sup> and the size of it was 15×70 mm. Prior to the experiments, part of the PA films was boiled in distilled water for 2 h (Sample 1, S1) while the other part films was treated in concentrated acetic acid at 20 °C for 0.5 h (Sample 2, S2). After that they were dried using a filter paper and kept in a desiccator over anhydrous CaCl<sub>2</sub>. The salts of potassium telluropentathionate (K<sub>2</sub>TeS<sub>4</sub>O<sub>6</sub>·1.5H<sub>2</sub>O), were prepared according to published procedure [6]. In the first stage, PA 6 films were chalcogenized from 1 to 5 h at 20 °C using an acidified (0.2 mol·dm<sup>-3</sup> HCl) 0.1 mol·dm<sup>-3</sup> solution of K<sub>2</sub>TeS<sub>4</sub>O<sub>6</sub>. In the second stage, PA samples were treated with the 0.1 mol·dm<sup>-3</sup> solution of cadmium acetate, (Cd(CH<sub>3</sub>COO)<sub>2</sub>·2H<sub>2</sub>O), for 10 min at the temperatures of 70, 80, 90 °C.

After preparation of both parts of samples, they were analysed by XRD technique on the Bruker D8 Advance diffractometer. PA 6 films were scanned over the range 2θ = 3–70° at a scanning speed of 1° min<sup>-1</sup> using a coupled two theta/theta scan type. This analysis determined structural characterization of the obtained materials.

Results obtained by XRD analysis indicated the composition and size of the crystals which formed the PA 6 films. The samples contain these compounds and elements: hexagonal cadmium telluride, orthorhombic cadmium sulphide, monoclinic sulphur and tellurium. The crystal material size is quite similar to each other, and it is mostly dependent on the preparation method. However, results show that in the S1 samples crystals sizes would increase consistently when increasing the chalcogenization time and the temperature of cadmium acetate. Meanwhile in the S2 samples crystals sizes were not consistent. It creates presumption that part of PA 6 surface was exposed to acetic acid and the layers of materials were covered unevenly.

XRD analysis showed that both S1 and S2 samples layers contain similar size crystals, nevertheless the biggest crystals were obtained on the surface of the S1 sample which was chalcogenized 1 hour and treated with 90 °C cadmium acetate solution.

## References:

1. L. W. McKeen, 8-Polyamides (Nylons). *Film Properties of Plastics and Elastomers*, p. 187-227 (2017).
2. Tec-Sánchez, J.A., Arias, A.I.O., Aguilar-Vega, M. et al. Preparation and Characterization of Flexible, Transparent and Thermally Stable Aromatic Co-polyamides. *Chin J Polym Sci* **37**, 136–141 (2019).
3. Mosayeb Naseri, D.M. Hoat, J.F. Rivas-Silva, Gregorio H. Cocolletzi, Electronic structure, optical and thermoelectric properties of cadmium chalcogenides monolayers. *Optik*, Vol. 210 (2020).
4. K. Punitha, R. Sivakumar, C. Sanjeeviraja, V. Ganesan, Influence of post-deposition heat treatment on optical properties derived from UV–vis of cadmium telluride (CdTe) thin films deposited on amorphous substrate. *Applied Surface Science*, Vol. 344, p. 89-100 (2015).
5. R. S. Kapadnis, S. B. Bansode, A. T. Supekar et al., Cadmium Telluride/Cadmium Sulfide Thin Films Solar Cells: A Review. *ES Energy & Environment*, **10**, p. 3-13 (2020).
6. Foss O., Salts of Monotelluropentathionic Acid. *Acta Chemica Scandinavica*. Vol. 3, p. 708–716. (1949)

# In-situ Synthesis of Calcium Phosphate Bioceramics Derived from Eggshells to Improve Strength and Fire Resistance of Scots Pine Wood

Gabija Navašinskaitė, Denis Sokol

*Institute of Chemistry, Faculty of Chemistry and Geosciences, Vilnius University, Naugarduko st. 24, LT – 30225, Vilnius*

*\*gabija.navasinskaite@chgf.stud.vu.lt*

Being a natural raw material with great mechanic and thermal insulation properties, which ensures a comfortable indoor climate, timber remains one of the prime choices for energy-efficient construction [1]. Compared to steel or concrete constructions, wooden ones require the least energy resources for the manufacturing purposes as well as have the smallest GHG emission rate [2]. However, wood-based constructions are inferior to steel or concrete based ones in terms of being a fire hazard and being more prone to weathering, which makes the surface of wood more susceptible to microorganisms such as bacteria and microscopic fungi [3]. Although scientists have already developed many ways to modify the wood as a means to improve its properties, the vast majority of them are costly and not environment-friendly [4].

The goal of this work is to enhance physicochemical properties of wood by utilizing eggshells as a  $\text{CaCO}_3$  source for bioceramic-reinforced wood materials. Egg production industry is an important part of EU agriculture. Eggshells which consist of 96% of mineral calcite are, however, considered waste material. Calcite is a compelling source of calcium and serve as a precursor for carbonated hydroxyapatite, a biocompatible ceramic material, i.e. not harmful or toxic to living organisms [5]. The in-situ synthesis of carbonated hydroxyapatite subsequently lead to wood mineralization, as seen in Figure 1. To an even greater extend, fighting the war against climate change and trying to minimize  $\text{CO}_2$  emission, the successful incorporation of mineral calcite within the wood matrix will result in a  $\text{CO}_2$  storing hybrid wood material.

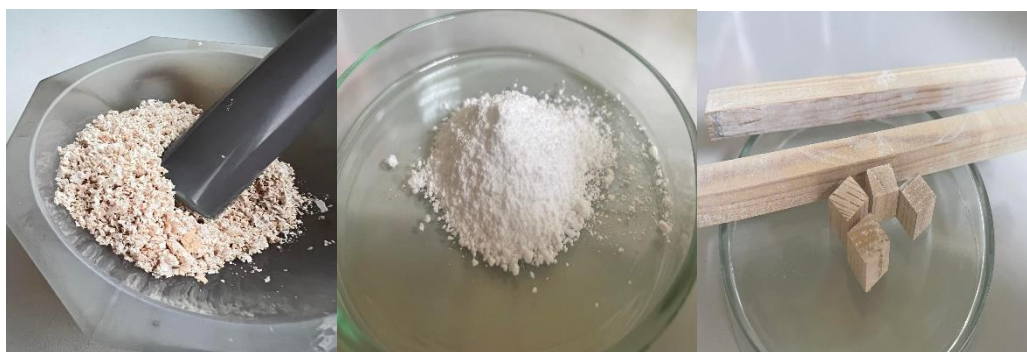


Fig. 1. Photos of grinded waste eggshell (left),  $\text{Ca}(\text{OAc})_2$  produces from eggshells (middle) and successfully mineralized pine wood with calcium phosphate bioceramics (right).

The main aim of the work is the reinforcement of locally produced pine wood with biocompatible calcium phosphate (CaP)-based ceramics to enhance mechanical strength and fire-retardancy.

## References

1. Kuzman, Manja & Grošelj, Petra. (2012). Wood as a construction material: Comparison of different construction types for residential building using the analytic hierarchy process. *Wood Research*. 57. 591-600.
2. Upton, B., Miner, R., Spinney, M., & Heath, L. S. (2008). The greenhouse gas and energy impacts of using wood instead of alternatives in residential construction in the United States. *Biomass and Bioenergy*, 32(1), 1–10.
3. Rowell, R.M. *Handbook of Wood Chemistry and Wood Composites*, 2nd ed.; CRC Press, Taylor and Francis Group: Boca Raton, FL, USA, 2012.
4. Hill Callum A. S. 2006. *Wood Modification: Chemical Thermal and Other Processes*. Chichester England: John Wiley & Sons.
5. K. Ronan and M. B. Kannan, *ACS Sustain Chem. Eng.*, 2017, 5, 2237.

# UV/Vis Investigation of Cu<sub>x</sub>S Thin Films Deposited on Polypropylene by Chemical Bath Technique

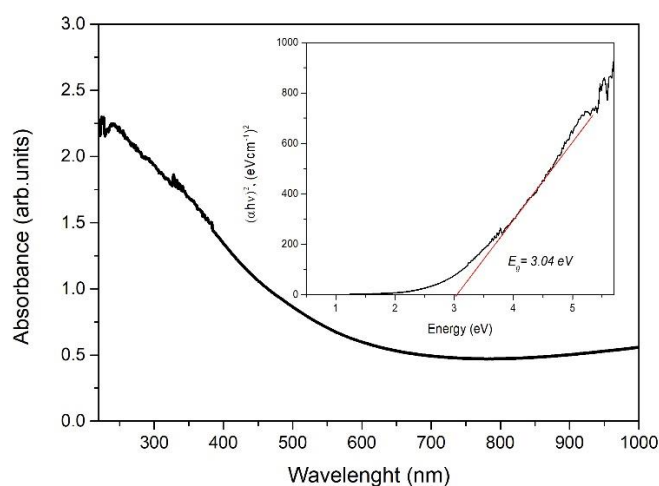
Neringa Petraškauskienė\*, Rasa Alaburdaitė, Edita Paluckienė

Department of Physical and Inorganic Chemistry, Kaunas University of Technology, Lithuania

\*Corresponding author, e-mail: neringa.petrasauskiene@ktu.lt

Copper sulfide (Cu<sub>x</sub>S) is a wide-band-gap p-type semiconductor material with modern applications ranging from industrial to biomedical. Various polymers, modified by copper sulfides, represent a new class of materials – composites with novel properties. Polymers, modified by Cu<sub>x</sub>S, are used as conductive substrates for the deposition of metals and semiconductors; as gas sensors functioning at temperatures tending to room temperature; as polarizers of infrared radiation; and as active absorbents of radio waves. Electrically conductive Cu<sub>x</sub>S films can be prepared by the chemical bath technique [1]. Polypropylene (PP) is a low-cost thermoplastic polymer with great chemical, physical, and mechanical properties.

Cu<sub>x</sub>S thin films were deposited on PP (density 0.9 g·cm<sup>-3</sup>, 150 μm thick) using CuCl<sub>2</sub> and Na<sub>2</sub>S<sub>2</sub>O<sub>3</sub> mixture for 16 h. The deposition process was carried out by repeating such deposition cycles up to 3 times. The aim of this work was to obtain Cu<sub>x</sub>S thin films by the chemical bath deposition method and to determine the effect of the variation of the number of cycles of deposition on the optical properties with a view to ascertaining the possible applications. UV/Vis absorption spectroscopy is a powerful tool for investigating the optical properties of a material.



**Fig. 1.** UV/Vis absorbance spectrum and plot of  $(\alpha h\nu)^2$  against  $h\nu$  (inset).

Fig.1 shows that the absorbance of Cu<sub>x</sub>S films (after 3 cycles of deposition) is generally high in the UV region (200-450 nm) and low in the visible spectrum (550-900 nm).

The variation of  $(\alpha h\nu)^2$  with  $h\nu$  is linear, indicating that a direct transition is present. Extrapolating the straight line portion of the plot of  $(\alpha h\nu)^2$  against  $h\nu$  to the energy axis for zero absorption coefficient gives an optical bandgap energy value of 3.04 eV.

## References

1. E. Balciaunaite, N. Petrasauskiene, R. Alaburdaite, G. Jakubauskas, E. Paluckiene, Surf. Interfaces, **21** (2020) 100801-100808.

# Simulating Microwave Field Distribution in a Novel Superconducting EPR Microresonator

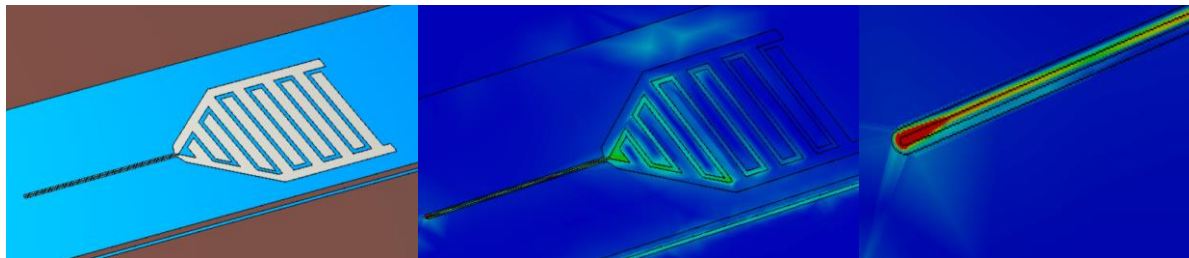
I. Pocius<sup>1,\*</sup>, P. Verbaitytė<sup>1</sup>, J. Banys<sup>1</sup>, M. Šimėnas<sup>1</sup>

<sup>1</sup>Faculty of Physics, Vilnius University, Sauletekio 9, LT-10222 Vilnius, Lithuania

\*ignas.pocius@ff.stud.vu.lt

Electron paramagnetic resonance (EPR) is a technique used to study and manipulate electron spins in various functional materials. Recently, major advances in EPR sensitivity were achieved using planar superconducting microresonators [1,2]. However, microresonators fabricated from conventional superconductors have severe limitations for conventional EPR due to their low temperature of operation. For this reason, microresonators fabricated from high- $T_c$  superconductors are gaining attention [3].

Here, we explore a novel planar “airplane” microresonator geometry coupled to a co-planar waveguide (Fig. 1) using the CST Microwave Studio computational electromagnetics tool. We analyze the distribution and homogeneity of the microwave magnetic field produced by the microresonator. Our results show that the highest magnetic field density is concentrated on the inductor region, although the undesirable contribution from the capacitor is also significant. We discuss ways to further improve the resonator design.



**Fig. 1.** Model of an “airplane” type resonator on a co-planar waveguide. Colour coding represents the intensity of the microwave magnetic field of the microresonator. The inductor region is emphasized in the enlarged figure.

## References

1. A. Bienfait, et al., Reaching the quantum limit of sensitivity in electron spin resonance, *Nature Nanotechnology* **11**, (2016) 253-257.
2. J.J.L. Morton, P. Bertet, Storing quantum information in spins and high-sensitivity ESR, *Journal of Magnetic Resonance* **287**, (2018) 128-139.
3. Ghirri, A. *et al.* YBa<sub>2</sub>Cu<sub>3</sub>O<sub>7</sub> microwave resonators for strong collective coupling with spin ensembles, *Appl. Phys. Lett.* **106**, 184101 (2015).

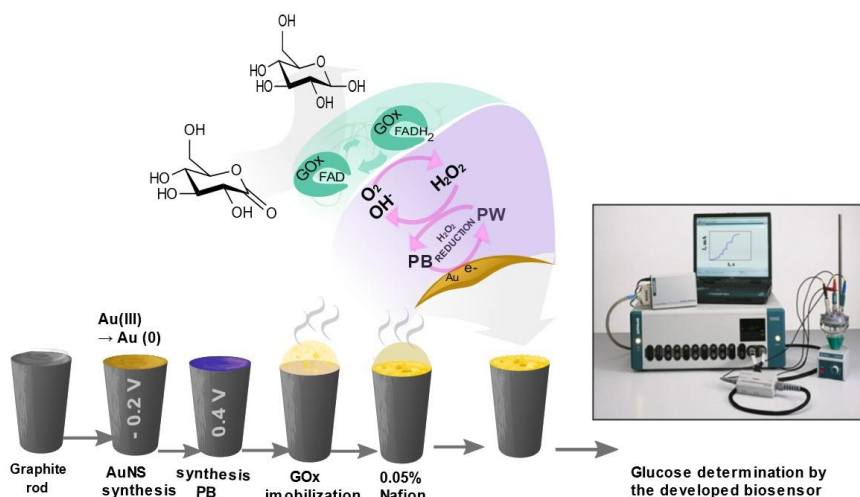
# Reagentless Electrochemical Glucose Biosensor Based on Electrochemically Deposited Gold Nanostructures and Prussian Blue

L. Sakalauskiene<sup>1</sup>, A. Popov<sup>1</sup>, B. Brasiunas<sup>1</sup>, A. Ramanaviciene<sup>1</sup>

<sup>1</sup>NanoTechnas—Center of Nanotechnology and Materials Science, Faculty of Chemistry and Geosciences, Vilnius University Vilnius, Lithuania  
e-mail: laura.sakalauskiene@chgf.vu.lt

As the number of people with diabetes increases every year, sensitive, selective, easy-to-use, and fast methods for determination of glucose level in the blood are greatly needed. Electrochemical biosensors based on immobilized enzymes have received considerable attention due to their exceptional selectivity, low limit of glucose detection, and high sensitivity [1]. The performance of such biosensors can be improved by the application of various metal nanoparticles and Prussian blue (PB) well known as an “artificial peroxidase”. Electrochemical glucose biosensors based on PB can register the electrocatalytic reduction of hydrogen peroxide ( $H_2O_2$ ) produced during enzymatic oxidation of glucose. The application of PB and gold nanostructure (PB/AuNS) composite on the electrode could additionally provide some advantages for the glucose biosensor characteristics. The synthesis of PB on AuNS ensures proper immobilization of PB on the electrode surface and helps to solve PB stability problem. Additionally, AuNS create a favourable microenvironment for retaining biological activity of immobilized enzymes [2].

In this work graphite rod (GR) electrode was electrochemically modified with AuNS and PB. Novel glucose biosensor was constructed using modified electrode by immobilizing glucose oxidase (GOx) and coating the surface with 0.05% solution of Nafion. The SEM images of AuNS/GR and PB/AuNS/GR electrodes confirmed that Prussian blue was successfully synthesized on the AuNS/GR electrodes. The biosensor based on Nafion/GOx/PB/AuNS/GR electrode exhibited excellent sensitivity for the  $H_2O_2$  produced during enzymatic reaction. The registered current response of the developed biosensor is proportional to glucose concentration in the range from 0.025 to 10.00 mM.



**Fig. 1.** Main steps of GR electrode modification and application of Nafion/GOx/PB/AuNS/GR electrode for the determination of glucose.

## References

1. L. Yan, K. Miao, P. Ma, X. Ma, R. Bi, and F. Chen, “A feasible electrochemical biosensor for determination of glucose based on Prussian blue – Enzyme aggregates cascade catalytic system,” *Bioelectrochemistry*, vol. 141, p. 107838, 2021, doi: 10.1016/j.bioelechem.2021.107838.
2. C. Wang *et al.*, “Glucose biosensor based on the highly efficient immobilization of glucose oxidase on Prussian blue-gold nanocomposite films,” *J. Mol. Catal. B Enzym.*, vol. 69, no. 1–2, pp. 1–7, 2011, doi: 10.1016/j.molcatb.2010.12.002.

# Effect of the Acid Sulphate Solution Additives on the Active Real Surface Area of the Electrodeposited Copper Honeycomb-Like Structures

B. Serapinienė\*, J. Juodkazytė, A. Selskis, R. Juškėnas, R. Ramanaukas

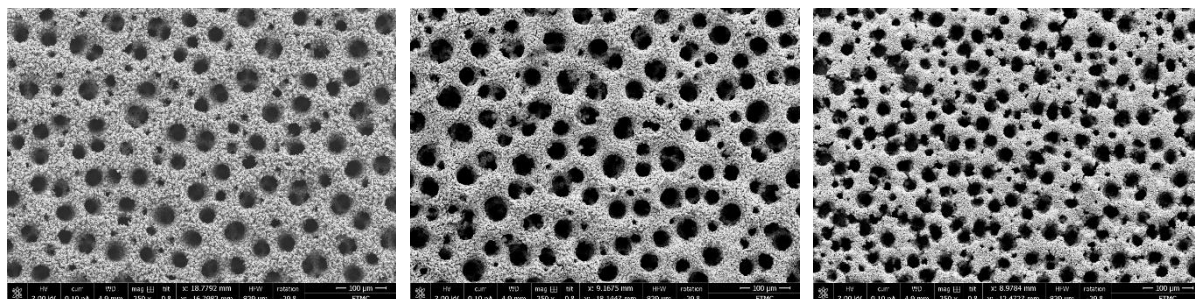
Center for Physical Sciences and Technology, Saulėtekio al. 3, LT-10257 Vilnius, Lithuania

\*Corresponding author, e-mail: birute.serapiniene@ftmc.lt

Reduction of greenhouse gas emissions is the main goal of Paris Agreement [1]. Electrochemical reduction of CO<sub>2</sub> is one of key solutions to this agreement. Metallic Cu-based nano catalysts have demonstrated to be promising for selective CO<sub>2</sub> reduction to HCOOH, CO, CH<sub>4</sub>, C<sub>2</sub>H<sub>4</sub> and C<sub>2</sub>H<sub>6</sub> with relatively high efficiency [2]. Smooth, polycrystalline or single crystal Cu electrodes are characterized by low catalytic activity for this process. Meanwhile, nanostructured Cu electrodes have been extensively explored as its open porous structure exhibits large electrochemical activity for CO<sub>2</sub> reduction.

Copper foams with highly open porous dendritic nanostructure have been successfully produced by electrodeposition process using hydrogen bubbles as dynamic templates. The pore sizes and wall structures of the foams are tunable by adjusting the deposition conditions [3]. Addition of the additives to the electrodeposition bath is simpler condition change.

The aim of this research was to find easy, fast and reliable real electrochemically active surface area measurement method for the evaluation of Cu honeycomb-like structure electrode deposited in an acid sulphate solution containing HCl and polyethylene glycol (PEG) additives. Accordingly, the real electrochemically active surface area of Cu honeycomb-like electrodes was assessed by the Cu oxidation-reduction (Cu<sub>2</sub>O monolayer formation) and underpotential deposition (UPD) of Pb monolayer methods. Surface of Cu honeycomb-like electrodes was analyzed with Scanning Electron Microscopy (SEM) (Fig. 1), while its phase composition and the grain size were evaluated using X-Ray diffraction (XRD).



**Fig. 1.** SEM images of Cu honeycomb-like structure made by electrodeposition (3 A/cm<sup>2</sup> current density for 20 s) respectively: 0,5 M CuSO<sub>4</sub> + 2,5 M H<sub>2</sub>SO<sub>4</sub> electrolyte, 0,5 M CuSO<sub>4</sub> + 2,5 M H<sub>2</sub>SO<sub>4</sub> + 1 mM HCl electrolyte, 0,5 M CuSO<sub>4</sub> + 2,5 M H<sub>2</sub>SO<sub>4</sub> + 1mM HCl + 0,1 mM PEG (2000) electrolyte.

XRD analysis revealed that the deposited Cu honeycomb-like structures were composed from Cu and Cu<sub>2</sub>O phases, while the grain sizes of the both of them varied around ~21 nm and ~26 nm respectively and were not influenced by the addition of chloride or PEG in the deposition electrolyte. Meanwhile, the determined values of electrochemical active surface area of the deposited sample showed, that addition of HCl into deposition solution yields ~1.7 times greater surface area, compared with the electrode, deposited from the solution without additives.

## References

1. <https://unfccc.int/process-and-meetings/the-paris-agreement/the-paris-agreement>
2. Xie, H., Wang, T., Liang, J., Li, Q., & Sun, S., Nano Today, Elsevier, UK, 2018.
3. Shin, H. C., & Liu, M., Chemistry of Materials, American Chemical Society, US, 2004.



# Optically Active Yttrium Aluminum Garnet and Silica Glass System

M. Skruodiene<sup>1\*</sup>, M. Leimane<sup>1</sup>, G. Inkrataite<sup>2</sup>, M. Kemere<sup>1</sup>, A. Sarakovskis<sup>1</sup>

<sup>1</sup> Institute of Solid State Physics, University of Latvia, 8 Kengaraga Street, LV-1063 Riga, Latvia

<sup>2</sup> Institute of Chemistry, Vilnius University, 24 Naugarduko Street, Vilnius, LT-03225 Vilnius, Lithuania

\*monika.skrudiene@cfi.lu.lv:

Silica glass is a typical amorphous material, which does not have secondary phases and grain boundaries. Glasses are the most well-known candidates for their better transparency, mechanical stability, thermal resistivity, and chemical durability. However, in the late '60s when glass-ceramics were discovered. Since then, many studies have been conducted on glass-ceramics (GC) materials as a completely new field of materials that could improve the needed properties. Doping glass with alkali, alkaline earth metal, transition metal, and/or lanthanide ions allows the development of phosphors for a variety of applications, including lighting and display devices such as light-emitting diodes, optical fibers, plasma display panels, safety signals, biological sensing, biological imaging, photocatalysts, and many others.

Garnet crystal structure is a very important matrix for optical applications. A wide variety of transition and/or rare-earth ions used as dopants to this matrix are extensively discussed over years. Cubic yttrium aluminum oxide is an attractive laser host material and a promising candidate for high-temperature structural applications, of its high chemical and thermal stability [1-3]. In the presented work, particles of yttrium/yttrium-lutetium/lutetium aluminum garnet doped with cerium ions were encapsulated in silica glass obtained by the sol-gel method are characterized. The morphology, glass composition, structure modification, and optical properties were analyzed. The main goal was to verify structural changes of the glass when the different concentrations of dopants are used into optically active glass.



**Fig. 1.** Photo of samples with different concentrations of phosphor: YLuAG:0.5 % Ce@SiO<sub>2</sub>, YAG:0.5 % Ce@SiO<sub>2</sub> and LuAG:0.5 % Ce@SiO<sub>2</sub>

## References

1. L. Skuja, N. Ollier, K. Kajihara, K. Smits, A. Silins, J. Phys. Stat. Sol., **218** (2021) 2100009.
2. S. Grandi, P. Mustarelli, S. Agnello, M. Cannas, A. Cannizzo, J. Sol-Gel. Sc. Tech., **26** (2003) 915-918.
3. G. Inkrataite, M. Kemere, A. Sarakovskis, R. Skaudzius, J. Alloys. Compd. **875** (2021) 160002.

# Influence of Grain Size on Properties of Lanthanum Manganite Nanocrystals and Nanoceramics

**R. Tomala<sup>1,\*</sup>, A. Łukowiak<sup>1</sup>, D. Karpinsky<sup>2</sup>, P. Gluchowski<sup>3</sup>, D. Kujawa<sup>3</sup>,  
Y. Gerasymchuk<sup>1</sup>, M. Ptak<sup>1</sup>, W. Stręk<sup>1</sup>**

<sup>1</sup> *Institute of Low Temperature and Structure Research, Polish Academy of Sciences, Wrocław Poland*

<sup>2</sup> *Namangan Engineering-Construction Institute, Namangan, Uzbekistan*

<sup>3</sup> *Nanoceramics Inc., Wrocław, Poland*

*\*Corresponding author, e-mail: R.Tomala@intibs.pl*

Multiferroic materials exhibit two or three primary ferroic properties, such as ferromagnetism, ferroelectricity or ferroelasticity, in the same phase. These materials are broadly investigated mainly due to their magnetoelectric properties that can be useful in random access memory, magnetometers, antennas, sensors, or voltage-tunable inductors [1]. In addition to magnetoelectric effect, other intriguing behaviors have been observed in nanostructured systems, that can be applied in photovoltaics, photocatalysis, photostriction, electrochromism, and gas-sensing [2]. Currently, it is particularly interesting to study new materials (other than BiFeO<sub>3</sub>) and composites as well as continue studies of the size-effect on the properties of nanostructures.

The presentation will give information on the fabrication of nanosized lanthanum manganite and nanoceramic prepared from the LaMnO<sub>3</sub> powder. Synthesis of nanocrystals was based on the self-combustion method where urea was used as a fuel and different annealing temperatures were used in the post-synthesis treatment. The nanoceramics were obtained using the high-pressure low-temperature method. The structure, crystallites' size, and properties of the nanocrystals and nanoceramics were analyzed and compared.

## Acknowledgment

The research has received funding from the European Union's Horizon 2020 research and innovation programme under the Marie Skłodowska-Curie grant agreement No. 778070—TransFerr—H2020-MSCA-RISE-2017.

## References

1. N. A. Spaldin, R. Ramesh, *Nature Mater.*, **18** (2019) 203.
2. S. Shevlin, *Nature Mater.*, **18** (2019) 191.

# Overview of Donors in Silicon for Spin-Based Quantum Technologies

Justinas Turčak<sup>1\*</sup>, Jūras Banys<sup>1</sup>, Mantas Šimėnas<sup>1</sup>

<sup>1</sup>Faculty of Physics, Vilnius University, Sauletekio 9, LT-10222 Vilnius, Lithuania

\*justinas.turcak@ff.stud.vu.lt

One of the necessary requirements for constructing a quantum computer [1] is a relatively long quantum coherence time in comparison to computational time. Donors in silicon have been proposed as a viable option for spin-based quantum technologies including spin ensemble quantum memories [2,3], offering both: easy qubit manipulation and robustness to external perturbations. The latter being enhanced at so-called ‘clock-transitions’, which increase the spin coherence time several orders of magnitude – up to several seconds for Bi dopant [4].

Here, we explore feasibility of group-VI donors in Si [5,6] for electron spin-based quantum technologies from theoretical standpoint. We derive transition frequency dependencies on magnetic field from spin Hamiltonian equations. This allows us to analytically find points representing both magnetic and electric field ‘clock-transitions’.

## References

1. D. P. DiVincenzo, The Physical Implementation of Quantum Computation, *Fortschritte der Physik*, **48**, 771-783 (2000).
2. B. E. Kane, A silicon-based nuclear spin quantum computer, *Nature*, **393**, 133-137 (1998).
3. A. Morello et al., Single-shot readout of an electron spin in silicon, *Nature*, **467**, 687-691 (2010).
4. G. Wolfowicz et al., Atomic clock transitions in silicon-based spin qubits, *Nature technology*, **8**, 561-564 (2013).
5. R.L. Nardo et al., Spin relaxation and donor-acceptor recombination of Se<sup>+</sup> in 28-silicon, *Physical Review B* **92**, 165201 (2015).
6. M. Šimėnas et al., Spin coherence of near-surface ionised <sup>125</sup>Te<sup>+</sup> donors in silicon, *Phys Rev Lett* in press (2022) arXiv:2108.07654

# Substitution Effects on the Stability and Electrochemical Properties of $\text{NaTi}_{2-x}\text{M}_x(\text{PO}_4)_3$ ( $\text{M} = \text{Zr(IV)}, \text{Hf(IV)}$ ) Anodes for Aqueous Sodium Ion Batteries

S. Tutlienė\*, J. Pilipavičius, J. Juodkazytė, L. Vilčiauskas

<sup>1</sup>Center for Physical Sciences and Technology, Savanorių ave. 231, LT-02300 Vilnius, Lithuania

\*Corresponding author, e-mail: skirmante.tutliene@fmc.lt

The climate change is forcing to diminish  $\text{CO}_2$  emissions immediately and globally. The great part of negative impact is coming from energy production. So, the move from fossil fuel to renewable energy resources is urgent. However, the electricity grid adaptation to the usage of sustainable energy, like sun and wind, is challenging. The need for reliable, cheap, and environmentally friendly energy storage technologies is one of the major unsolved problems. Nowadays, the Li-ion batteries are the dominant energy storage technology; however, imminent problems, like material criticality and ecological issues are pushing for alternatives. The promising candidate, especially in stationary energy storage technology, is aqueous Na-ion based batteries. Consequently, NASICON-structured  $\text{NaTi}_2(\text{PO}_4)_3$  (NTP) phosphate framework has been in the spotlight and continues to be investigated as the negative electrode material. Despite high regard, there are several problems for future applications to be resolved: NTP electrodes' degradation at aqueous electrolyte during long cycling procedure and self-discharge. When cycling rate is low at 1M  $\text{Na}_2\text{SO}_4$  (aq.) electrolyte, the pure NTP degrades noticeably.

Nonetheless, it is known that compounds' elemental composition variation changes their properties; so, the conductivity and crystal structure of NASICON-structured NTP can be altered. Therefore, partial replacement of  $\text{Ti}^{4+}$  by  $\text{Zr}^{4+}$  or  $\text{Hf}^{4+}$  was investigated. In this work we present the results of electrochemical properties and cycling stability in aqueous electrolytes when NTP is substituted with Zr(IV) or Hf(IV). The morphology, crystal structure and phase purity were determined by using SEM and XRD analysis methods. Moreover, Cyclic voltammetry and Galvanostatic charge/discharge cycling were performed to investigate the stability of the electrodes from sintered samples.

## Acknowledgement

This project has received funding from the European Regional Development Fund (Project No. 01.2.2-LMT-K-718-02-0005) under grant agreement with the Research Council of Lithuania (LMTLT).

# ESEEM Spectroscopy of Methyl Group Quantum Tunneling in Co<sup>2+</sup>-Doped Dimethylammonium Zinc Formate

Gediminas Usevičius<sup>1\*</sup>, Vidmantas Kalendra<sup>1</sup>, Andrea Eggeling<sup>2</sup>, Daniel Klose<sup>2</sup>, Gunnar Jeschke<sup>2</sup>, Andreas Pöppl<sup>3</sup>, Jūras Banys<sup>1</sup>, Mantas Šimėnas<sup>1</sup>

<sup>1</sup>Faculty of Physics, Vilnius University, Sauletekio av. 9, 10222 Vilnius, Lithuania

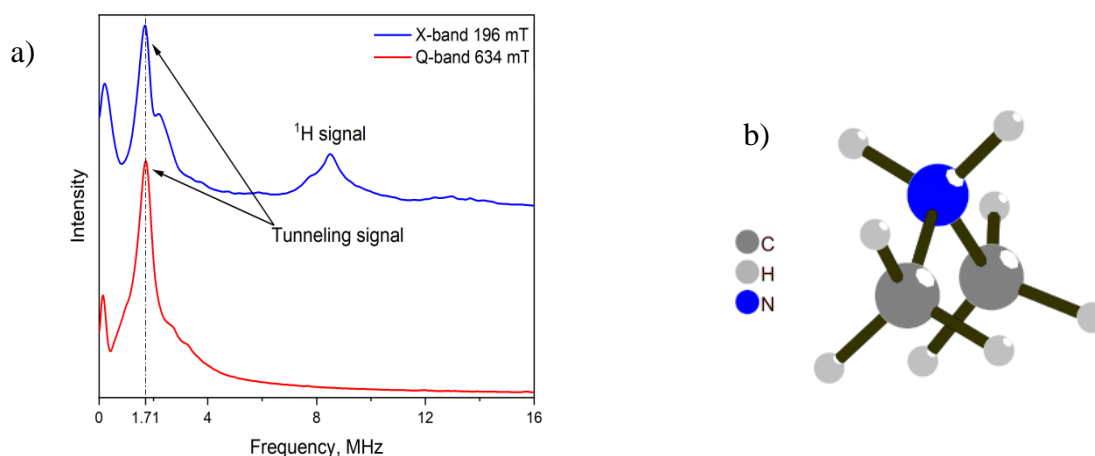
<sup>2</sup>Department of Chemistry and Applied Biosciences, ETH Zürich, Vladimir-Prelog-Weg 2, 8093 Zürich, Switzerland

<sup>3</sup>Felix Bloch Institute for Solid State Physics, Leipzig University, Linnéstr. 5, 04103 Leipzig, Germany

\*Gediminas Usevičius, gediminas.usevicius@ff.vu.lt

Methyl groups are ubiquitous functional groups in chemistry making them an abundant motif of organic and hybrid materials. At low temperature, the methyl group acts as a quantum rotor and undergoes quantum tunneling. Recently, quantum tunneling of methyl groups was observed using electron spin echo envelope modulation (ESEEM) spectroscopy in Mn<sup>2+</sup>-doped [(CH<sub>3</sub>)<sub>2</sub>NH<sub>2</sub>][Zn(HCOO)<sub>3</sub>] (DMAZn:Mn) hybrid perovskite [1]. Despite this and subsequent studies [2, 3], many unsolved problems remain, including the influence of relaxation times on observing the tunnel splittings.

In this work, we use Co<sup>2+</sup> as a paramagnetic center to study the methyl group tunneling in [(CH<sub>3</sub>)<sub>2</sub>NH<sub>2</sub>][Zn(HCOO)<sub>3</sub>] (DMAZn:Co) hybrid perovskite. The tunneling signal appears as a field-independent line in three-pulse ESEEM spectra (Fig. 1). By comparing our results with the Mn<sup>2+</sup> case, we investigate how paramagnetic dopants with different spin Hamiltonians and relaxation times affect the rotation barrier and thus the methyl group tunneling.



**Fig. 1.** (a) Three-pulse ESEEM spectra of DMAZn:Co obtained at 193 and 634 mT at 5 K. We observe a field-independent signal at 1.7 MHz, which originates from tunneling of the two methyl groups of the DMA cation shown in (b).

## References

1. M. Šimėnas, D. Klose, M. Ptak, K. Aidias, M. Mączka, J. Banys, A. Pöppl, G. Jeschke. *Sci. Adv.* 6, eaba1517 (2020).
2. G. Jeschke. *Appl. Magn. Reson.* 1, 17 (2021).
3. J. Soetbeer, L. F. Ibáñez, Z. Berkson, Y. Polyhach, G. Jeschke, *Phys. Chem. Chem. Phys.* 23, 5352 (2021).

# Lanthanide Oxalates: Synthesis, Structure, and Applications

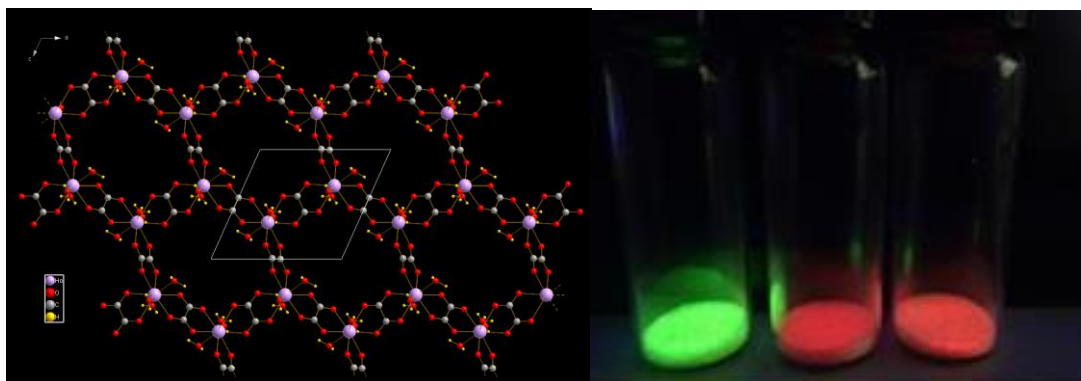
D.V. Ciesarová<sup>1</sup>, I. Kabitakis<sup>2</sup>, I. Císařová<sup>1</sup>, A. Alemayehu<sup>1</sup>, K. Lang<sup>2</sup>, J. Demel<sup>2</sup>, V. Tyrpekl<sup>1,\*</sup>,

<sup>1</sup> Department of Inorganic Chemistry, Faculty of Science, Charles University, Hlavova, 2030 Prague, Czech Republic

<sup>2</sup> Institute of Inorganic Chemistry of the Czech Academy of Sciences, 250 68, Husinec-Řež 1001, Czech Republic

\*Corresponding author, e-mail: vaclav.tyrpekl@natur.cuni.cz

Present work deals with the synthesis of lanthanide oxalates monocrystals, their structure determination and possible applications. Since oxalates are inexpensive and convenient salts used in the technology of transition metals, lanthanoids and actinoids. All this is thanks to their low solubility in aqueous solutions. Even though, the synthesis and properties oxalates might be considered as mastered, the opposite is true. We have developed a new synthetic route enabling growth of large crystals appropriate for crystal structure determination [1]. We focused predominantly on the heavy lanthanides, for which the literature showed large discrepancies in the structures and presence of crystalline water. Figure 1 shows the structure of Ho(III) oxalate hexahydrate (left) and one of the possible applications in optics - Tb(III) (green), Eu(III) (red), and Eu(III)-Tb(III) (1:1) (orange) oxalate powders under 365 nm excitation. Additionally, oxalates can be easily converted into oxides with possible application in solid oxide fuel cells and catalysts [2].



**Fig. 1.** Simplified sketch of the Ho(III) oxalate hexahydrate structure (left), Tb(III) (green), Eu(III) (red), and Eu(III)-Tb(III) (1:1) (orange) oxalate powders under 365 nm excitation (right).

## References

1. A. Alemayehu, A. Zakharanka, V. Tyrpekl, ACS Omega, **7** (2022) 12288-12295.
2. A. Alemayehu, D. Zákutná, S. Kohúteková, V. Tyrpekl, J. Amer. Ceram. Soc. **105** (2022) 4621-4631.

# Formation and Investigation of Cobalt Sulfide Layers on the Surface of Polyamide 6

Klaudija Vaičiukynaitė<sup>1,\*</sup>, Skirma Žalėnienė<sup>1</sup>

<sup>1</sup>Kaunas University of Technology, Radvilenu St. 19, LT-50254 Kaunas, Lithuania

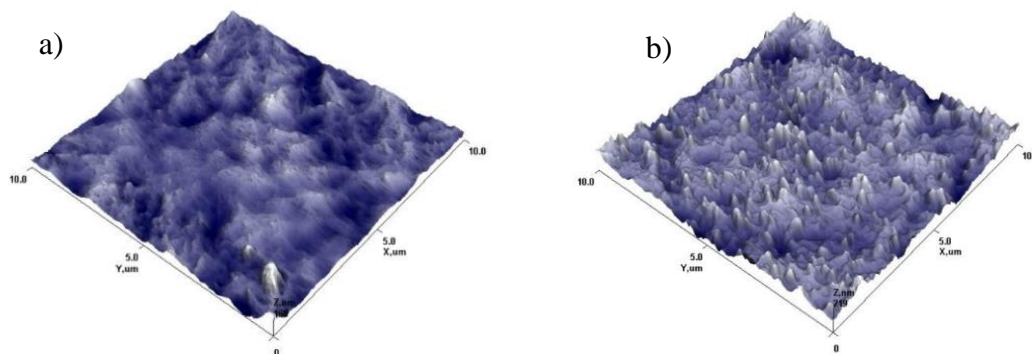
\*klaudija.vaiciukynaitė@ktu.lt

Nowadays, supercapacitors have a worldwide interest due to their high-power density and length of service. For this reason transition metal sulfides are being studied as a substance for energy storage because they can exist in several structures and demonstrates exceptional electrical conductivity [1]. The perfect example could be cobalt sulfides that have the above properties and might be used in lithium-ion or rechargeable alkaline batteries (as anodes), magnetic materials and catalysts. Nevertheless, despite these excellent possessions, scientists still face difficulties in synthesizing pure material. However, it is known, that conditions like temperature, reactant concentration and reaction time has the largest impact on the formation of certain structures that determine the properties and application of the resulting material [2].

The aim of this work is to form semiconductors cobalt sulfide layers on the surface of polyamide 6 and to investigate the properties of the obtained thin films using various analysis.

Polyamide 6 films used in this research were obtained from Ensinger (Germany). Before the experiment, PA films were boiled in distilled water for 2 h. After that, PA 6 films were kept in pentathionic acid ( $\text{H}_2\text{S}_5\text{O}_6$ ) from 1.0 to 5.0 h at room temperature. After interaction with acid, samples were treated with the  $0.16 \text{ mol}\cdot\text{dm}^{-3}$  solution of cobalt sulphate, ( $\text{CoSO}_4 \cdot 7\text{H}_2\text{O}$ ) for 10 minutes at different temperatures – 60, 70 and 80 °C (5 samples for each temperature).

After the formation of cobalt sulfide layers on PA 6 surfaces, films were investigated using X-ray diffraction (XRD) and atomic force microscopy (AFM) analysis. Morphological studies showed that sample demonstrates the best properties when sulfurized for 1 hour and kept in a cobalt salt solution at 60 °C - it has the most homogeneous surface possibly due to the evenly formed layer of  $\text{Co}_x\text{S}_y$  (Fig. 1 (a)). Meanwhile, when sample was sulfurized for 5 hours and kept at 80 °C temperature cobalt salt solution, the roughest surface was obtained because it failed to form the layer of cobalt sulfides (Fig. 1 (b)).



**Fig. 1** Images of atomic force microscopy (AFM) analysis: a – PA 6 sample sulfurized for 1 hour and kept in a cobalt salt solution at 60 °C temperature; b – PA 6 sample sulfurized for 5 hours and kept in a cobalt salt solution at 80 °C temperature

## References

1. W. Yang, et al. Chemical Engineering Journal, **434** (2022) 134473.
2. Q. Wang, et al. CrystEngComm, **13** (2011) 6960-6963.

# Hydration Properties of Mayenite and Gypsum Mixture

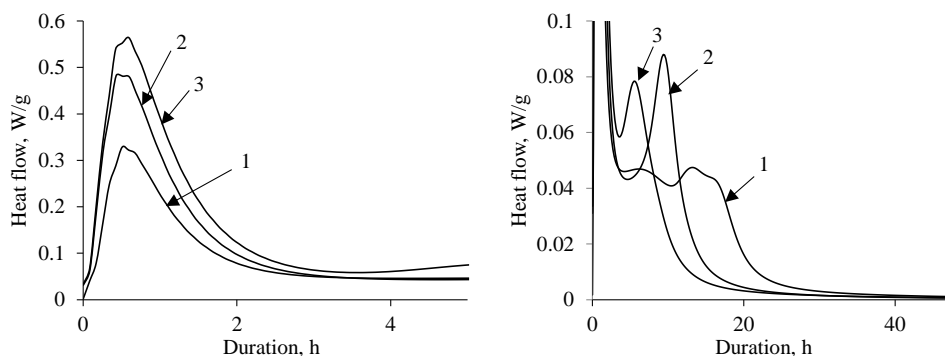
K. Vasiliauskiene<sup>1,\*</sup>, A. Eisinis<sup>1</sup>

Department of Silicate Technology, Kaunas University of Technology, Radvilenu 19, LT-50270 Kaunas,  
\*Kristina.ruginyte@ktu.lt

Mayenite ( $\text{Ca}_{12}\text{Al}_{14}\text{O}_{33}$ ) is a highly interesting functional material not only in view of its unique crystal structure but also for its variety of possible applications: catalysis (oxidation and reduction, ammonia synthesis), environmental sensors and  $\text{CO}_2$  sorbent materials [1,2]. In addition to the aforementioned possibilities of using mayenite, it is also constituent part of compounds in calcium aluminate and calcium sulfoaluminate cement clinkers [3]. It should be noted that, mayenite additives accelerates ettringite formation and change Portland cement hydration mechanism [4]. For this reason, the hydration experiments of mayenite and gypsum mixture samples were performed.

Mayenite synthesis was carried out in two stages: hydrothermal synthesis (4 h, 130 °C) and calcined (1 h, at 350 °C). Dry primary mixtures with differences mass ratio of gypsum and mayenite: 1.755 (labelled: CA1\_2.5); 0.855 (labelled: CA1\_5) and 0.555 (labelled: CA1\_7.5) were mixed. These ratios were calculation, which corresponds to the mentioned compounds mass ratio in OPC with mayenite additives (a partial replacement of the OPC at 2.5; 5 and 7.5 % by weight of the total cementitious material). The heat release kinetics of the samples was investigated with an isothermal calorimeter at 25 °C for 60 h when the ratio of the primary water/solid mixtures was equal to 0.75.

It was determined that in all samples initial reaction start slowly because maximum heat evolution rate was observed after 40 min of hydration. It should be emphasized that hydration at this stage is accelerated by mayenite because this effect grows as the mayenite level increases (Fig. 1). Besides, the accelerating effect began after 4-5 h of hydration in all samples and the maximum values of heat flow of the second exothermic reaction were determined, when mayenite amount decrease, i.e. 0.08 W/g at 8 h, 0.085 W/g at 10 h and 0.047 W/g at 13 h. After 72 h of hydration, the highest quantity of the total heat (~460 J/g) was obtained in the CA1\_5 mixture, while in the CA1\_7.5 and CA1\_2.5 samples, were slightly lower and reached very similar values (>450 J/g). In order to determine the mineralogical composition of hydration products, CA1\_2.5, CA1\_5, CA1\_7.5 mixture was hydrated using ratio of water/cementitious mixtures 0.75 at 25 °C, which were characterized by XRD, STA, and FT-IR analysis.



**Fig. 1.** The heat evolution rate of mayenite and gypsum mixture, curves: 1 – CA1\_2.5, 2 – CA1\_5 and 3 – CA1\_7.5 samples during the early stage of hydration (a water/solid ratio of 0.75).

## References

1. R. Cucciniello et al., Mayenite based supports for atmospheric  $\text{NO}_x$  sampling, *Atmos. Environ.*, 79 (2013)66-71
2. Hongjie Wu et al.,  $\text{CO}_2$  methanation over  $\text{Ru}/12\text{CaO}\cdot 7\text{Al}_2\text{O}_3$  catalysts: Effect of engaged anions on catalytic mechanism, *Appl. Catal.*, 595(2020)474
3. M. CarmenMartín-Sedeño et al., Aluminum-rich belite sulfoaluminate cements: Clinkering and early age hydration, *Cem. Concr. Res.*, 40(2010)359-369
4. K. Baltakys et. al., The Effect of calcined mayenite on the hydration of ordinary Portland cement, *Ceramic. Int.*, 2022.



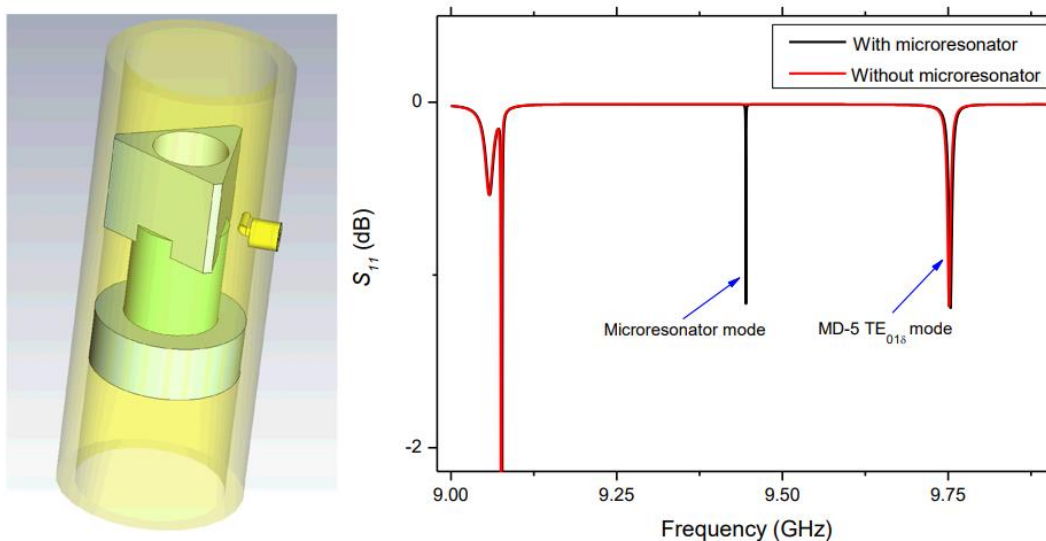
# Coupling of Microwaves to a Planar EPR Microresonator Via a 3D Cavity

Paulina Verbaitytė<sup>1\*</sup>, Gediminas Usevičius<sup>1</sup>, Vidmantas Kalendra<sup>1</sup>, Jūras Banys<sup>1</sup>, Mantas Šimėnas<sup>1</sup>

<sup>1</sup> Faculty of Physics, Vilnius University, Sauletekio 9, LT-10222 Vilnius, Lithuania  
[paulina.verbaityte@ff.stud.vu.lt](mailto:paulina.verbaityte@ff.stud.vu.lt)

Electron Paramagnetic Resonance (EPR) is a broadly used technique to study and manipulate electron spins across different disciplines covering quantum information, material science, physics and biology. However, in conventional EPR spectroscopy, sensitivity often limits the range and type of systems that can be studied. Recently, major advances in EPR sensitivity were achieved using planar superconducting microresonators [1,2]. However, these applications were limited to very low temperatures and spins in substrates of the resonators severely limiting the applicability of such resonators for conventional EPR samples. Thus, the full potential and compatibility of such microresonators to study a more general spin systems remains to be shown, which requires solving of several problems such as a convenient coupling to the driving microwave field.

Here, we explore the feasibility of microwave coupling to a planar EPR microresonator using a standard 3D cavity. First, we use CST Microwave Studio computational electromagnetics tool to simulate frequency response of a Bruker MD-5 dielectric ring resonator (Fig. 1). Our simulations successfully reproduce the resonance frequency of about 9.75 GHz of the  $TE_{018}$  mode of the resonator, which is revealed in the calculated frequency response of the  $S_{11}$  scattering parameter (Fig. 1). Then we use this model as a basis to simulate microwave coupling to a planar microresonator placed into an EPR tube, which is then inserted into the dielectric ring resonator. Our simulation successfully produces additional resonance frequency of microresonator on substrate (Fig. 1). We compare our simulation results with the experimental observations and further discuss the best coupling geometry.



**Fig. 1.** Model of a Bruker MD-5 dielectric resonator (left) and simulation of its microwave response with and without inserted microresonator at X-band (right).

## References

1. Bienfait, et al., Reaching the quantum limit of sensitivity in electron spin resonance, *Nature Nanotechnology* **11**, 253-257 (2016).
2. J.J.L. Morton, P. Bertet, Storing quantum information in spins and high-sensitivity ESR, *Journal of Magnetic Resonance* **287**, 128-139 (2018).

# Electrochemical Prussian Blue-based Hypochlorite Sensor

G. Žižiūnaitė<sup>1\*</sup>, A. Valiūnienė<sup>1</sup>, P. Virbickas<sup>1</sup>

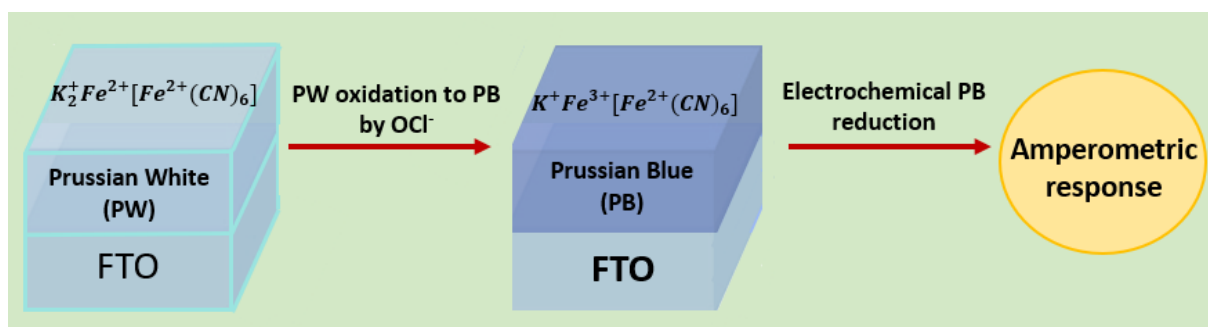
<sup>1</sup>Vilnius university, Institute of Chemistry, Naugarduko str. 24, LT-03225, Vilnius, Lithuania

\*Gerda Žižiūnaitė, e-mail: gerda.ziziunaite@chgf.stud.vu.lt

Prussian blue (iron hexacyanoferrate, PB) is a synthetic coordination compound [1], which due to its electrocatalytic and electrochromic properties is used for manufacturing of electrochemical devices [2], including electrochemical sensors [3,4]. Redox transitions between oxidated and reduced forms, Prussian Blue and Prussian White (PW) can occur both electrochemically and chemically, therefore quantitative detection of PB-reduced species is possible. PB gained its name as “artificial peroxidase” due to its highly selective reduction of hydrogen peroxide, which happens as a result of unique electrocatalytic mechanism – redox reaction occur as oxidator gets entrapped in crystal lattice of PB, therefore only certain species (such as O<sub>2</sub>, H<sub>2</sub>O<sub>2</sub>) that are small enough in size to enter the crystal lattice can be reduced [1].

In this research, electrochemical hypochlorite (OCl<sup>-</sup>) sensor was created by electrochemically depositing a layer of Prussian blue on a glass slide coated with tin oxide (glass|FTO|PB). Such electrochemical sensor could potentially be applied for detection of hypochlorite in water that was disinfected by the means of chlorination.

In order to characterize glass|FTO|BM analytical response as reduction of hypochlorite, optical absorption and cyclic voltammetry investigations were carried out. The possible impact of ions commonly found in hypochlorite-containing solutions (OCl<sub>3</sub><sup>-</sup>, OCl<sub>4</sub><sup>-</sup>) for analytical signal was analysed.



**Fig. 1.** Schematic representation of the glass|FTO|PB-based amperometric hypochlorite sensor.

## References

1. Biao Kong, Cordelia Selomulya, Gengfeng Zheng, Dongyuan Zhao. New faces of porous Prussian blue: interfacial assembly of integrated hetero-structures of sensing applications, *Chemical Society Reviews*, 44(22), 7997–8018 (2015).
2. C. D. Wessells, S. V. Peddada, M. T. McDowell, R. A. Huggins, Y. Cui, Nickel hexacyanoferrate nanoparticle electrodes for aqueous sodium and potassium ion batteries, *Nano Letters*, 11(12), 5421–5425 (2011).
3. A. Valiūnienė, G. Kavaliauskaitė, P. Virbickas, A. Ramanavičius, Prussian blue based impedimetric urea biosensor, *J. Electroanal. Chem.*, 895, 115473 (2021).
4. P. Virbickas, A. Valiūnienė, A. Ramanavičius, Towards electrochromic ammonium ion sensors, *Electroch. Commun.*, 94, 41–44 (2018).

# The Performance of Waste Nanomaterial in the Remediation of a Real Aluminum Anodizing Wastewater

E. Zubrytė\*, A. Gefenienė, R. Ragauskas, S. Jankauskas, R. Ramanauskas

State research institute Center for Physical Sciences and Technology<sup>1</sup>, Public Institution. Savanorių ave. 231, LT-02300 Vilnius, Lithuania

\*Corresponding author, e-mail: edita.zubryte@ftmc.lt

Aluminum is a metal anodized on a large scale. The anodising process consists of various pre-treatment and post-treatment stages and consumes a lot of water [1-2]. Aluminum, especially in the form of  $\text{Al}^{3+}$ , is considered the potential toxic to ecosystem and human health [3]. Different techniques have been used for the treatment of wastewater from the aluminum anodizing industry [3-5]. The search of alternative absorbents that can be used for the removal of aluminum is of great environmental interest. Limited information is available on aluminum removal from a real anodizing wastewater. The main objective of this study was to evaluate the use of groundwater deironing residuals (GDR) as a low-cost and environmentally friendly waste nanomaterial for the simultaneous removal of aluminum and color from the aqueous phase. Different GDR characterization methods were involved to ascertain and understand the action of solid waste in the aluminum removal process. SEM and TEM studies showed that the amorphous GDR consist of agglomerated 50-100 nm spherical particles. The calcination of GDR resulted in the formation of a crystalline cubic phase of maghemite and hexagonal phase of  $\text{SiO}_2$ . Elemental composition of the waste nanomaterial and chemical states of the elements were determined by X-ray fluorescence spectroscopy, EDX and XPS analysis. The GDR is the mesoporous-macroporous material rich in iron(III) oxides and oxyhydroxides with the BET surface area of about  $35 \text{ m}^2 \text{ g}^{-1}$ . The surface charge distribution of the GDR at various solution pH values were determined from  $\text{pH}_{\text{zpc}}$ . Batch studies were carried out to treat a real aluminum anodizing wastewater. The optimal conditions and parameters were determined. Aluminum ( $\text{Al}^{3+}$ ) concentrations were monitored by inductively coupled plasma-optical emission spectrometry. Simultaneous removal of aluminum species and wastewater color took place. The optimal remediation conditions were selected by varying the waste nanomaterial dosage, the aqueous phase acidity/basicity and remediation pathway. pH of the wastewater was regulated to achieve the desired transformations of aluminum species because at  $\text{pH} < 4$ , aluminum exists in the form of  $\text{Al}^{3+}$ , at  $\text{pH} > 8$ ,  $\text{Al}(\text{OH})_4^-$  is predominant and in the range of  $4 < \text{pH} < 6$ ,  $\text{Al}(\text{OH})_2^+$ ,  $\text{Al}(\text{OH})^+$  and  $\text{Al}(\text{OH})_3$  species exist [6]. According to the obtained results, the possible mechanism of the aluminum removal may be chemical precipitation, complexation and adsorption. The experiments demonstrated that a two-stage treatment using waste nanomaterial provided a near-100% aluminum removal efficiency.

The waste nanomaterial may be a promising alternative adsorbent for the removal of aluminum in the small-scale manufacturing facilities.

## References

1. N. Ates, N. Uzal, Environ. Sci. Pollut. Res., **25** (2018) 22259-22272.
2. J.O. Ighalo, I.A. Obiora-Okafo, K. Dulta, F.O. Omoarukhe, C.A. Igwegbe, S.O. Ebhodaghe. Water Conservation Science and Engineering, **7** (2022) 65-76.
3. L. Delgadillo-Velasco, V. Hernández-Montoya, L. A. Ramírez-Montoya, M. A. Montes-Morán, Ma. del Rosario Moreno-Virgen, N. A. Rangel-Vázquez, J. Mol. Liq. **323** (2021) 114586.
4. O. Kaan Türk, A. Zoungrana, M. Çakmakci. J. Environ. Chem. Eng. (2022) 108036.
5. B. Yuzer, M. Iberia Aydin, H. Yildiz, B. Hasançebi, H. Selcuk, Y. Kadmi, Chem. Eng. J. **434** (2022) 134755.
6. T. T. N. Nguyen & M. S. Lee. Geosyst. Eng. **22** (2019) 232-238.

# INDEX

---

## A

Afonina, A. ....	39
Alaburdaitė, R. ....	56, 69
Aleksandravičius, E. ....	53
Alemayehu, A. ....	78
Antuzevics, A. ....	54
Astrauskytė, D. ....	57
Aukštakojytė, R. ....	23, 43

---

## B

Baba, M. A. ....	33
Back, M. ....	26
Baltakys, K. ....	25
Baltrūnas, D. ....	38
Banys, J. ....	70, 75, 77, 81
Barkauskas, J. ....	23, 29, 43, 49
Baublytė, M. ....	44
Beganskienė, A. ....	38, 47, 64
Borak, B. ....	32
Brasiūnas, B. ....	71
Brimas, E. ....	42
Budrevičius, D. ....	58

---

## C

Ciesarová, D. V. ....	78
Císařová, I. ....	78

---

## D

Dambrauskas, T. ....	25
Damolskis, M. ....	52
Demel, J. ....	78
Dėnas, N. ....	59
Diliautas, R. ....	38
Dobilaitė, V. ....	66
Drazdys, M. ....	57
Drazdys, R. ....	57
Dzvinka, M. ....	60

---

## E

Eggeling, A. ....	77
Eisinas, A. ....	80
Ežerskytė, E. ....	20

---

## G

Gaidukevič, J. ....	23, 29, 43, 46, 49
Gailevičius, D. ....	53, 57
Gailiūtė, N. ....	61
Galvanauskas, K. ....	57

Garškaitė, E. ....	38
Gefenienė, A. ....	83
Gerasymchuk, Y. ....	32, 62, 74
Getautis, V. ....	21
Gluchowski, P. ....	74
Grieciūtė, D. ....	17, 37, 54, 63
Grigoravičiūtė, I. ....	39, 50
Grinevičiūtė, L. ....	57
Gudavičiūtė, L. ....	31

---

## H

Hałubek-Głuchowska, K. ....	32
Hayashi, K. ....	19

---

## I

Inkrataitė, G. ....	45, 73
---------------------	--------

---

## J

Jankauskas, S. ....	83
Januškevičius, J. ....	51
Jeschke, G. ....	77
Jucienė, M. ....	66
Juodėnas, M. ....	33
Juodkazytė, J. ....	72, 76
Jušėnas, R. ....	31, 72

---

## K

Kabašinskas, E. ....	63
Kabitakis, I. ....	78
Kalendra, V. ....	77, 81
Karalkevičienė, R. ....	46
Kareiva, A. ....	17, 38, 39, 42, 46, 47, 48, 50, 51, 54, 58, 64
Karoblis, D. ....	38, 63, 64
Karpinsky, D. ....	48, 74
Katelnikovas, A. ....	20, 54
Kaušaitė-Minkštienė, A. ....	27
Kavaliauskaitė, G. ....	65
Kemere, M. ....	45, 73
Khinevich, N. ....	33
Kirdeikienė, A. ....	31
Kizalaitė, A. ....	17, 37
Klimavičius, V. ....	17, 54
Klimkevičius, V. ....	20
Klose, D. ....	77
Klydžiūtė, G. ....	47
Knozowska, K. ....	22
Kozłowski, M. ....	23
Krunks, M. ....	30
Krylova, V. ....	66
Kujawa, D. ....	74
Kujawa, J. ....	22
Kujawski, W. ....	22
Kyshkarova, V. ....	41

---

**L**

Lang, K. ....	78
Laurikėnas, A. ....	64
Leimane, M. ....	73
Li, G. ....	22
Linkaitė, G. ....	50
Lisytė, V. ....	27
Liudžiūtė, M. ....	67
Lukavičiūtė, L. ....	47
Łukowiak, A. ....	32, 62, 74

---

**M**

Malinauskas, M. ....	53, 57
Mardosaitė, R. ....	33
Matijūnas, M. ....	56
Mažeika, K. ....	38
Melnyk, I. ....	40, 41
Merkininkaitė, G. ....	53
Meyer, G. H. ....	34
Mikoliūnaitė, L. ....	24
Mudring, A.-V. ....	28
Mykolaitis, J. ....	33

---

**N**

Navašinskaitė, G. ....	68
Niaura, G. ....	24, 38, 48, 49
Nurakhmetov, T. ....	64

---

**P**

Pakalniškis, A. ....	48, 58
Paluckienė, E. ....	69
Pauliukaitė, R. ....	23, 43
Pazyłbek, S. ....	64
Peckus, D. ....	33
Petrašauskienė, N. ....	69
Pilipavičius, J. ....	31, 76
Pocius, I. ....	70
Popov, A. ....	27, 71
Pöppel, A. ....	77
Ptak, M. ....	62, 74

---

**R**

Rabu, P. ....	16
Račkauskas, S. ....	33
Ragauskas, R. ....	83
Raišeliėnė, R. ....	50
Ramanauskas, R. ....	31, 72, 83
Ramanavičienė, A. ....	27, 71
Ramanavičius, S. ....	18
Raudonis, R. ....	42, 64
Raudonytė-Svirbutavičienė, E. ....	17, 46, 47, 63
Rimkutė, G. ....	49

---

**S**

Sakalauskienė, L. ....	71
------------------------	----

Šakirzanovas, S. ....	52, 53
Sarakovskis, A. ....	45, 73
Selskis, A. ....	31, 72
Serapinienė, B. ....	72
Šerpytis, L. ....	52
Šimėnas, M. ....	70, 75, 77, 81
Skaužius, R. ....	44, 45, 48, 58
Skrudienė, M. ....	73
Sokol, D. ....	44, 61, 68
Stankevičiūtė, Ž. ....	51
Steponavičiūtė, M. ....	20
Stręk, W. ....	62, 74
Szymański, D. ....	32, 62

---

**T**

Talaikis, M. ....	24, 38
Tamulevičienė, A. ....	33
Tamulevičius, S. ....	33
Tamulevičius, T. ....	33
Taujenis, L. ....	52
Tomala, R. ....	62, 74
Turčak, J. ....	75
Tutlienė, S. ....	76
Tyrpekl, V. ....	78

---

**U**

Uazyrkhanova, G. ....	64
Usevičius, G. ....	77, 81

---

**V**

Vaclavikova, M. ....	40
Vaičiukynaitė, K. ....	79
Valiūnienė, A. ....	59, 65, 82
Vasiliauskiene, K. ....	80
Verbaitytė, P. ....	70, 81
Vilčiauskas, L. ....	35, 76
Virbickas, P. ....	59, 65, 82
Vištorskaja, D. ....	64

---

**W**

Wędzyńska, A. ....	62
--------------------	----

---

**Y**

Yang, T. C.-K. ....	51
Yankovych, H. ....	40

---

**Z**

Žalėnkiėnė, S. ....	67, 79
Žambžickaitė, G. ....	24
Žarkov, A. ....	17, 37, 38, 46, 47, 54, 63, 64
Žižiūnaitė, G. ....	82
Zubrytė, E. ....	83

Functional Inorganic Materials, abstract book, 86 pages.

Vilnius University Press  
9 Saulėtekio Av., III Building, LT-10222 Vilnius  
info@leidykla.vu.lt, [www.leidykla.vu.lt/en/](http://www.leidykla.vu.lt/en/)  
[www.knygynas.vu.lt](http://www.knygynas.vu.lt), [www.journals.vu.lt](http://www.journals.vu.lt)